Investigating the localization and functional significance of adenine phosphoribosyltransferase1 in *Arabidopsis* chloroplasts

by

Kaluhannadige Rasanie Eranka Padmathilake

A thesis
presented to the University of Waterloo
in fulfillment of the
thesis requirement for the degree of
Master of Science
in
Biology

Waterloo, Ontario, Canada, 2014

AUTHOR'S DECLARATION

I hereby declare that I am the sole author of this thesis. This is a true copy of the thesis, including any required final revisions, as accepted by my examiners.

I understand that my thesis may be made electronically available to the public.

Abstract

Adenine phosphoribosyltransferase (APT) is a housekeeping enzyme that catalyses the principal route of adenine recycling in plants. Of the five *APT* genes encoded in the *Arabidopsis* genome, *APT1* is the most highly expressed. The *APT1* locus encodes two polypeptides: APT1.1 and APT1.2 with *APT1.1* being the slightly larger of the two due to having extra exon at its 5' end. This exon contains a predicted chloroplast targeting sequence. The *APT1* mutants *apt1-3* and *oxt1*, have low levels of APT activity, in the range of 1-6% that of the wild type, and increased adenine content (i.e. *oxt1* chloroplasts have 12-fold more adenine than WT plastids). The first aim of this study was develop a system to test whether the increased adenine in plastids of *apt1* mutants is essential for their oxidative stress tolerance. A second objective was to determine the localization of APT1.1 in chloroplasts.

The adenine deaminase (ADE) activity encoded by the *AAH1* gene of *Saccharomyces cerevisiae* was transferred into *apt1* mutants with the objective of reducing the adenine content at chloroplasts. A targeting sequence was fused with the coding sequence of *AAH1* to direct ADE activity into the plastid. The construct was first introduced into WT plants under control of the constitutive *UBQ10* promoter, and the transgene subsequently transferred to *apt1-3* and *oxt1* mutants by genetic crossing. Additional constructs containing the coding sequence for green fluorescent protein (GFP) fused to either the transit sequence or the C-terminus of the *AAH1* sequence were created to verify the import of ADE into plastids. Transformants were evaluated for the presence of the *AAH1* transgene, transcript, protein and enzyme activity. The expression of the ADE-GFP fusion protein was analyzed by confocal microscopy and immunoblotting. ADE enzyme activity was assayed using a coupled spectrophotometric method. Finally, chloroplast subfractionation followed by immunoblotting was used to investigate the chloroplast localization of APT1 in WT plants.

While immunoblotting and polymerase chain reaction assays of cDNA prepared from the transgenic lines provided evidence that they expressed the full-length ADE transgene, ADE enzyme activity in leaf extracts was undetectable. Confocal microscopy showed that the ADE-GFP was imported successfully into plastids. Subfractionation of WT chloroplasts indicated that APT1.1 is localized in the membrane fraction. However it is yet to be confirmed whether APT1 is attached to the outer envelope membrane or one of the internal membranes (inner envelope membrane or thylakoid membrane).

Acknowledgements

First of all I would like to thank my supervisor Dr. Barbara Moffatt for her exceptional guidance, support and encouragement and direction in conducting proper scientific research. For her unending motivation that kept me on track and made me perform the lab work enthusiastically.

My thanks goes to my committee members (not in a particular order), Dr. Simon Chuong, Dr. Todd Holyoak, Dr. Allison McDonald and Dr. Matthew Smith, for their invaluable constructive criticism and suggestions during committee meetings. Special thanks to Dr. Chuong and Dr. Holyoak for letting me work in their labs. Very special thanks for Dr. Trevor Charles for keeping trust on me.

I would like to extend my heartiest thanks for all past and present Moffatt and Chuong lab members especially to Sang, Terry, Ishari, Sarah, Cherry, Maye and Nimhani.

I wish to thank all the technicians in the Department of Biology especially to Yong, Dale, Mishi, Adrian, Lynn and Daryl for their various technical support for this research work. I would also like to thank the lab members of Dr. Holyoak, Dr. Chuong, Dr. Lolle, Dr. Glick, Dr. Charles and Dr. Heikkila for letting me use their facilities and teaching me various techniques.

Lastly, I would like to thank my husband Wenura, my dad, my mom, grand-parents, my one and only sister, brother-in-law and chooty Nilesi for being with me each and every moment in last two and half years with me though I was several thousand miles away from them physically.

Dedication

To my family in Canada

Ishari, Nandana, Dylan and Dyanna Jayabahu

Table of Contents

List of Figures

List of Tables

List of Abbreviations

AAH1	Adenine aminohydrolase1
Aah1p	Adenine aminohydrolase1 polyclonal antibody
ADE	Adenine deaminase.
AMP	Adenosine monophosphate
$(NH_4)_2SO_4$	Ammonium sulphate
APT	Adenine phosphoribosyltransferase
AT	3-amino-1, 2, 4-triazole
ATP	Adenosine triphosphate
BA	Benzyladenine
BSA	Bovine Serum Albumin
BSO	Buthionine sulfoximine
cDNA	Complementary deoxyribonucleic acid
CDS	Coding sequences
CK	Cytokinin
ClpC	Caseinolytic protease subunit C
DAP	2, 6-diaminopurine
dATP	Deoxyadenosine triphosphate
DEPC	Diethylpyrocarbonate
ECL	Enhanced Chemiluminescence
EDTA	Ethylenediaminetetraacetic acid
eFP	Electronic Fluorescent Pictograph
GDH	Glutamate dehydrogenase

GFP	Green fluorescent protein
GTP	Guanosine Triphosphate
H_2O_2	Hydrogen Peroxide
HEPES-KOH	[2-hydroxyethyl]-1-piperazineethanesulfonic acid-KOH
HS	HEPES sorbitol
HPLC	High-Performance Liquid Chromatography
HRP	Horseradish Peroxidase
Hsp_{70}	Heat Shock Protein 70 kDa
IC	Intact Chloroplasts
IP	Intact Protoplasts
IPTG	Isopropyl β-D-1-thiogalactopyranoside
K_M	Michaelis-Menten constant
V_{max}	Maximum velocity of an enzyme reaction
M	Membrane Fraction
Met	Methionine
MS	Murashige-Skoog
NaCl	Sodium chloride
NAD^+	Nicotinamide-adenine-dinucleotide
NADH	Reduced nicotinamide- adenine-dinucleotide
NADPH	Reduced nicotinamide- adenine-dinucleotide-phosphate
NaH_2PO_4	Sodium dihydrogen phosphate
NCBI	National Center for Biotechnology Information
NH_4Cl	Ammonium chloride
O^{2-}	Superoxide

oxt1	Oxidative Stress Tolerance 1
PAGE	Polyacrylamide gel electrophoresis
PCR	Polymerase chain reaction
PBS-T	Phosphate buffered saline-Tween
PPDB	Plant Proteome Database
PRPP	5-phosphoribosyl-1-pyrophosphate
PsaD	D subunit of photosystem I (PSI)
RbcL	Rubisco large subunit
ROS	Reactive Oxygen species
RT	Room temperature
SAHH	S-Adenosyl Homocysteine Hydrolase
SDS	Sodium Dodecyl Sulfate
SUBA	SUB-cellular location database for *Arabidopsis*
TAIR	The *Arabidopsis* Information Resource
tFd	Transit peptide sequence for ferredoxin
Tic	Translocon at the inner envelope membrane of chloroplast
Toc	Translocon at the outer envelope membrane of chloroplast
UTR	Untranslated Region

Chapter 1
Introduction

1.1 Arabidopsis thaliana

Arabidopsis thaliana (L.), commonly known as Thale Cress, belongs to the family Brassicaceae. Although this family is rich in economically important crop plants, *Arabidopsis* is considered as weed. With time, it has gained prominence as the most extensively used model plant not only for plant molecular genetic studies but also for studying biological structural and functional processes common to all eukaryotes (Meinke *et al.* 1998). Columbia and Landsberg are the most commonly used ecotypes for genetic and molecular studies involving *Arabidopsis* (Meinke *et al.* 1998).

A number of characteristics of *Arabidopsis* make it useful for plant science research. As a small plant of 15-20 cm in height, it needs only a little space to grow to maturity. Therefore, this plant can be easily maintained under greenhouse conditions or under fluorescent lights in a growth chamber. It is a self-pollinating plant and can be crossed easily, if required. A single plant can produce over 5,000 seeds (Meinke *et al.* 1998) and it completes its life cycle within 7-8 weeks depending on the growth conditions (Pyke 1994). These latter two features help to produce a large number of plants within a short period of time.

Arabidopsis has a small genome of 125 Mb with about 25,498 genes arranged in five chromosomes. Its nuclear genome is completely sequenced and well documented (*Arabidopsis* Genome Initiative 2000; Bevan and Walsh 2005). There are several databases of compiled genetic and molecular observations of *Arabidopsis* with The *Arabidopsis* Information Resource (TAIR, www.*Arabidopsis*.org) database being the most comprehensive. TAIR includes information on gene structure, gene expression, gene product information, DNA and seed stocks, genetic and physical markers, genome maps,

publications, as well as information about the *Arabidopsis* research community. The data on gene product functions are updated weekly based on the latest publications and community data submissions (TAIR 2014). This genomic information aids the isolation of genes and studies of gene expression and gene regulation during plant development. To date numerous mutants have been identified and characterized in a variety of areas such as mutants resistant to biotic stresses (e.g. pest and pathogen resistant), and abiotic stresses (e.g. drought, salinity, high temperature); mutants useful in bio-remediation, protein therapeutics and plant metabolism. This thesis is focused on understanding the phenotype of a mutant deficient in adenine salvage metabolism.

Previous studies by Sukrong *et al.* (2012) reported on *Arabidopsis* mutants in a gene encoding adenine phosphoribosyltransferase (APT) (At1g27450) that were oxidative stress tolerant as a result of the *apt* mutation. A key focus of the research outlined in this thesis was to understand the consequences of APT deficiency on stress tolerance; a second aspect explored the subcellular localization of APT isoforms.

1.2 Adenine Phosphoribosyltransferase

Adenine phosphoribosyltransferase (APT) (EC 2.4.2.7) is an essential enzyme that is constitutively expressed in most living organisms (Sarver and Wang 2002). It acts as a salvage enzyme for the recycling of adenine into adenosine monophosphate (AMP) (Figure 1-1). APT catalyzes the reaction between adenine and 5-phosphoribosyl-1-pyrophosphate (PRPP) and produces AMP and, the byproduct, pyrophosphate (PPi) (Bashor *et al.* 2002). The reaction is achieved by Mg^{+2} dependent transfer of the phosphoribosyl group from PRPP to adenine (Groth and Young 1971). AMP is a precursor for ATP and dATP synthesis (Figure 1-1).

APT activity has an additional role in plant metabolism. It converts cytokinin (CK) bases, a class of phytohormones that are derivatives of adenine, to their corresponding nucleotide forms (Allen *et al.* 2002). For example, Moffatt *et al.* (1991) showed that the metabolism of the CK base benzyladenine (BA) is strongly decreased in *Arabidopsis* plants that are APT1-deficient, when the CK is exogenously supplied. The conversion of a CK base to its nucleotide is believed to inactivate the hormone (Schwartzenberg *et al.* 2007).

1.2.1 Purine metabolism

Purine metabolism is synthesis and break down of purines in organisms. Adenine and uridine nucleotides are important in the synthesis of nucleic acids and as cofactors in metabolism (Zrenner *et al.* 2006). Adenine nucleotides are the main nucleotide form for energy metabolism. Zrenner *et al.* (2006) explained the compartmentalization of adenine nucleotide synthesis in leaves as 45% in plastid stroma, 46% in cytosol and 9% in mitochondrial matrix (Zrenner *et al.* 2006).

There are two principle routes for purine nucleotide metabolism: *de novo* synthesis and the salvage pathway (Moffatt and Ashihara 2002). The *de novo* pathway is very energy consuming and it starts with small molecules such as amino acids, carbon dioxide, phosphoribosyl pyrophosphate, and aspartate. *De novo* synthesis of adenine nucleotides is 10-step-pathway requires seven ATPs (Senecoff *et al.* 1996). It is assumed that the large demand of nucleotides of growing and dividing cells is supplied by *de novo* synthesis (Zrenner *et al.* 2006). The synthesis of adenine nucleotides by breaking down of complex molecules is known as salvage pathway (Zrenner *et al.* 2006). According to Zrenner *et al.* (2006) non growing cells may be able to maintain their nucleotide pools mainly by salvage pathway. APT plays an important role here. The salvage pathway demands less energy compared to *de novo* synthesis (Zrenner *et al.* 2006). Moffatt and Ashihara (2002) reviewed

that only one reaction in salvage pathway requires ATP (phosphorylation of nucleosides to nucleotides). According to Moffatt and Ashihara (2002) and Zrenner *et al.* (2006) salvage pathway and *de novo* synthesis are mainly found in the cytosol and in the chloroplast, respectively.

As explained earlier APT metabolizes adenine into AMP which is then converted into ADP and finally into ATP. The *apt* mutants of *Arabidopsis* have increased level of adenine than does WT (Facciuolo 2009 and Sukrong *et al*. 2012). In addition, Shkolnik (2009) reported that *apt* mutants express increased level of adenine in chloroplasts. This tells metabolism of adenine into AMP by APT in other words salvage pathway of adenine nucleotides metabolism takes place in chloroplasts as well as in cytosol. On the other hand, it suggests the de novo synthesis pathway which lead the adenine accumulation takes place in both cytosol and chloroplasts.

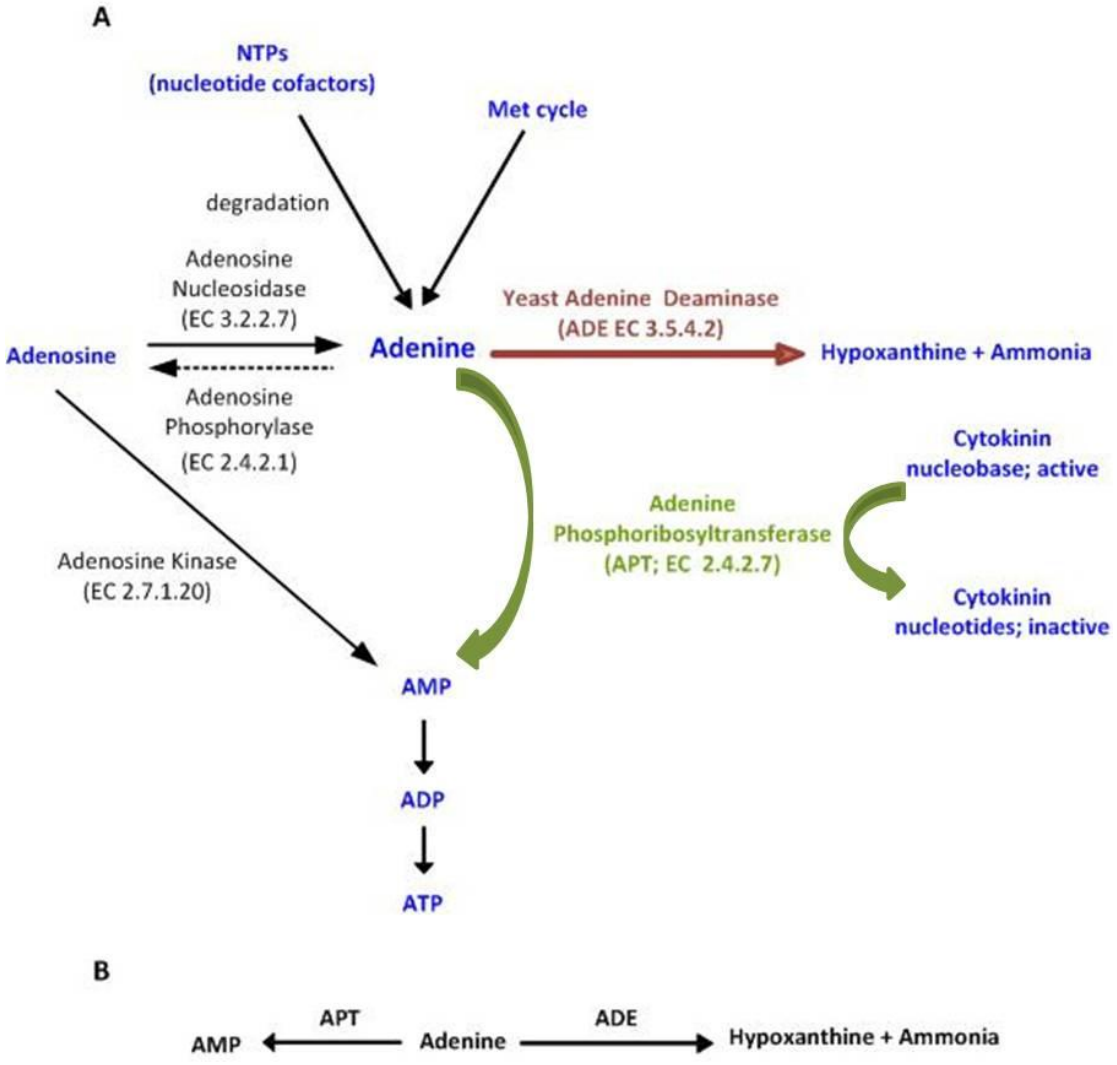

Figure 1-1: A Schematic diagram of involvement of APT and ADE in adenylate metabolism

A: A schematic diagram showing the major components of metabolism that produce or interconvert adenine and CKs. Green lines represent the involvement of APT in adenine and CK metabolism in plant cells while red lines represent the effect of adding of ADE. In plants, adenine is produced by three key routes: the methionine (Met) cycle enzyme, methylthioadenosine nucleosidase (EC 2.4.2.28); the degradation of nucleotide cofactors, and the metabolism of adenosine by adenosine nucleosidase (EC 3.2.2.7). Adenine can be converted back to adenosine by adenosine phosphorylase (EC 2.4.2.1). Adenine is mainly metabolized by APT and adenine deaminase (ADE). APT catalyzes the conversion of CK bases to their corresponding nucleotides; B: Adenine metabolism by APT and ADE: adenine is metabolized into AMP by APT and into hypoxanthine and ammonia by ADE. Yeast ADE was transformed into *Arabidopsis* plants in this study as it does not exist naturally in plants (NCBI 2014).

1.2.2 Five *Arabidopsis APT* genes and their protein products

APT is a single copy housekeeping gene in most organisms including *Saccharomyces cerevisiae* (Shi *et al.* 2000). In contrast, there are several plant species reported to have multiple *APT* genes. For example, in 2006, Zhou and colleagues found two forms of *APT* in rice (*Oryza sativa*) and in 2008, Wu and colleagues identified three *APT* genes in maize (*Zea mays*). As outlined in the NCBI database (www.ncbi.nlm.nih.gov), there are five genes in *A. thaliana*: *APT1* (*At1g27450*) (Moffatt and Somerville, 1988), *APT2* (*At1g80050*) (Schnorr *et al*. 1996), *APT3* (*At4g22570*) (Allen *et al.* 2002), *APT4* (*At4g12440*) and *APT5* (*At5g11160*) (TAIR, 2014). These five isoforms share 89% amino acid sequence similarity (Facciuolo 2009). The expression of each isoform varies within the plant. According to TAIR (2014), APT1, APT2, APT3 and APT5 are transcribed in leaf (leaf apex, leaf lamina base, petiole, guard cells), shoot system (shoot apex, stem), flower (petal, sepal, carpel, stamen, pedicel, pollen, inflorescence meristems), seeds (cotyledon, hypocotyls, embryo), and root, while APT4 is transcribed in guard cells, hypocotyl, flower, vascular leaves, leaf apex, shoot apex

and root. Figure 1-2 shows the Electronic Fluorescent Pictograph (eFP) browser representation of available transcriptome data (University of Toronto; bar.utoronto.ca/efp/cgi-bin/efpWeb.cgi).

Figure 1-3 shows how eFP browser depicts the available data on the subcellular localization of APT1, APT2, APT3, APT4 and APT5 in the *Arabidopsis* cell. APT1 localizes in cell wall, cytosol, chloroplasts and mitochondria whereas, APT2, APT3, APT4 and APT5 localize only in the cytosol subcellularly. There are experimental publications that relate with these eFP prediction results. As example Allen *et al.* (2002) reported APT1, APT2, and APT3 are localize in cytosol and Schnorr *et al.* (1996) explained APT2 is in cytosol.

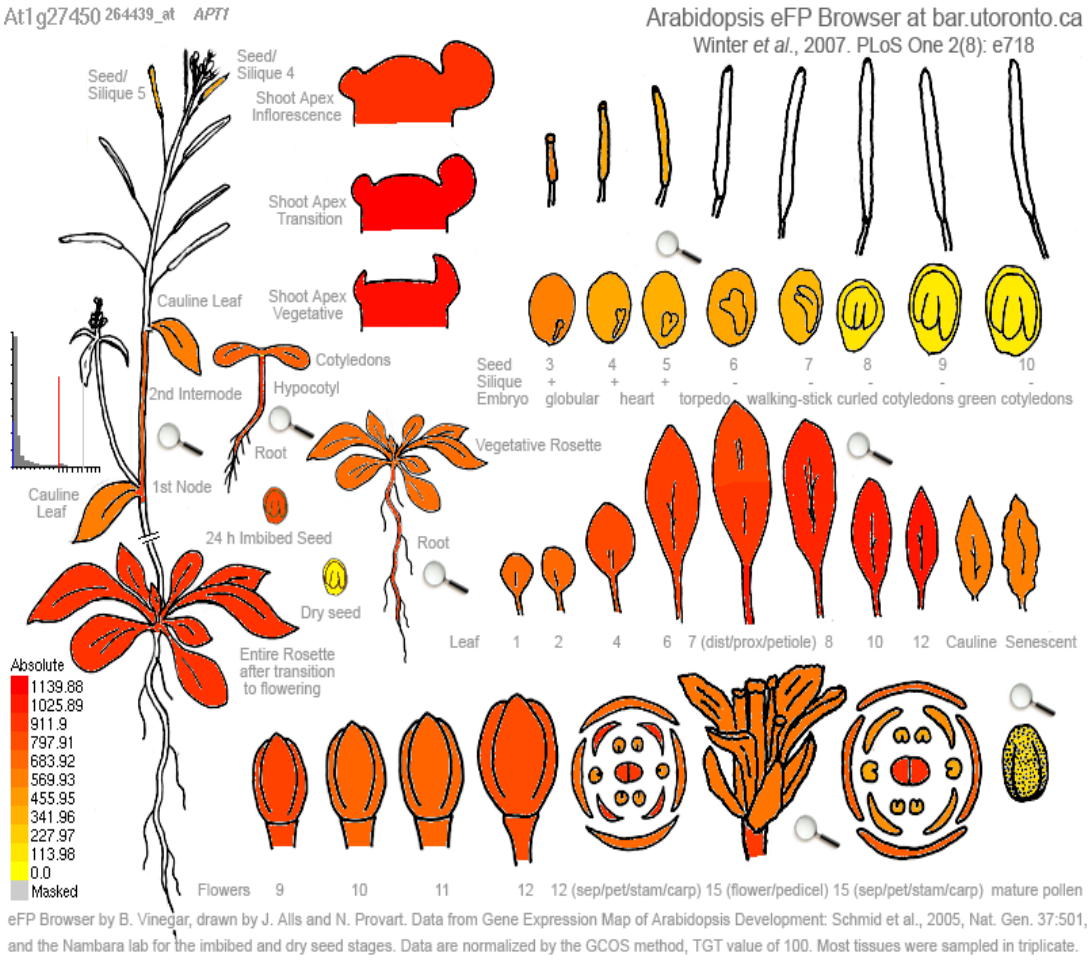

Figure 1-2: Schematic representation of comparative analysis of *APT1* (At1g27450) transcripts in different organs throughout development of *Arabidopsis*

The predicted organ *APT1* transcript abundance correlated with the Map of *Arabidopsis* development of Schmid *et al*. (2005), the AtGenExpress Consortium data (Abiotic Stress - Kilian *et al.* 2007, Biotic Stress, and the Chemical and Hormone Series), cell-type or seed-specific data and other data. The image was taken from electronic Fluorescent Pictograph (eFP) browser which is available at bar.utoronto.ca/efp/cgi-bin/efpWeb.cgi (Dec 12, 2013). The colours indicate the intensity of transcript availability within the indicated organ (red is the highest, whereas white is the lowest).

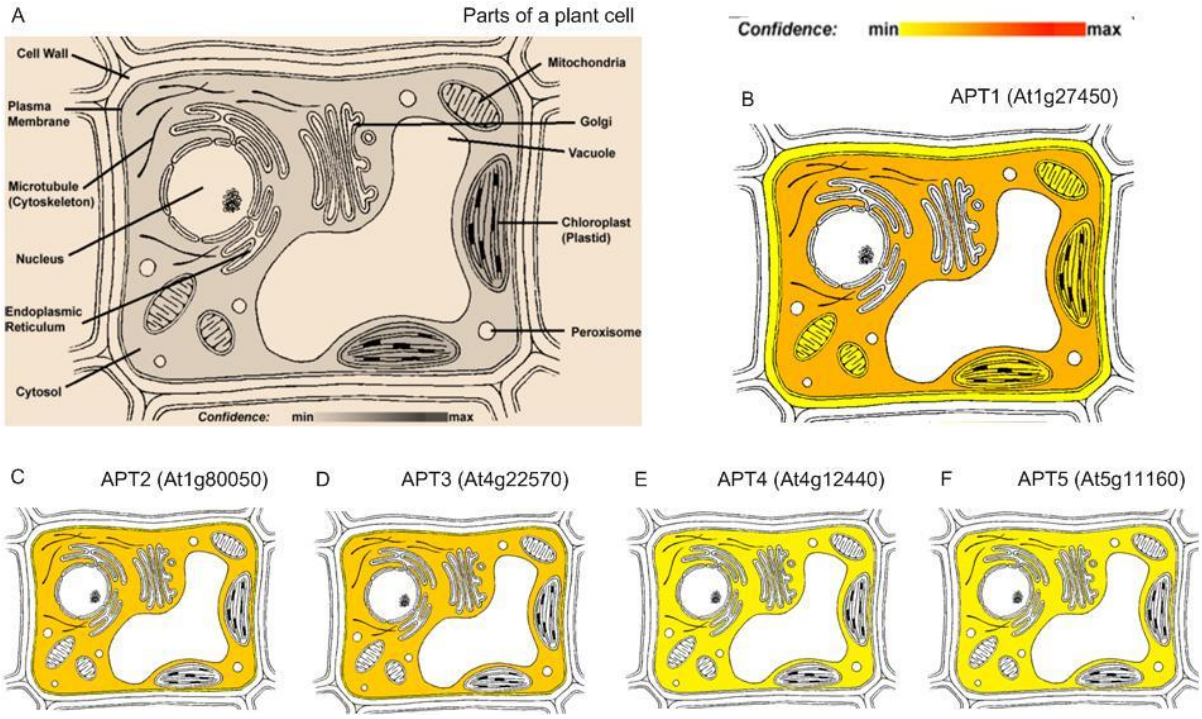

Figure 1-3: Schematic representation of localization of APT1 (At1g27450), *APT2* (*At1g80050*), *APT3* (*At4g22570*), *APT4* (*At4g12440*) and *APT5* (*At5g11160*) in *Arabidopsis* cell

The image is the eFP depiction of the predicted subcellular localization of APT1, APT2, APT3, APT4 and APT5 proteins as predicted in Heazlewood *et al.*'s SUBA database (bar.utoronto.ca/cell_efp/cgi-bin/cell_efp.cgi [May 01, 2014]). A-compartments of a typical plant cell; B- APT1 is predicted to be localized in cytosol, mitochondria, and chloroplasts of the cell; C- APT2 localizes in the cytosol, D-APT3 localizes in the cytosol, E- APT4 localizes in the cytosol, F-APT5 localizes in the cytosol. The colors indicate the intensity of transcript availability in the cell (dark yellow to light yellow indicates higher to lower expression of APT).

1.2.2.1 APT1

APT1 accounts for most of the APT activity in Arabidopsis leaves based on the observation that a mutation in *APT1* eliminates ~99% of the APT activity detected in leaf crude extract (Moffatt and Somerville 1988). According to the information in TAIR, At1g27450 encodes a polypeptide of 243 amino acids with a predicted molecular weight of 26.4 kDa (TAIR 2014). Based on APT enzyme activity assessments in various plant organs, Lee and Moffatt (1994) demonstrated that APT activity is present in crude protein extracts isolated from flowers, roots, stems and leaves. They determined APT is more abundant in flower buds and root tips than in other parts of the plant. Zhang *et al.* (2002) showed that the strongest expression of APT1 is in young buds.

Drawing on *in vivo* feeding study results, Zhang *et al.,* (2002) reported that APT1 has a similar kinetic activity when using adenine and CK bases as substrates (1.5-9.6 µmol/min mg protein). According to Schnorr *et al*. (1996), adenine is the most efficient substrate for APT1.

1.2.2.2 APT2

Schnorr *et al.* (1996) sequenced the APT2 gene before the complete genome sequence was available and reported that APT1 and 2 both contain 5 introns in the same positions, but these vary in their length and nucleotide composition. The APT2gene predicts a polypeptide with 192 residues and a molecular weight of 21 kDa (Schnorr 1996). Based on sequencing data and subcellular fractionation experiments, Allen *et al*. (2002) confirmed that APT2 is localized in the cytosol.

Schnorr and colleagues (1996) reported that APT2 is transcribed in roots, stems, siliques, flower meristems, and cultured cells, based on RNase protection assays. Furthermore, they noted that APT2 is not present where active forms of CKs are not present such as mature

leaves. According to Moffatt and colleagues (2001), APT2 transcripts are specifically expressed in the floral receptacle parenchymal cells around the xylem vessels where dividing and growing cells need CKs.

Schnorr *et al.* (1996) confirmed that recombinant APT1 and APT2 recovered from *E. coli* have similar K_M values for adenine. APT2 has a higher affinity for CKs as compared to APT1. Allen and colleagues (2002) determined both APT1 and APT2 prefer adenine as a substrate, based on their activities on adenine and BA. Furthermore, they reported that APT1 is 180-fold more effective than APT2 in the metabolism of adenine whereas; APT2 is 250-fold more active than APT1 on BA.

1.2.2.3 APT3, APT4, and APT5

APT3 encodes a polypeptide with 183 residues with a predicated molecular weight of 20.4 kDa (Allen *et al.* 2002). According to TAIR (2014), APT3 is transcribed in leaves, flowers, roots, seeds and stems. Based on immunoblot results of subcellular fractions Allen *et al*. (2002) showed APT3 to be present in the cytosol. In addition, they reported that APT3 metabolizes adenine at a rate 31-35 times lower than APT1 does. However, APT2 and APT3 have higher affinities for CKs than does APT1.

As documented in TAIR, APT4 is transcribed in leaves, flowers, roots and shoot apices; APT5 is expressed in leaves, flowers, roots, shoot apices, stems, seeds, pollen and embryos. APT4 and APT5 genes predict polypeptides with 182 and 191 residues, respectively and molecular weights 20.4 kDa and 20.8 kDa, respectively.

In 2000, Itali and colleagues used GFP translational fusions to determine that APT is localized in the cytosol of barley cells (*Hordeum vulgare* L.). Using immunofluorescence localization Zarella-Boitz *et al.* (2004) confirmed APT is localized in the cytosol of *Leishmania donovani* cells. Zybailov *et al.* (2008) confirmed it further by proteomic analysis of *Arabidopsis* plastids. They analyzed ten independent Arabidopsis chloroplast preparations by noLC-Q-TOF and nanoLC-LTQ-Orbitrap mass spectrometry (MS) and identified 1325 proteins. Since it was a mass scale analysis the reliability might be debatable. Therefore, the first part this research focuses to study the localization of APT in chloroplasts.

1.2.3 APT1 isoforms

The analysis of expressed sequence tag collections revealed the presence of two transcripts arising from the *APT1* locus: APT1.1 and APT1.2 (Facciuolo 2009). *APT1.1* is longer than *APT1.2* due to the presence of an additional 5' terminal exon, while the other six exons are common to both gene models and transcripts as shown in Figure 1-4 (Facciuolo 2009). According to various subcellular localization prediction programs APT1.1 is localized in chloroplasts (Table 1). Besides the difference between *APT1.1* and *APT1.2* made by the presence of the first exon, each has a unique 5' UTR region. The 5' UTR of *APT1.1* is upstream of the methionine codon of exon 1 while, the APT2 5' UTR resides in the first intron (Facciuolo 2009).

As explained in Section 1.2.1, Itali *et al*. (2000), Allen *et al*. (2002), Zarella-Boitz *et al.* (2004), and Zybailov *et al.* (2008) reported APT as a cytosolic localized protein. In contrast, Hochstadt-Ozerand Stadtman (1971) detected APT in membrane vesicles in *Escherichia coli*. However, Ashihara and Ukaji (1985) detected APT activity in chloroplasts of spinach (*Spinacia oleracea*) leaves purified by differential centrifugation and discontinuous Percoll density gradients.

The results of subcellular localization prediction programs propose the destination of APT1.1 to be in chloroplasts as shown in Table 1. All the aforesaid programs predicted APT1.2 to be in the cytosol (the data are not shown). Facciuolo (2009) explained the additional first exon contains a predicted chloroplast targeting sequence and demonstrated the localization of APT1.1 in chloroplasts by green fluorescent protein (GFP) translational fusion protein studies. Facciuolo transformed *Arabidopsis* with a construct of GFP fused to the C-terminus of APT1.1 under the expression of the actin promoter (act_{pro}:APT1.1-2GFP); the transformants contained punctate bodies localized in the chloroplasts. He noted that Exon 1 alone is sufficient for this localization by using a APT_{pro}:Ex1-GFP construct. However, Facciuolo concluded that his studies were not able to determine if the APT1.1 was localized within chloroplast or just on the outer envelope of the organelle.

Table 1: Bioinformatic predictions on plastid localization of APT1.1

MultiLoc, WoLF PSORT, TargetP, and Predator predict APT1.1 is localized in plastids. (Modified from Facciuolo 2009)

Program	Probability of chloroplast localization	Website	Reference
MultiLoc	0.98	http://wwwbs.informatik.unituebingen.de/Services/MultiLoc/	Hoeglund *et al*. 2006
WoLF PSORT	0.86	http://wolfpsort.org/	Horton *et al*. 2007

TargetP	0.881	http://www.cbs.dtu.dk/services/TargetP/	Emanuelsson *et al*. 2000
Predator	0.45	http://urgi.versailles.inra.fr/predotar/predotar.html	Small *et al*. 2004

1.3 *Arabidopsis apt1* mutants

1.3.1 *apt1-3* mutant

The first APT1-deficient mutant lines were identified by Moffatt and Somerville in 1988. The mutants were selected based on their ability to grow on Murishige-Skoog (MS) medium supplemented with 2,6-diaminopurine (DAP). DAP becomes toxic to plants only if converted into its nucleotide form by the action of APT (Moffatt, 1994). Moffatt and Somerville (1988) reported three mutants of *APT1: apt1-1, apt1-2 and apt1-3.* Once the mutants are transferred to soil they grow slower than WT plants (Moffatt and Somerville, 1988; Allen *et al.* 2002).

Most interestingly, *apt1-2* and *apt1-3* mutants are completely male sterile while *apt1-1* is partially male sterile with 2% of seed production of WT (Moffatt and Somerville 1988). Their residual fertility is proportional to the APT activity measured in leaf extracts: *apt1-1, apt1-2 and apt1-3* have 10-15%, 2% and 1% of WT level of APT activity, respectively. Moffatt and colleagues (1992) proposed that this male sterility might be due to abnormal pollen development of mutant plants. Several explanations were suggested to account for the association between male sterility and APT deficiency: inadequate ATP availability during

microsporogenesis; accumulation of adenine causing inhibition of methylthioadenosine nucleosidase activity, and an imbalance in CK metabolism during pollen development (Facciuolo 2009; Zhang *et al.* 2013). In this study I used the most deficient APT 1 mutant, *apt1-3* that contains a point mutation in the splice acceptor site (3' splice site) of exon 4 (Figure 1-4). *apt1-3* does not express either APT1.1 or APT1.2 (Facciuolo 2009).

1.3.2 Oxidative stress tolerant 1 (*oxt*1): an APT1-deficient mutant

The APT1-deficient *oxt1* mutant was identified by Sukrong and colleagues (2012) using a screen designed to detect oxidative stress tolerant mutants within a population of T-DNA mutagenized seeds. As Sukrong *et al*. (2012) explain reactive oxygen species (ROS) cause intracellular damage to cells. Molecules such as H_2O_2, OH^-, and O_2^- are ROS in the system. Catalase and glutathione reductase are two of the enzymes which play important roles in scavenging ROS from the system. They used 3-amino-1, 2, 4-triazole (AT), a catalase inhibitor, and buthioninesulfoximine (BSO), a γ-glutamylcysteinyl synthetase (the first enzyme of the cellular glutathione biosynthetic pathway) inhibitor, to induce oxidative stress in the growth medium. AT, and BSO stimulate a non-lethal degree of oxidative stress to *Arabidopsis* plants by elevating H_2O_2 levels, and suppressing glutathione biosynthesis, respectively.

Seeds were grown in MS medium supplemented with 2 µM AT and 400 µM BSO. WT root growth is inhibited under these conditions resulting in chlorosis, and with prolonged exposure, death of the seedling. According to Sukrong *et al.* (2012), *oxt1* seedlings tolerate two-fold higher AT concentrations than do WT seedlings. Facciuolo (2009) found *apt1-3* is also tolerant to the oxidative stress induced AT and BSO.

The *oxt1* mutant contains a T-DNA insertion within the first intron of *APT1*, 40 bp upstream of exon II in the *APT1.1* gene model, as shown in Figure 1.4 (Sukrong *et al.* 2012). Based on transcript abundance assays, *APT1.1* is not expressed in *oxt1*, while *APT1.2* is expressed at only 1% of the transcript abundance found in WT (Facciuolo 2009). Sukrong and colleagues (2012) confirmed that the *oxt1* phenotype was due to a single dominant-acting mutation by segregation analysis. This mutation made the mutant line tolerant to diverse forms of chemically induced oxidative stresses. Importantly, this mutant shows good vegetative growth although it is comparatively slower than WT (Sukrong *et al.* 2012). Moreover, *oxt1* displays relatively delayed flowering (i.e. 3–5 days later under 16-h light conditions on soil) and increased biomass. For instance, Sukrong and colleagues (2012) showed *oxt1* seedlings grown under 16-h light conditions for 21 days on MS supplemented with sucrose reached 10% greater biomass than WT plants. In addition to its tolerance to chemically induced oxidative stresses and H_2O_2, it was also tolerant to high temperatures (Sukrong *et al*. 2012).

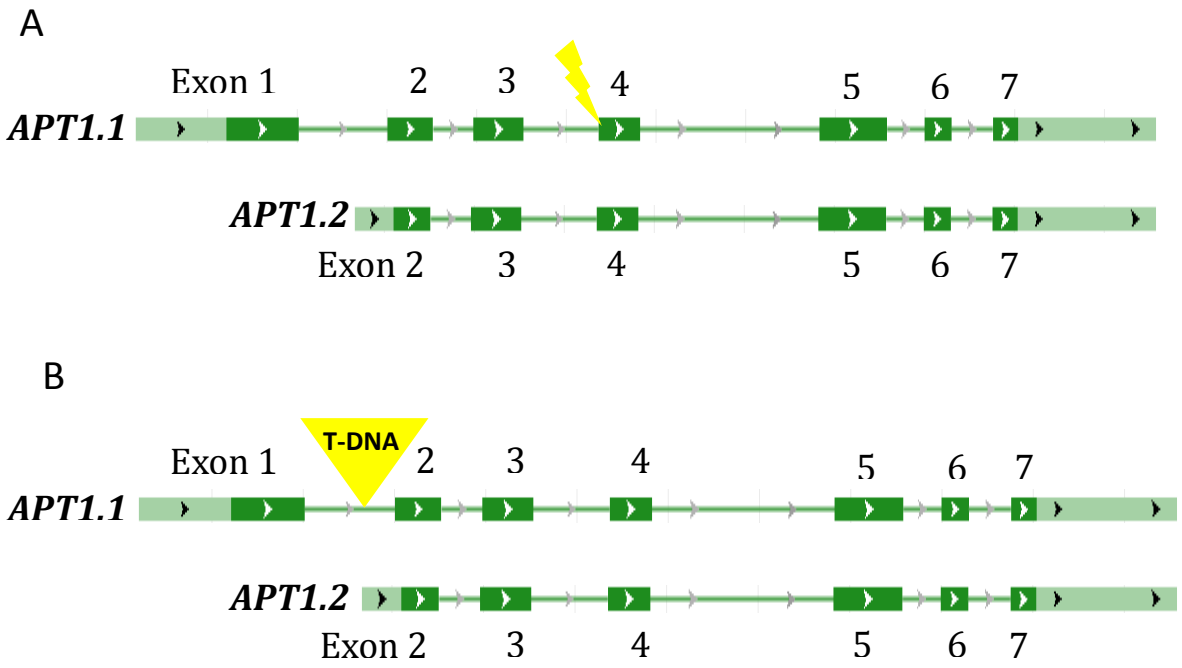

Figure 1-4: Schematic diagram of mutations in *APT1.1* in *apt1-3* and *oxt1*

APT1.1 contains seven exons while *APT1.2* contains only 6 exons. The additional exon in *APT1.1*, Exon 1, encoded a putative plastid targeting sequence. The dark green boxes, light green boxes, and light green lines represent exons, UTRs, and introns, respectively. A: The point mutation in *apt1-3* is at the splice acceptor site of exon 4 in *apt1-3*; B: The T-DNA insertion is at intron 1 (40 bp upstream of exon 2) in *oxt1*. Neither APT1.1 nor APT1.2 is expressed in *apt1-3* while APT1.2 expresses 1% in transcript abundance in *oxt1.* Modified from National Center for Biotechnology Information database (www.ncbi.nlm.nih.gov/gene/839636#reference-sequences)

1.4 Stress tolerance and adenine concentration

Perhaps not surprisingly, APT-deficient mutants have a higher adenine content in leaf extracts as compared to the corresponding WT samples: *oxt1* has 1.5-fold and *apt1-3* has 6-fold more adenine than WT (N=four biological replicates) (Sukrong *et al.* 2012). The APT1-deficient mutants also have a higher tolerance to oxidative stress compared to WT plants, as evaluated by their root lengths and dry plant mass (Sukrong *et al.* 2012). Based on HPLC analyses of the contents of chloroplasts separated using sucrose gradients, *oxt1* chloroplasts contain 12-fold more adenine than do WT chloroplasts (Shkolnik *et al*. 2009). According to Sukrong *et al.* (2012), an exogenous supply of adenine ranging from 5 to 150 µM results in improved growth in WT plants under oxidative stress. Based on these observations, Sukrong *et al.* (2012) suggested that there may be a relationship between adenine content of the plant and the oxidative stress tolerance.

1.5 Oxidative stress tolerance

Drought, flood, extreme temperatures, salt, heavy metals and oxidative stress are the major abiotic conditions that account for 50% of average crop yield losses worldwide annually (Wang *et al.* 2003). Oxidative stress is also a key abiotic factor that causes a series of morphological, physiological, biochemical and molecular alterations resulting in abnormal plant growth, development and ultimately poor crop production (Wang *et al*. 2001a). Oxidative stress results when there is an imbalance between the generation and the removal of ROS. These are intermediates such as hydrogen peroxide, singlet oxygen, hydroxyl radicals and superoxide radicals. ROS are normal byproducts of aerobic metabolism particularly associated with signaling pathways (such as ion channels); they are commonly removed by antioxidants. In contrast, under salinity, drought, extreme temperatures like other stress conditions, and during processes such as programmed cell

death (e.g. formation of aerenchyma in aquatic plants) and pathogen defense, ROS are in excess as a result of overwhelming the antioxidant capacity of the cell (Mittler 2002). Since ROS are highly reactive they can damage the cell structure and function with the absence of proper removal mechanisms and lead to oxidative destruction of the cell (Cho and Seo 2004; Mittler 2002).

Superoxide dismutase, catalase, peroxidase, and ascorbate peroxidase are some of the enzymes involved in antioxidant systems in plant cells, effectively protecting them from ROS damage (Cho and Seo 2004). Kruzniak (2002) suggested the majority of plant injuries are caused by environmental stresses related with oxidative stress caused by ROS.

There are many genetically engineered oxidative stress tolerant plants. Transgenic tobacco plants overexpressing CuZn superoxide dismutase from pea plants have an enhanced tolerance to an herbicide called methyl viologen which leads to the accumulation of toxic levels of H_2O_2 in plants (Gupta 1992). Tobacco plants engineered to overexpress *E. coli* catalase showed tolerance to photo oxidative stress and to methyl viologen (Shikanai *et al.* 1998; Miyagawa *et al*. 2000). Transgenic *Brassica juncea* plants overexpressing *E. coli* γ-glutamylcysteine have higher glutathione content and enhanced cadmium tolerance (Pilon-Smith *et al.* 2000).

An understanding of the oxidative stress tolerance of *apt1* mutants might lead to a new means to produce stress tolerant crops. Based on the findings of Facciuolo (2009), Shkolnik (2009), and Sukrong *et al.* (2012), the increased adenine content of *apt1* mutants might be the reason for their oxidative stress tolerance. To test this hypothesis I wanted to introduce an enzyme into the *apt1* mutants that would reduce their adenine content and test the transformants for a change in their oxidative stress tolerance. I chose the enzyme adenine deaminase (ADE) for this purpose.

1.6 Adenine deaminase

Adenine deaminase (ADE) (EC 3.5.4.2) is also known as adenine aminohydrolase, adenase and ADase (Kidder 1977; Nygaard *et al.* 1996). ADE catalyzes the reaction between adenine and H_2O, where hypoxanthine and ammonia are made as products (Kamat *et al*. 2011). The resulting hypoxanthine can react with PRPP to form inosine monophosphate, which is then converted into guanosine monophosphate (Pospisilova *et al.* 2008). The direct deamination of adenine has been reported only in bacteria (such as *Bacillus subtilis, and E. coli*); and lower eukaryotes (such as *Aspergillus nidulans, S. cerevisiae, and S. pombe*) (Ribard *et al.* 2003; Nygaard *et al.* 1996).

The ADE gene in *S. cerevisiae* is also known as Adenine aminohydrolase1 (AAH1; Gene ID: 855581) (Pospisilova *et al.* 2008). According to Pospisilova *et al.* (2008) the enzyme has a molecular mass of 39.633 kDa and its temperature and pH optima are in the range of 30-37^{o}C and at pH 7, respectively. Its K_M for adenine was reported to be 55 µM. In 1977 Kidder and others found the pH optimum of yeast adenine deaminase is between 6.0 and 7.5. They determined this enzyme is very stable upon heating, but that dilution increases its sensitivity to heat. They showed that the AAH1 enzyme loses less than 10% of its activity after 60 min exposure at 55^{o}C and 20% loss of activity after 5 min at 65^{0}C.

Since Shkolnik (2009), and Sukrong *et al.* (2012), found that the adenine content of *oxt1* mutants is 12-times higher than the adenine in WT chloroplasts, my research focused on the targeting of yeast ADE into *Arabidopsis* chloroplasts with the help of a chloroplast transit peptide.

1.7 Plastids

Plastids are organelles characteristic of plant cells. There are several types of plastids; all originate from a form called a proplastid which is a type of cytosolic body. Differentiation of

proplastids depends on the cell type, developmental stage of the plant and external factors. For instance, chloroplasts contain chlorophylls to absorb sunlight in photosynthetic cells; chromoplasts in flowers contain carotenoids to attract pollinators, and amyloplasts in roots and tubers are used to store starch (Pyke 1999). Later in development, chloroplasts transition into gerontoplasts during leaf senescence (Biswal 2012). Chloroplasts are the sites of photosynthesis in plants. Other than photosynthesis, other important metabolic activities such as lipid biosynthesis, nitrogen and sulfur assimilations, amino acid synthesis and purine metabolism also occur in plastids (Keeling, 2004).

1.7.1 Chloroplast structure

Chloroplasts are highly structured organelles. They contain three distinct membrane systems: outer-envelope-membrane, inner-envelope-membrane, and thylakoid membrane. The thylakoid membrane contains photosynthetically active protein complexes (Soll and Schleiff 2004). The thylakoids are disc shaped internal structures that consist of a thylakoid membrane and thylakoid lumen. Stacks of thylakoids are called grana. Grana are interconnected by non-stacked regions called stroma lamellae. There are several membrane-protein complexes associated with the thylakoid membrane: the light-harvesting systems I and II; photosystems I and II; cytochrome b_6f; and ATP synthase. Light harvesting complex II, photosystem II are incorporated in the granum thylakoid; the light harvesting system I, photosystem I and ATP synthase are associated with stroma thylakoids. Cytochrome b_6f is distributed equally in both types of lamellae. Due to having the light harvesting complex, the thylakoid membrane is the site for the conversion of light energy into chemical energy, ATP and NADPH, also known as light dependent reactions of photosynthesis (Daum *et al.* 2010). The space between the thylakoid membrane and chloroplast inner membrane is filled with stroma. The stroma contains the enzymes that make up the Calvin cycle (or ATP- and NADPH- dependent reactions) of photosynthesis

(Berg *et al*. 2002).The Calvin cycle is the process in which CO_2 is converted into glucose using NADPH and ATP formed in the light reactions (Berg *et al*. 2002).

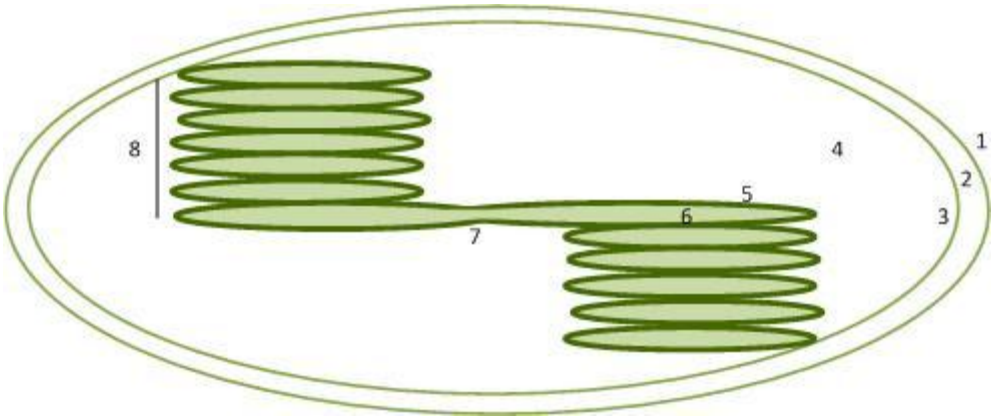

Figure 1-5: Schematic diagram of a longitudinal section of a chloroplast

Chloroplasts are the sites of photosynthesis in plants. They are double membranous organelles. A stack of thylakoids is called a granum and there are number of grana in one chloroplast although only two are shown here. The space between thylakoids and the inner membrane is filed with stroma. 1: outer envelope membrane, 2: inter membrane space 3: inner envelope membrane, 4: stroma, 5: thylakoid membrane, 6: thylakoid lumen, 7: stroma lamellae, 8: granum (a stack of thylakoid).

1.7.2 Import of proteins into chloroplasts

Some proteins synthesized in the cytosol are translocated into different organelles to perform their specific activities. The localization of proteins from cytosol to the correct organelle or sub-organellar compartment depends on a specific amino acid sequence in the

protein itself; in the case of plastid targeting this is called a 'transit peptide' (Agne and Kessler, 2007).

Transit peptides typically contain 20-70 amino acids (Agne and Kessler, 2007). Although the whole sequence of a transit peptide is important in binding and import of the pre-protein, the N-terminal region of 6-14 residues is the vital part for the initial interaction with the import apparatus. A second region, often located within residues 15-25, is important for the interaction with a component in the inner membrane (Bruce 2000). Transit peptides are rich in hydroxylated residues such as serine and threonine and deficient in acidic residues (Bruce 2001, Agne and Kessler, 2007). Transit peptides are recognized by chloroplast import receptors and bound reversibly (Agne and Kessler, 2007). Then the preproteins are bound with outer envelope irreversibly (Agne and Kessler, 2007). In 2001, Bruce showed two possible modes of interaction between the chloroplast envelope and chloroplast-specific-transit peptides: an ionic interaction between the anionic phospholipids of the chloroplast outer membrane and basic amino acids in transit peptides and, hydrogen bonding between galactose head groups of glycolipids and the hydroxyl groups of transit peptides (Bruce 2001, Bhushan *et al.* 2006, Lung, 2012).

When polypeptides enter the chloroplast stroma their transit peptides are cleaved off by an enzyme called the stromal processing peptidase. After the initial cleavage, one or a few N-terminal amino acids may be removed by a second stromal protease (Bruce 2001). There are several sequence-based computational predictors for cleavage sites including ChloroP (Emanuelsson *et al*. 1999) and TargetP (Emanuelsson *et al*. 2000). The results of previous analyses of the amino acid sequence of APT1.1 are shown in Table 1. Databases based on the results of large scale proteomic experiments such as Plant Proteome DataBase (PPDB) (ppdb.tc.cornell.edu) and SUB-cellular location database for *Arabidopsis* proteins (SUBA) (www.suba.bcs.uwa.edu.au) also provide evidence for the plastid localization of APT1.1.

In this study I used the transit peptide from ferredoxin to direct the yeast ADE into *Arabidopsis* plastids. Ferredoxin is a chloroplast protein that is encoded in the nuclear genome and synthesized in the cytosol and subsequently imported into plastids (Smeekens *et al.* 1989). Smeekens and colleagues made deletions in the processing site of the ferredoxin precursor molecule to define the transit peptide sequence. The particular sequence I used originated from *Bienertia sinuspersici* that was developed and tested by Terry Lung (Lung 2012).

1.7.3 Chloroplast import apparatus

The import of proteins into chloroplasts begins with binding of the preprotein with several cytosolic factors. First, the transit peptide binds with Heat Shock Protein 70 kDa (Hsp70) to keep the preprotein unfolded and in an import competent state. This allows it to be translocated through a channel in the outer membrane that has a small diameter limited to the proteins with no secondary structure (i.e. Toc 75). In addition to that, the unfoldase activity of the envelope also contributes to keep the preprotein sequence unfolded (Bruce 2001). Apart from Hsp70, the preprotein binds with a 14-3-3 protein, thereby forming a guidance complex. Formation of guidance complex increases the specificity of chloroplast import (Bruce 2001, Agne and Kessler, 2007).

When an unfolded preprotein reaches the chloroplast outer membrane, its transit peptide directs its import. There are two protein complexes called the translocon at the outer envelope membrane of chloroplast (Toc) and the translocon at the inner envelope membrane of chloroplast (Tic) that mediate these steps. The different Toc and Tic components are named according to the molecular weights in kDa calculated at their first discovery (e.g. Toc34, i.e. molecular weight of 34 kDa) (Jarvis and Soll 2001, Reinbothe, 2014).

1.7.4 The import of polypeptides at the outer chloroplast membrane and inner membrane

The Toc complex consists of Toc64, Toc159, Toc34 and Toc75 (Jarvis and Soll 2001, Agne and Kessler 2007, Richardson *et al.* 2014). The complexes made of Toc75, Toc34 and Toc159 are minimal size of 800 kDa and stoichiometry estimated at 3:3:1 or 4:4:1 (Schleiff *et al*., 2003; Kikuchi *et al.,* 2006; Chen and Li, 2007). Pre-proteins are unloaded at Toc64 and localized to the outer lipid bilayer for recognition by other Toc proteins. Toc159 and Toc34 are GTPase receptors, which recognize preproteins. Toc75 is β-barrel channel protein, which provides a voltage-gated ion channel through the outer membrane (Jarvis and Soll 2001).

Protein translocation from the cytosol to the inter-membrane space of chloroplasts needs a low concentration of ATP and GTP. However, protein translocation from the inter-membrane space to stroma via inner envelope membrane needs a higher concentration of ATP in the stroma. The inner membrane translocation requires the involvement of Tic proteins. Tic20 and Tic21 are channel proteins. Tic110 assemble the preprotein import motor, which consists of Hsp93 and caseinolytic protease subunit C (ClpC) and Tic40 (Jarvis and Soll 2001; Kessler and Blobe 1996).

1.7.5 Other routes for protein import into chloroplasts

There are certain proteins translocated to chloroplasts via alternative import pathways, without the involvement of conventional transit peptides (Jarvis 2008). For instance, in 2002, Miras and colleagues showed an ATP-dependent pathway that did not rely on functional Tic/Toc machinery. In addition, there are some proteins imported to chloroplasts after pre-binding with their substrate, for instance, NADPH: protochlorophyllide oxidoreductase binds with its substrate protochlorophyllide (Reinboth *et al.* 1995).

1.8 Objectives of the research outlined in this thesis and the associated hypotheses

Part of my research was focused on developing a system to test whether the increased plastid adenine content of *Arabidopsis apt1* mutants is essential for their oxidative stress tolerance. The yeast ADE was used to reduce the adenine levels in the mutants. The constructs with yeast ADE were first introduced into WT *Arabidopsis* plants and subsequently transferred to the *apt1-3* and *oxt1* mutants by genetic crossing.

The second part of my research was focused on determining the plastid localization of APT1.1 in WT *Arabidopsis* plants.

1. To test the relationship between adenine content and oxidative stress tolerance of *Arabidopsis*

   H1- Yeast ADE can be expressed in *Arabidopsis* plants.

   H2-Yeast ADE is active in transgenic *Arabidopsis* plants

   H3-Yeast adenine deaminase activity can be targeted to chloroplasts by the ferredoxin transit peptide.

   H4- Increased adenine content in chloroplasts enhances plant stress tolerance of *apt1* mutants

2. To detect the localization and compartmentalization of native APT1.1 in chloroplasts

   H1- Native APT1.1 localizes in chloroplasts

   H2-APT1.1 localizes in a chloroplast membrane

Chapter 2
Materials and methods

2.1 Chemicals and supplies

Chemicals used in this study were of analytical grade and purchased from Sigma-Aldrich, BioShop Canada Inc., BioBasic, New England Biolabs, BioRad or Thermo Scientific (Canada) unless otherwise specified. T4 DNA ligase, restriction enzymes, and Phusion High-Fidelity DNA Polymerase were purchased from New England Biolabs (Canada).DNA sequencing was provided by the Sanger Sequencing Facility at The Centre for Applied Genomics (The Hospital for Sick Children, Canada).

2.2 Plant Propagation and growth conditions

Arabidopsis seeds (ecotype Columbia) were grown in a soil mixture or in sterile culture depending on the requirement of each experiment.

2.2.1 Growth in soil

Seeds (around 100-200) were sown in cell packs in size of 19.5x13x5 cm^3 (length x width x height) containing 1:1 soil mixtures of Sunshine LC1 mix and Sunshine LG3 Germination mix (SunGro Horticultural Inc., USA) that was previously saturated with water; the seeds were stratified at 4^oC in the dark for 48 h, covered by a plastic dome to maintain humidity. Trays containing 6 cell packs were transferred to a growth chamber that provided long-day conditions of 16-h light (150±20 µmol $m^{-2}s^{-1}$photo-synthetically active radiation) and 8-h dark at 22^oC. When the first two true leaves were visible the plastic lid was opened. Plants

were then fertilized with 20:20:20 fertilizer (Plant Products Co. Ltd., Canada) once a week and watered from the top carefully every other day without letting them dry. Seeds were ready for harvesting approximately 7-8 weeks after sowing.

2.2.2 Growth in agar media

Seeds were surface sterilized with chlorine gas as follows. They were placed in open microfuge tubes in a chromatography tank that could be sealed well. A beaker containing 100 mL of 0.5% (v/v) bleach (Javex™) was set beside the seed; chlorine gas was produced by adding 3 mL of concentrated hydrochloric acid to the bleach; the tank lid was closed quickly. The seeds were incubated for a minimum of 1.5 h (Cadenas and Packer, 2013).

The sterile seeds were sown on ½ strength Murashige-Skoog basal medium containing Gamborg's vitamins (Sigma-Aldrich, Canada) supplemented with 0.05% (w/v) 4-morpholineethanesulfonic acid, and 0.8% (w/v) agar, at a pH of 5.7-5.8. The seeded culture plates (140 mm diameter x 20 mm height) were sealed with breathable tape and kept at 4^{o}C in dark conditions for 48 h. Afterwards, the plates were transferred to a tissue culture chamber (TC7, Conviron, Canada) with 16 h light and 8 h dark (50- 80µmol m^{-2} s^{-1}photo-synthetically active radiation) at 20^{o}C.

If needed, seedlings were transplanted into individual pots of 6x6x8 cm^3 containing the soil mixture (Sunshine LC1 mix and Sunshine LG3 Germination mix in 1:1 ratio); they were maintained as described above for soil-grown plants.

2.3 Transformation of *Arabidopsis* with yeast ADE expression constructs

2.3.1 Constructs used to transfer yeast ADE into WT

Three constructs containing the yeast ADE coding sequence were made by Yong Li, a technician in the Moffatt lab prior to my arrival: 1. *UBQ10*$_{pro}$:yeast ADE (*UBQ10*-ADE); 2. *UBQ10*$_{pro}$:tFd-yeast ADE (*UBQ10*-tFd-yeast ADE) and 3. *UBQ10*$_{pro}$:tFd-yeast ADE-GFP (*UBQ10*-tFd-yeast ADE-GFP).

The first construct contained the constitutive promoter *UBQ10* and coding sequence of yeast ADE. The second construct contained an additional transit peptide sequence from *B. sinuspersici* ferredoxin (tFd) to target the ADE polypeptide into chloroplasts. The third construct contained a GFP coding sequence fused to the C-terminus of the tFd-yeast ADE sequence; this construct was designed to verify that the transit sequence was functioning as expected. All three constructs were cloned into the pSAT6 vector and the insert was subcloned into the binary vector pZP (Tzfira et al., 2005) that confers resistance to glufosinatebammonium (Basta) on transformants.

2.3.2 Generation of transgenic plants by the dipping method

The transgenes were introduced using Agrobacterium tumefaciens-mediated transformation via the "dipping" method developed by Clough and Bent (1998). Arabidopsis WT plants were grown for about 4 and half weeks as described in 2.2.1 until they came up with first set of flowers but had not yet set seeds. The Agrobacterium strain GV3101 carrying the plasmids outlined in the previous section were grown overnight with shaking in 3 mL of Luria-Bertani media supplemented with 300 mg/L spectinomycin, 25 mg/L rifampicin and 25 mg/L gentamycin at 28°C. The culture was then added to 250 mL fresh LB media with the same antibiotics and incubated at 28^{o}C until it reached an optical density at

600 nm of 0.8. The culture was centrifuged for 20 min at 5500 g, at 4^{o}C using the SLA1500 rotor of Sorvall Legend XTR centrifuge. The pellet was re-suspended in 5% (w/v) sucrose solution containing 0.05% of Silwet L-77 (Lehle Seeds, USA). The shoot parts of plants were dipped in *Agrobacterium* culture solution for 2 to 3 seconds with gentle agitation. After dipping, the plants were returned to their trays and left in the lab covered for 16 to 24 h to maintain high humidity. The plants were moved to a growth chamber and maintained as outlined in section 2.2.1. T1 seeds were sown in cell packs. When plants were 10 days old, selection for transformants was started by daily spraying with 0.067% (v/v) of the herbicide Wipeout™ (Wilson Laboratories Inc., Canada) that contains Basta. Spraying of Basta was continued for 7 days. The surviving T1 plants were transplanted into individual pots for further research. The seeds of individual T2 lines containing *UBQ10$_{pro}$*:tFd-yeast ADE were grown on ½ strength MS media (as explained in section 2.2.2) supplemented with glufosinate ammonium (Crescent chemicals Co., New York) at 25 µg/ml ratio and lines in which all T3 seeds germinated normally on the selection media were considered to be homozygous for the transgene.

2.4 Detection of the protein expression in transgenic lines

2.4.1 Preparation of crude leaf extracts

A rosette leaf from T1 plants selected by BASTA as described in section 2.4.2 were ground in pre-chilled glass homogenizers (Kontes, USA) with pre-chilled protein extraction buffer (50 mM Tris [pH 7.5], 1 mM EDTA, 8 mM $MgCl_2$, 1 mM PMSF) in buffer to leaf weight 100 µl:100 mg ratio. The lysates were centrifuged at 10,000 g for 10 min at 4^{o}C (F45-24-11 for centrifuge 5415R; Eppendorf Canada Ltd., Canada). The supernatant (crude extract) was used for protein concentration using the Bradford assay (Bradford, 1976) following the manufacturer's instructions using Bovine Serum Albumin (BSA) as the standard.

2.4.2 Detection of protein by immunobloting

Protein samples (prepared as explained in section 2.5.1), 12 µg from each, were loaded and resolved by SDS PAGE as explained in section 2.3.5 and immunoblotted as outlined section 2.3.6 with an anti-αAah1p primary antibody (polyclonal rabbit antibody raised against the N terminal amino acids (# 1-177) of *S. cerevisiae* ADE (a gift of Dr. Ivo Frébort, Biotechnological and Agricultural Research Centre, Hana, Czech Republic).

2.5 Detection of activity of yeast ADE in transgenic lines

2.5.1 Over expression and purification of recombinant yeast ADE

ADE was recovered from *E. coli* BL21 (DE3) cells carrying the vector pET 100 with the *S. cerevisiae AAH1* gene under control of the lac promoter. The plasmid was the gift of Dr. Ivo Frébort, Biotechnological and Agricultural Research Centre, Hana, Czech Republic.

Three mL of overnight culture was used to inoculate 300 mL of LB broth supplemented with 1% (w/v) glucose and 100 µg/mL of ampicillin and grown at 37^{o}C, with shaking at 250 rpm to an optical density of 0.6 when measured at 600 nm. ADE expression was induced with the addition of 0.2 mM isopropyl β-D-thiogalactoside (IPTG) and incubated at 18^{o}C, with shaking at 200 rpm for 16 h. The cells were pelleted by centrifugation at 10,000g for 20 min, resuspended in 2.5% (v/v) lysis buffer (50 mM NaH_2PO_4 [pH 8], 300 mM NaCl, 10 mM imidazole, 0.5% (v/v) Triton X-100, and 10% (v/v) glycerol) and lysed by emulsification (Emulsiflex®-C3, High pressure homogenizer, Avestin Inc., Canada).

The bacterial cells were recovered by centrifugation twice at 20,000 *g*, at 4^{o}C for 20 min and ADE was purified by immobilized metal affinity chromatography. A column of a 1 ml resin (Qiagen, Canada) bed volume was prepared and in a gravity-flow chromatography column

according to the manufacturer's instructions. The column was equilibrated with 5 column volumes of binding buffer (50 mM NaH_2PO_4 [pH 8], 300 mM NaCl, 10 mM imidazole, and 10% (v/v) glycerol) followed by loading of the clarified soluble fraction. After the flow-through was collected, the resin was washed with 20 column volumes of binding buffer and the bound proteins were eluted with elution buffer (50 mM NaH_2PO_4 [pH 8], 300 mM NaCl, 300 mM imidazole, and 20% (v/v) glycerol). The purified protein was concentrated in 1x PBS buffer by ultra-filtration using a Nanosep 10K centrifugal device (Pall Life Sciences, USA). The eluted protein was quantified by Bradford assays (Bradford, 1976) with the Protein Assay Dye Reagent Concentrate (Bio-Rad), based on manufacturer's instructions. Additional 20 µL aliquots of each fraction were prepared, frozen in liquid nitrogen and stored at -80^{o}C for further use as needed. The protein was confirmed by immunoblotting using an anit-αAah1p primary antibody as explained in 2.5.2.

Thereafter, for gel analysis, 20 µl of each stage of the enzyme purification process: before IPTG induction, after IPTG induction, soluble fraction, insoluble fractions, flow through, wash and elutions (with elution buffer with 300 mM imidazole and 500 mM imidazole) were resolved by SDS gel and stained with Coomassie Blue R-250 (0.025% Coomassie Brilliant Blue, 40% methanol, 10% acetic acid). The affinity purified recombinant protein was confirmed by immunoblotting using an anti-αAah1p primary antibody as explained in section 2.5.2.

2.5.2 Enzyme activity assay

2.5.2.1 Assay reagent optimization

The ADE enzyme activity present in recombinant protein preparations and crude extracts of transgenic lines expressing the yeast *AAH1* gene was measured using the coupled enzyme activity assay described by Kamat *et al*. (2011) with slight modifications. This assay involves

a coupled reaction. First, yeast ADE catalyzes the reaction between adenine and PRPP and produces hypoxanthine and ammonia. The produced ammonia then reacts with oxo-ketoglutarate (oxo-ketoglutarate or α-ketoglutaric acid) and oxidizes reduced-nicotinamide--adenine-dinucleotide-phosphate (NADH) into nicotinamide-adenine-dinucleotide-phosphate (NAD^+) with byproducts glutamate and H_2O. The second reaction is catalyzed by glutamate dehydrogenase (GDH). The oxidation of NADH was measured at 340 nm.

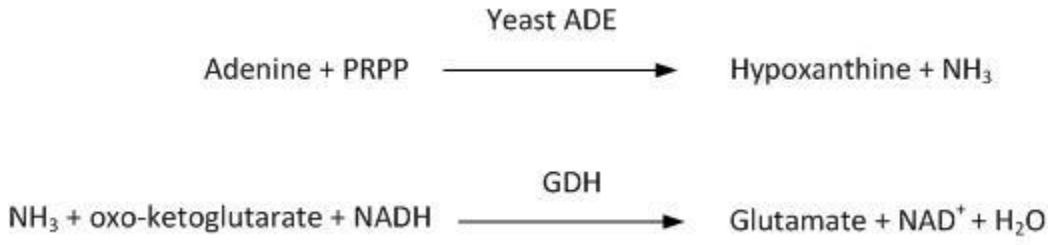

Figure 2-1: Coupled assay of NADH oxidation

Adenine is metabolized to hypoxanthine and ammonia in the presence of yeast ADE. The ammonia and oxo-ketoglutarate oxidize NADH into NAD^+ catalyzed by GDH.

The stock solutions for the assay were prepared as follows: 1.25 mM NADH, 1 M oxo-ketoglutarate, 5 mM adenine and 10 mg/mL GDH were dissolved in 50 mM HEPES (pH 7.5); adenine, oxo-ketoglutarate, and GDH stocks were prepared fresh for each assay. The stocks of 1 M HEPES (pH7.5) and 1.25 mM NADH were stored at 4^oC and -20^oC, respectively. Since NADH can be degraded by light the stock containing tube was covered by aluminum foil. GDH was dissolved by inverting tube gently so as to limit incorporating any air bubbles.

The reaction mixture contained 20 mM HEPES (pH 7.5), 0.25 mM NADH, 25 mM α-ketoglutaric acid as explained in Kamat *et al.* (2011). A Cary 100 UV-Vis spectrophotometer (Agilent Technologies, USA) was used to monitor the oxidation of NADH at 340 nm at 30^{o}C.

Several parameters of the assay had to be established before it was used to assay the ADE enzyme activity in transgenic plant extracts. First, the amount of GDH needed to couple the two reactions was determined by running the assay with 100 mM NH_4Cl in place of adenine for the reaction shown in Figure 2-2 (Robb *et al*. 1992), as amount suggested by Kamat *et al.* (2011), 4 µg/mL, was not enough to maintain the reaction.

$$NH_4Cl + NADH + \text{oxo-ketoglutarate} \xrightarrow{GDH} \text{Glutamate} + NAD^+ + H_2O$$

Figure 2-2: GDH- catalyzed reaction of NH_4Cl, NADH, and oxo-ketoglutarate

NH_4Cl, NADH, oxo-ketoglutarate react together and form glutamate and H_2O while oxidizing NADH into NAD^+. GDH catalyzes the reaction.

To optimize the quantities of each reagent in the assay, the calculated amounts (based on Kamat *et al.* (2011) of HEPES (pH 7.5), NADH, oxo-ketoglutaric acid and distilled water were added into the cuvette and stirred well with a plastic stirrer. After waiting 1-2 minutes GDH was added and the solution was mixed well as described for the previous step. Finally, 5 µl of recombinant yeast ADE (with a concentration of 2.7 µg μl^{-1}) was added to start the reaction.

2.5.2.2 Evaluation of K_M of recombinant yeast ADE for adenine

Since the given K_M value of yeast ADE for adenine reported in Kamat *et al*. (2011) is 55 µM, the assay was started with three lower concentrations (i.e. 20, 30, 40 µM) and five higher concentrations (55, 100, 120, 150, 200, 250 µM) than 55 µM of adenine. Since the range of concentrations with higher values was not enough to reach to a plateau of Michaelis-Menten graph the adenine concentrations were extended up to 700 µM of adenine as shown in Figure 3.6.

2.5.2.3 Assay of ADE activity in crude leaf extracts

After optimization of the reagent quantities, the order that the reagents were added was evaluated. HEPES-KOH (pH 7.5), oxo-ketoglutarate, NADH, and dH_2O were added first followed by GDH, recombinant yeast ADE and, finally, adenine as shown in Figure 3.5. The objective was to detect enzyme activity following the addition of the plant protein crude extract.

Thereafter, the crude leaf extracts prepared from the homozygous transgenic lines were added in place of the recombinant yeast ADE and mixed well. After waiting for 1-2 minutes GDH was added and followed by mixing. I observed a slight oxidation after adding protein crude extract before adding the substrate, adenine. As a solution, the protein crude extracts were desalted by a homemade G-25-Sephadex column as explained in Schoor (2007) (as shown in section 2.6.2.4 and by Nanosep 10K OMEGA centrifugal devices (Pall Life Sciences, Canada).

2.5.2.4 Desalting of protein crude extracts

The Sephadex G25 was soaked in 50 mM HEPES (pH 7.2) overnight (i.e. 1 g of G25 in 5 ml of buffer). The excess buffer was drained off and replaced with fresh buffer. The swollen beads were autoclaved to reduce contamination and stored at 4^{o}C. The column was prepared by adding 1.2 mL of swollen Sephadex to a 1.5 mL microfuge tube and allowing the beads to settle. After marking the level excess buffer was allowed to drain off through a hole which was made at the bottom of the tube by a 28 gauge needle which was as large enough to drain off the solution and small enough to not allow beads to drain out. Then swollen beads were filled in to the tube until the bead level came to previously marked level. Then this column was placed in a small glass test tube (13 x 100 mm). The excess buffer was removed by centrifugation at 13,200 rpm in swinging bucket centrifuge for 15 s at room temperature. Then the column was transferred to a new test tube. After adding 100 µl of protein crude extract the column was centrifuged for 15 min at 13,200 rpm at 4^{o}C.

2.5.2.5 Ammonium sulphate precipitation

2.5.2.5.1 Crude protein extraction

Leaf extracts were prepared in a 4^{o}C cold room to avoid protein denaturation. First, 10 g of leaves of four-weeks-old-plants were ground with 20 mL of protein extraction buffer (50 mM Tris-HCl, 8 mM $MgCl_2$, 1 mM EDTA, 1 mM phenylmethylsulfonyl fluoride) using a prechilled porcelain motar and pestle. To remove the debris, the resulting slurry was centrifuged at 10,000 g for 15 min at 4^{o}C, in a fixed-angle rotor (F45-25-11 for centrifuge 5415R; Eppendorf Canada Ltd, Canada).

2.5.2.5.2 Ammonium sulphate precipitation

Ammonium sulphate precipitation and dialysis were conducted in the 4^{o}C cold room. The required amount of ammonium sulphate was calculated to make the solution 60% saturated using ammonium sulphate calculator provided by Encor biotechnology Inc. (www.encorbio.com/protocols/AM-SO4.htm). Thereafter finely ground ammonium sulphate was added to the protein crude protein extract little by little while stirring on a magnetic stirrer at a speed that did not allow a froth to form. After adding the complete amount of measured ammonium sulphate, the solution was stirred for another 2 hs. The sample was centrifuged at 16,000 g at 4^{o}C for 1 h and the resulting pellet was resuspended in 500 µL of 50 mM HEPES (pH 7.5); the sample was dialyzed to remove ammonium sulphate.

2.5.2.5.3 Dialysis

The resuspended ammonium sulphate precipitate was transferred into a dialysis bag (Spectra/Por®, Canada; molecular weight cut-off of 6-8,000) which was sealed with clips. The volume of the bag was two times larger than that needed for the actual sample size so that there was room to accommodate dilution of the sample. The dialysis bag containing the sample was placed in a beaker containing 200 volumes of 50 mM HEPES (pH 7.5) relative to the sample volume and gently stirred at 4^{o}C. The buffer was replaced twice after 3 h each time and changed a third time for dialysis overnight. The next day the sample was concentrated with a Nanosep 10K centrifugal device.

2.6 Detection of ADE transgenes at gene level

2.6.1 Plant genomic DNA extraction

One mature rosette leaf of a 4-week-old soil grown *Arabidopsis* plant was homogenized in 50 µl of extraction buffer (0.2 M Tris-HCl pH 7.2, 0.25 M NaCl, 0.025 M EDTA, 0.5% (w/v) SDS) in a 1.5 mL microfuge tube with a blue plastic pestle. After homogenization an additional 350 µL of extraction buffer was added to the tube and mixed well by vortexing. Next the homogenate was centrifuged for 2 min at 13,200 rpm following which 300 µL of the resulting supernatant was transferred to a new tube. An equal volume of isopropanol was added and the solution was mixed by invertion. After a 5 min incubation period at room temperature the DNA was pelleted by centrifugation at 13,200 rpm for 5 min and the supernatant was removed. The pellet was air dried and resuspended in 100 µl of PCR-grade water (UV treated milliQ water for 90 sec).

2.6.2 Reverse transcription polymerase chain reaction detection of transgenes

2.6.2.1 RNA extraction

Small-scale RNA extractions were carried out using a chromatography-based kit (BioBasic Inc., Canada) according to the manufacturer's instructions. The RNA work bench was cleaned by RNase ERASE^{TM} (MP Biomedicals LLC, Canada). The microfuge tubes, pipette tips, spatulas, and plastic pestles were autoclaved and cleaned with RNase ERASE^{TM} prior to use.

Fifty mg of expanded leaf tissue from each 4- to 5-week-old plant analyzed where added to a 1.5 ml microfuge tube and ground thoroughly with a plastic blue pestle. Next, 450 µL of Rlysis-PG buffer was added to the tube and mixed with the sample by inverting the tube; it

was incubated at room temperature for 5 min to make sure all the cells were lysed. After incubation the sample was centrifuged at 12,000 g for 5 minutes in a fixed-angle rotor (F45-24-11 for centrifuge 5415R; Eppendorf Canada Ltd., Canada) at RT (24^{o}C) and 400 µL of the supernatant was transferred to a new tube. Next, 200 µl of ethanol was added and the sample was mixed by inversion. The solution was transferred to the spin column, centrifuged at 12,000 g for 30 seconds at RT using the fixed-angle rotor and flow-through was discarded.

The column was washed by the addition of 0.5 mL of pre-chilled Universal GT solution followed by centrifugation at 12,000 g for 30 seconds at RT in a fixed-angle rotor; the flow through was discarded. Next, 0.5 mL of Universal NT solution was added and centrifuged at 12,000 g for 30 seconds and the flow through was again discarded. Thereafter centrifugation was repeated at 12,000 g for 30 seconds at RT to remove any residual ethanol. Then the column was put to a new centrifuge tube, 30 µL of RNase free water was added and kept at RT for 2 minutes. The column was placed in a new microfuge tube and centrifuged at 12,000 g for 30 seconds at RT in fixed-angle rotor and analyzed the concentration of RNA by a Nanodrop.

2.6.2.2 Evaluation of RNA quality

The integrity of the RNA samples was evaluated by denaturing agarose gel electrophoresis. The gel comb and tray which were stored in 3% (v/v) H_2O_2; these were rinsed with diethylpyrocarbonate (DEPC) treated water and cleaned with RNase ERASE^{TM} before use. All the glassware was wrapped in foil and baked to kill RNase prior to use. The gel was prepared by mixing 5 mL of 0.2 M3-(N-morpholino) propanesulfonic acid, 44 mL of DEPC-treated water and 0.74 g of agarose were microwaved for 1-2 min, until the agarose was

thoroughly dissolved; 600 µL of formaldehyde was added once the solution had cooled to 50^{o}C.

To evaluate the quality of the RNA samples, 2.5 µg of each was mixed with 2x loading dye and the volume made up to 20 µL with DEPC-treated water. The samples were heated at 70^{o}C for 15 minutes, followed by 5 minutes chilling on ice. The samples were loaded onto the gel and electrophoresed at 80-100 V for 20-30 minutes. The pattern and intactness of the ribosomal RNAs was evaluated under UV light using a gel documentation system by analysing the first (28S) and second (18S) rRNA bands. The 28S rRNA band was expected to be approximately twice as intense as the 18S rRNA band.

2.6.2.3 cDNA synthesis and RT PCR

Each RNA sample (1-2 µg) was mixed with 1 µL of 10x TURBO DNase buffer, 1 µL of TURBO DNase (Ambion, Canada), and the volume made up to 20 µL with RNase-free water; the mixture was incubated at 37^{o}C for 1 h and then chilled on ice for 5 min. The DNase reaction was stopped by the addition of 6 µL of well-mixed DNase inactivation reagent followed by a 2 min incubation at RT. The 10 µL sample was collected by a short centrifugation and mixed with 1 µL of AnchorT primer mixture (100 µM), and 1 µL of dNTP mix (10 mM). The mixture was heated at 65^{o}C for 5 minutes and chilled on ice for 5 minutes. The contents in the tubes were collected by centrifugation before the addition of 4 µL of 5x First-strand buffer, 2 µL of 0.1 M dichlorodiphenyltrichloroethane followed by gentle mixing and incubation at 42^{o}C for 2 minutes. Thereafter 1 µL of Superscript^{TM} II RT (Ambion, Canada) was added and mixed in by gently by pippetting the solution. The mixture was incubated at 42^{o}C for 1 h and then inactivated by heating at 70^{o}C for 15 minutes. The cDNA samples were stored at -20^{o}C.

One µL of yeast ADE was PCR amplified using the AdedeaF and AddeaR primers using the cycle conditions: 94°C 4:00 min, 36 cycles of 94°C 30 sec, 52°C 30 sec, 72°C 1:15 min, and final elongation of 72°C 10 min.

Table 2: Primers used in the study

Name	Sequence (5' to 3')	T_m (^oC)
AdedeaF	GAG CAT CAC TTG CAT TTG GAA GG	56
AdedeaR	GAC TAC TTC GTC CAC TCT ACT TAA C	54
AdedeaNF	CTA AAT AGG TCG AGG AAT TAA ACG	55
AdedeaNR	GGC GTT CTT AGC GAT ACG ACC	56
pJET1.2 F	CGA CTC ACT ATA GGG AGA GCG GC	60
pJET1.2 R	AAG AAC ATC GAT TTT CCA TGG CAG	56
Actin2F	CCG ATG GTG AGG ATA TTC AGC C	56
Actin2R	TGT CAC GGA CAA TTT CCC GTT CTG C	60

2.7 Detection of APT1.1 localization by chloroplast subfractionation

The whole chloroplast subfractionation was done according the method explained in Lung (2012).

2.7.1 Isolation of *Arabidopsis* protoplasts

The methods for the isolation of protoplasts and chloroplast subfractions are based on a protocol reported by Yoo *et al*. (2007) and subsequently adapted by Lung (2012).

Enzyme buffer was prepared by incubating CS-mannitol buffer (0.4 M mannitol, 20 mM MES-KOH (pH 5.7), 20 mM KCl) at 70^{o}C for 10 minutes to degrade all the proteases if they were present. After cooling the solution to 55^{o}C, 1.5% (w/v) cellulase R-10 and 0.4% (w/v) macerozyme R-10 (Yakult Pharmaceutical, Japan) were added and incubated at 55^{o}C for 10 min. The solution was cooled further to room temperature before adding 0.1% (w/v) bovine serum albumin and 10 mM $CaCl_2$. Around 30 leaves from 2-to 3–week-old plants grown in cell packs were cut into 0.5-1 mm strips with double-sided razor blades. The strips were floated on 10 mL of enzyme buffer in a 115 mm diameter petri plate and vacuum infiltrated for 10 min. They were then kept in the dark at room temperature to continue the enzymatic digestion of the cell wall for 3 h. The resulting slurry of protoplasts was filtered by pouring the mixture slowly through a piece of 100 µm nylon mesh (Spectrum Lab Inc., USA). The filtrate was mixed with an equal volume of HS buffer (50 mM 4-[2-hydroxyethyl]-1-piperazineethanesulfonic acid-KOH (HEPES-KOH) (pH 7.3), 330 mM sorbitol) by gentle swirling in a 50 mL Falcon tube and protoplasts were collected by centrifugation at 100 g for 2 min using a fixed-angle rotor (F45-24-11 for centrifuge 5415R; Microfuge Canada Ltd., Canada). The supernatant was aspirated off by a pippette. The protoplast pellet was resuspended in 2 mL of HS buffer by gentle swirling.

The number of intact protoplasts was determined using a haemocytometer. The volume calculated to contain 50,000-60,000 protoplasts was measured and centrifuged at 100 g for 2 min. The resulting pellet of intact protoplasts was resuspended in 25 µL of solubilization buffer (50 mM Tris-HCl (pH 8), 5 mM ethylenediaminetetraacetic acid [EDTA] and 0.2% (w/v) Sodium dodecyl sulfate [SDS]), centrifuged at the 13,200 rpm at 4^{o}C for 15 minutes in a fixed-angle rotor (F45-24-11 for centrifuge 5415R; Microfuge Canada Ltd., Canada) to lyse the protoplasts and bring all the soluble and membrane proteins into the buffer; the supernatant (the total soluble protoplast fraction) was subsequently analyzed by immunoblotting.

2.7.2 Lysis of protoplasts

The remaining protoplasts were resuspended in HS buffer and lysed by passing the mixture through a layer of 10 µm nylon mesh using a home-made protoplast-rupturing device. The protoplast-rupturing device was made by cutting off the needle-fitting end of a 1 mL syringe barrel and the top part of a 0.5 mL microfuge tube to form a hollow tube and a slightly wider adaptor ring, respectively. Then a piece of 10 µm nylon mesh filter (Spectrum Lab Inc., Canada) was laid against the cut end of the hollow tube and held in place using the adaptor ring.

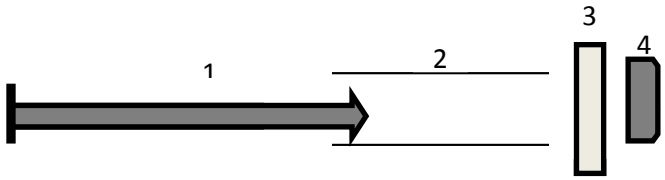

Figure 2-3: Filtering setup to break protoplasts

Home-made setup prepared for lysing protoplasts. A piece of nylon mesh was fitted between the adaptor ring, made by cutting the top part of 0.5 mL microfuge tube and needle-fitting end of a 1 mL syringe barrel. 1: Plunger, 2: 1 mL Syringe barrel, 3: nylon mesh (10 µm) and 4: Adaptor ring.

Thereafter, the protoplast suspension was transferred into the protoplast-rupturing device and forced through the mesh with the plunger slowly. All the subsequent steps were carried out in the cold. Approximately 50,000 protoplasts can be passed through one piece of mesh before it needs to be changed.

2.7.3 Percoll gradient purification of chloroplasts

The chloroplasts were isolated by density sedimentation through Percoll gradients containing 40% (v/v) and 85% (v/v) Percoll. Around 1 mL of lysed protoplast suspension was layered on 4 Percoll gradients (as 250 µL in each gradient) containing 500 µL of 40% upper Percoll solution (40% (v/v) Percoll, 50 mM HEPES-KOH (pH 7.3), 330 mM sorbitol, 1 mM $MgCl_2$, 1 mM $MnCl_2$ and 2 mM EDTA) and 500 µL of 85% lower Percoll solution (85% (v/v) Percoll, 50 mM HEPES-KOH (pH 7.3) and 330 mM sorbitol). The gradients were centrifuged at 2,000 g, at 4^{o}C for 10 min in a swinging-bucket rotor (A-8-11 for refrigerated centrifuge 5417R; Eppendorf Canada Ltd., Canada). After centrifugation, the intact chloroplasts located at the 40%/85% Percoll interface were aspirated with a pasture pipette, and each aliquot was diluted with 6 volumes of ice-cold HS buffer. The four suspensions were centrifuged at 750 g, 4^{o}C for 5 min to collect the intact chloroplasts.

Out of four pellets one pellet was resuspended in 25 µL of solubilization buffer, and centrifuged at the 13,200 rpm at 4 ^{0}C for 15 min in a fixed-angle rotor (F45-24-11 for centrifuge 5415R; Eppendorf Canada Ltd., Canada). The supernatant was resolved by SDS

polyacrylamide gel electrophoresis (PAGE) and subsequently immunoblotted as the total chloroplast fraction.

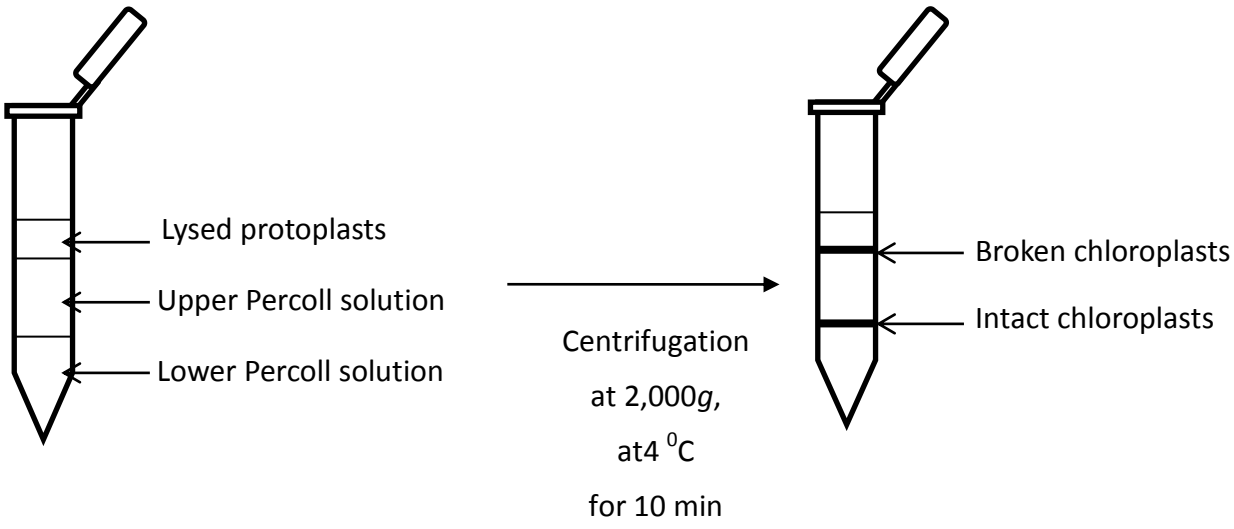

Figure 2-4: Percoll gradient purification

After centrifugation the lysed protoplasts with 40% upper and 85% lower Percoll gradient, the intact chloroplasts accumulated as a layer at the 40%/85% interface

2.7.4 Chloroplast subfractionation into membrane and stromal fractions

The remaining three pellets out of the total of four were pooled with 5.3 volumes of ice-cold 2mM EDTA and incubated on ice for 10 min. Then 1/16 volume of 4 M NaCl was added and the mixture centrifuged at the 13,200 rpm for 30 min at 4^{o}C in a fixed-angle rotor (F45-24-11 for centrifuge 5415R; Microfuge Canada Ltd., Canada). The resulting supernatant and the pellet were recovered separately.

To extract the proteins from stroma fraction, the recovered supernatant was mixed with 4 volumes of ice-cold acetone and incubated at -20^{o}C for at least 1 h and centrifuged at 13,200 rpm for 15 min at 4^{o}C in a fixed-angle rotor (F45-24-11 for centrifuge 5415R; Microfuge Canada Ltd., Canada). Next, the supernatant was removed as much as possible and placed in a Speed Vac for 10 min to remove acetone completely. The pellet was resuspended in 25 µL of solubilization buffer, centrifuged at the 13,200 rpm at 4^{o}C for 15 min in a fixed-angle rotor. The resulting supernatant was saved for immunoblot analysis as the chloroplast-stromal fraction.

2.7.5 Sodium Dodecyl Sulfate Polyacrylamide Gel Electrophoresis

SDS-PAGE was used to separate proteins in samples. SDS-PAGE was done with samples subfractionated as explained in sections from 2.3.1 to 2.3.4. Protein samples were analyzed in duplicate (except recombinant APT1) in two gels; the proteins resolved in gel1 were incubated with anti-APT1 antiserum and the proteins resolved in gel2 were incubated with antiserum recognizing Rubisco large subunit (anti-RbcL) or the PSI-D subunit of photosystem I (anti-PsaD). As my objective was to see if APT1 is presence in each fraction or not I did not quantified the samples. Protein samples (WT-IP, WT-IC, WT-M, WT-S, *oxt1*-IP and overexpressed recombinant APT1) were boiled with 1x SDS sample buffer (2% (w/v) SDS, 30% (v/v) glycerol, 72 mM Tris–HCl (pH 6.8), 0.12% (w/v) bromophenol blue and 6% (v/v) β-mercaptoethanol) for 5 min, and resolved by electrophoresis through polyacrylamide gels (12 % separating gel (2.5 mL of 0.375 M Tris-HCl (pH 8.8), 3 mL of 30% (w/v) acrylamide, 100 µL of 10% (w/v) SDS, 100 µL of 10% (w/v) ammonium persulphate and 10 µL of TEMED) and 5% stacking gel (312.5µL of 1M Tris-HCl (pH 6.8), 400 µL of 30% (w/v) acrylamide, 25 µL of 10% (w/v) SDS, 1.75 mL of distilled water, 2.5 µL of TEMED and 25 µL of 10% (w/v) ammonium persulphate) along with a pre-stained protein marker (Spectra^{TM} multicolor broad range protein ladder, Thermo Scientific, #26634). The samples were electrophoresed

at 60 V until the bromophenol blue entered the separating gel, after which the voltage was increased to 80 V until loading dye had just migrated off the end of the gel. In the case of resolving the APT1.1 and 1.2 polypeptides separated, the samples were electrophoresed longer (20 min after 15 kDa polypeptide marker migrated off the end of the gel).

2.7.6 Western blot analysis

Resolved proteins were transferred from SDS gels to nitrocellulose membranes in transfer buffer (48 mM Tris, 190 mM glycine, 0.0375% (w/v) SDS, and 20% (v/v) methanol) at RT using 20 V, 150 mA (constant current) for 45 min using a Trans-Blot Semi-Dry Electrophoretic Transfer Cell (Bio-Rad).Before the immunoblotting stage, the total protein on the membrane was stained with 0.2 % (w/v) Ponceau S prepared in 3 % (w/v) trichloroacetic acid). The membrane from gel 2 was cut in half, at the position of 50 kD marker. Next, the membranes were washed with phosphate buffered saline-Tween (PBS-T) buffer (1% (w/v) nonfat dry milk powder, 0.3% (v/v) Tween-20 in phosphate buffered saline), and blocked with 0.1% (w/v) polyvinyl alcohol in PBS for 30 seconds. After that, membrane 1 was incubated withanti-APT1 antiserum (diluted 1:5,000) (Facciuolo 2009). While the upper part of membrane 2 was incubated with anti-Rubisco large subunit antiserum (RbcL; diluted 1:7,500) (anti-APT1 and anti-RbcL were purified by previous lab members from Moffatt lab), the lower part of the membrane was incubated with an antibody specific for PSI-D subunit of photosystem I (1:5,000) (Agrisera, Canada) (dilutions based on Lung, 2012) which was diluted in PBS-T overnight at 4°C on a shaker.

After washing the membrane with PBS-T (3 times, 10 min minimum each wash), each membrane was incubated with an alkaline phosphatase-conjugated secondary antibody (anti-rabbit IgG, 1:10,000; Sigma-Aldrich) for 2 h at room temperature with shaking. After incubation and washing with PBS-T as described above, the membrane was placed in a plastic wrap envelope and incubated with Amersham ECL solution (250 µL of solution A and

6.25 µL of solution B for one membrane of 8x5 cm; (GE Healthcare, Canada) for 7 min. The membrane was placed in fresh plastic wrap and exposed to Amersham Hyperfilm ECL film (GE Healthcare, Canada), in the dark. The luminescent signal was revealed using a CP1000 photodeveloper (AGFA, Pointe Claire, Canada) and scanned as a digital image.

2.8 Detection of *UBQ10pro*:tFd-yeast ADE-GFP in transgenic lines

2.8.1 Detection the expression of *UBQ10pro*:tFd-yeast ADE-GFP by confocal microscopy

Fresh leaves from each plant line, mounted on slides with water were used as samples. GFP fusion protein expressions were visualized by confocal laser scanning microscopy (Carl Zeiss LSM 510; Jena, Germany). GFP was imaged using the excitation of an argon ion laser of 488 nm with a 505/530 nm bandpass filter. Visualization of chlorophyll autofluorescence was done using an optical filter, LP650, with excitation and emission wavelengths of 488 nm and 650 nm, respectively. Images were acquired using a 63X objective lens at a digital resolution of 64.3 x (zoom 1, 2 and 5).

The transgene was further analyzed by immunobloting as described in section 2.3.5 and 2.3.6 with the anti-αAah1p antiserum (diluted 1:10,000), and with an anti-GFP antiserum (diluted 1:4,000) (courtesy of Dr. Chuong and Dr. Lung, University of Waterloo, Canada). Both antisera were raised in rabbits.

2.9 Fixation of Arabidopsis leaf tissues

(Modified from the protocol explained in Lung, 2012 and based on personal communications with Dr. Chuong and S. Schoor, University of Waterloo)

For this experiment the second rosette leaf of 3 week-old plants of WT, *oxt1* and $APT1_{pro}$:Ex1–GFP were used. The leaves were cut into pieces of 2 mm thickness and dipped

in 1 mL of 0.02 M sodium phosphate buffer, pH 7.2 (prepared by mixing 28 mL of 0.2 M monobasic sodium phosphate and 72 mL of 0.2 M dibasic sodium phosphate) in microfuge tubes. The tissues in buffer were vacuum infiltrated for 4 min. Next, the tissues were fixed by dipping in a mixture of 0.1% (v/v) gluteraldehyde and 2% (v/v) paraformaldehyde and left on a rotator at 4^{o}C overnight. The next day the tissues were washed in 0.02 M sodium phosphate buffer by replacing the buffer four times (for 10 min in each time). Next the tissues were dehydrated in an ethanol series: 10%, 25%, 50%, 75% and 95%. The tissues were left in each solution for 2 hs with the first 30 min in each step being done in a vacuum infiltrator to facilitate the infiltration of ethanol into leaf tissues. After dehydrating the tissues in the series of ethanol concentrations the tissues were left in 100% ethanol at 4^{o}C overnight.

On the following day the dehydrated tissues were carried through a series of LR White as follows,

LR white : Ethanol ratio	duration
25% : 75%	2 h
50% : 50%	2 h
75% : 25%	2 h
100%: 0	overnight and then 1 h the following morning

To begin the embedding 100% LR White was poured into gelatin capsules (Electron MS, Canada) and individual leaf tissues were. The capsules were incubated at 65^{o}C for 48 hs to allow for polymerization.

Chapter 3

Results

The apt1 mutants, *oxt1* and *apt1-3,* have an increased content of adenine and are more oxidative stress tolerant than WT plants (Facciuolo 2009; Sukrong *et al.* 2012). The adenine content in *oxt1* chloroplasts is 12-times higher (i.e. 24 pmolesµg-1 chlorophyll) than in WT chloroplasts (Sukrong *et al.* 2012; Shkolnik 2009). The studies of these two mutants by Facciuolo (2009), Sukrong *et al.* (2012), and Shkolnik (2009), led to the hypothesis that the increased adenine content in *apt1* mutant chloroplasts underlies their oxidative stress tolerance. The first part of this thesis outlines how I introduced an ADE coding sequence into *Arabidopsis* plants and tested whether the transformants could be used to test this hypothesis.

The second part of my research focused on determining the subcellular localization of native APT1.1 in WT *Arabidopsis* plastids.

3.1 Developing a system to enzymatically reduce plastid adenine content in *Arabidopsis*

3.1.1 Expression of yeast ADE in WT *Arabidopsis*

ADE hydrolyzes adenine to hypoxanthine and ammonia (Brenda, 2013). There is no gene annotated to encode ADE in the *Arabidopsis* genome but this activity is well characterized in yeast species (Pospisilova *et al.* 2008). In NCBI BLAST search I could found adenosine deaminase and adenosine deaminase like proteins but ADE. Yeast ADE has a molecular weight of 39 630 Da making it relatively easy to clone and detect. A spectrophotometric enzyme assay to monitor its activity has been described (Escusa *et al.* 2006). In fact,

previous researchers had expressed the enzyme in *E. coli* and antibodies are available to detect its expression (Pospisilova *et al*. 2008).

Taken together these factors led Dr. Moffatt to propose that the yeast ADE gene could be used to lower the adenine content enzymatically in *Arabidopsis* if it was expressed using a plant promoter. The N-terminus of the ADE coding sequence was fused to a plastid targeting sequence so the enzyme would be imported into chloroplasts. A graduate student in Simon Chuong's lab at the time, Terry Lung, identified an effective targeting sequence of 32 bp from the ferredoxin gene of *Bienertia sinuspersici* (Lung, 2012); he made this sequence (tFd) available to me for the ADE expression in *Arabidopsis*. Three different constructs were prepared for this project; all were expressed from the constitutive *UBQ10* promoter (Grefen *et al.* 2010; Table 3). The first consisted of only the *UBQ10* promoter upstream of the coding region of the yeast *Aah1* gene ($UBQ10_{pro}$:yeast ADE). The second construct included the tFd transit sequence added in-frame to the ADE sequence ($UBQ10_{pro}$:tFd-yeast ADE). To make sure that the tFd sequence was functioning correctly, the coding region for GFP was added downstream of the ADE sequence in $UBQ10_{pro}$:tFd-yeast ADE thereby creating $UBQ10_{pro}$:tFd-yeast ADE-GFP.

Table 3: The constructs used to transform yeast ADE into WT plants

All clones were created in the pSAT6 backbone (Tzfira, 2005) and subsequently the insert was recloned into pZP which confers BASTA resistance on transformed plants.

Strain Number	Vector backbone	Insert
1938	pSAT6	*UBQ10*$_{pro}$:yeast ADE
1939	pSAT6	*UBQ10*$_{pro:}$tFd-yeast ADE
1940	pSAT6	*UBQ10*$_{pro}$:tFd-yeast ADE-GFP

These clones were created by previous members of the Moffatt lab before my arrival. I transferred them into *A*. *tumefaciens* and introduced them into Arabidopsis using the floral dipping method (Zhang *et al.* 2006). T1 transformants with one of the above three constructs were recovered. Transformants with *UBQ10*$_{pro:}$tFd-yeast ADE and *UBQ10*$_{pro:}$tFd-yeast ADE-GFP were used in further experiments in this study. The seeds transformed with *UBQ10*$_{pro:}$yeast ADE were not used in this study, although they were developed until F2 generation.

Thirty-two phenotypically normal lines transformed with the *UBQ10*$_{pro:}$tFd-yeast ADE transgene were recovered by BASTA selection. Sixteen of these lines were randomly selected and used to evaluate the expression of the transgene by immunoblotting. Crude leaf extracts of four-week-old plants were resolved by SDS-PAGE and blotted to a nitrocellulose membrane. The membrane was incubated with an antibody (αAah1p) raised

against recombinant ADE from *S. cerevisiae* (Pospisilova *et al*. 2008). Eleven plant extracts of the 16 tested showed evidence of antibody binding to a polypeptide of ~40 kDa, consistent with expression of yeast ADE (data not shown). All the 16 plants were retested; Figure 3.1 shows the results of this analysis for ten of the lines.

As I used a polyclonal antibody for the experiment (i.e. α-Aah1p), and the antiserum may bind to epitopes originating in polypeptides in addition to yeast ADE, it was not completely unexpected that there was evidence of antibody binding to multiple polypeptides in addition to the expected yeast ADE band at 40 kDa. Two of the strongest unidentified polypeptides observed were 63 and 29 kDa. These two non-specific bands were present in the WT extracts, as well. However, the 40 kDa band suspected to be ADE was not seen in WT samples (compare Figure 3.1 lanes WT and 3). Although this analysis does not unequivocally identify the 40 kDa polypeptide as ADE, it will be referred to as ADE for the remainder of this thesis.

Assuming these T1 lines to be heterozygous for the transgene, it was necessary to recover homozygous progeny for the consistency of the subsequent experiments. Plant lines #6 and #13, which are analyzed in lanes 4 and 9, respectively in the blot shown in Figure 3.1, were selected for further studies. They appeared to express the 40 kDa polypeptide at high and moderate abundance, respectively. These T1 plants were allowed to self-fertilize and the resulting T2 seed were reselected on BASTA. As shown in Figure 3.2 nine individual T2 plants of each line were grown and their progeny seeds (T3 generation) were germinated on BASTA-supplemented media. If all the T3 seeds tested were BASTA resistant, the line was assumed to be homozygous for the yeast ADE transgene. The lines hereafter referred to as homozygous lines 1 and 2 for *UBQ10*$_{pro}$:tFd-yeast ADE, were used for the rest of the studies.

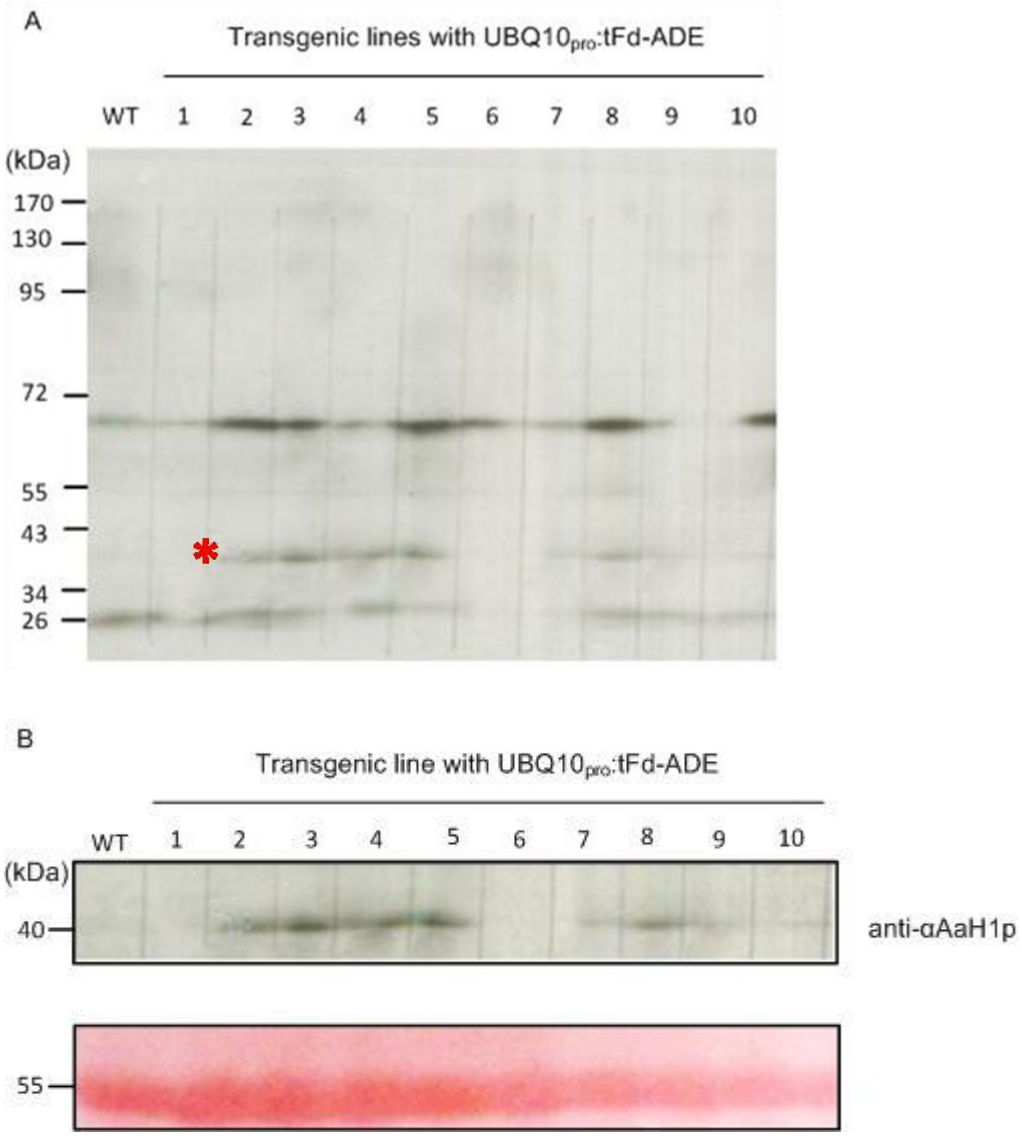
A
Transgenic lines with UBQ10pro:tFd-ADE
WT 1 2 3 4 5 6 7 8 9 10
(kDa)
170
130
95
72
55
43
34
26
*
B
Transgenic line with UBQ10pro:tFd-ADE
WT 1 2 3 4 5 6 7 8 9 10
(kDa)
40
anti-αAaH1p
55

Figure 3-1 Detection of yeast ADE in T1 plants transformed with *$UBQ10_{pro}$*:tFd-yeast ADE

Western blot analysis using the anti-αAaH1p antibody (1:10,000) to detect expression of the yeast ADE (40 kDa) in crude leaf extracts of ten (1 to 10) independent BASTA-resistant T1 lines recovered from an *Agrobacterium*-mediated transformation of WT with *$UBQ10_{pro}$*:tFd-yeast ADE. The quantity of protein that loaded in each lane was 12 µg. A WT protein crude extract was used as the negative control (WT lane). In addition to ADE band at 40 kDa, two other polypeptides of approximately 63 and 29 kDa were observed. These two non-specific bands were seen in the WT extracts, as well while ADE band was not. Samples were resolved by 10% SDS-PAGE and the bound antibody was detected using a rabbit secondary antibody conjugated to HRP. Exposure time was 2 minutes. A: the whole blot, ADE band of 40 kDa has shown with a red star; B: the 40 kDa region of the membrane shown in A and the 50 kDa region of same membrane stained with Ponceau to reveal the presence of RbcL to evaluate the consistency of the protein loading.

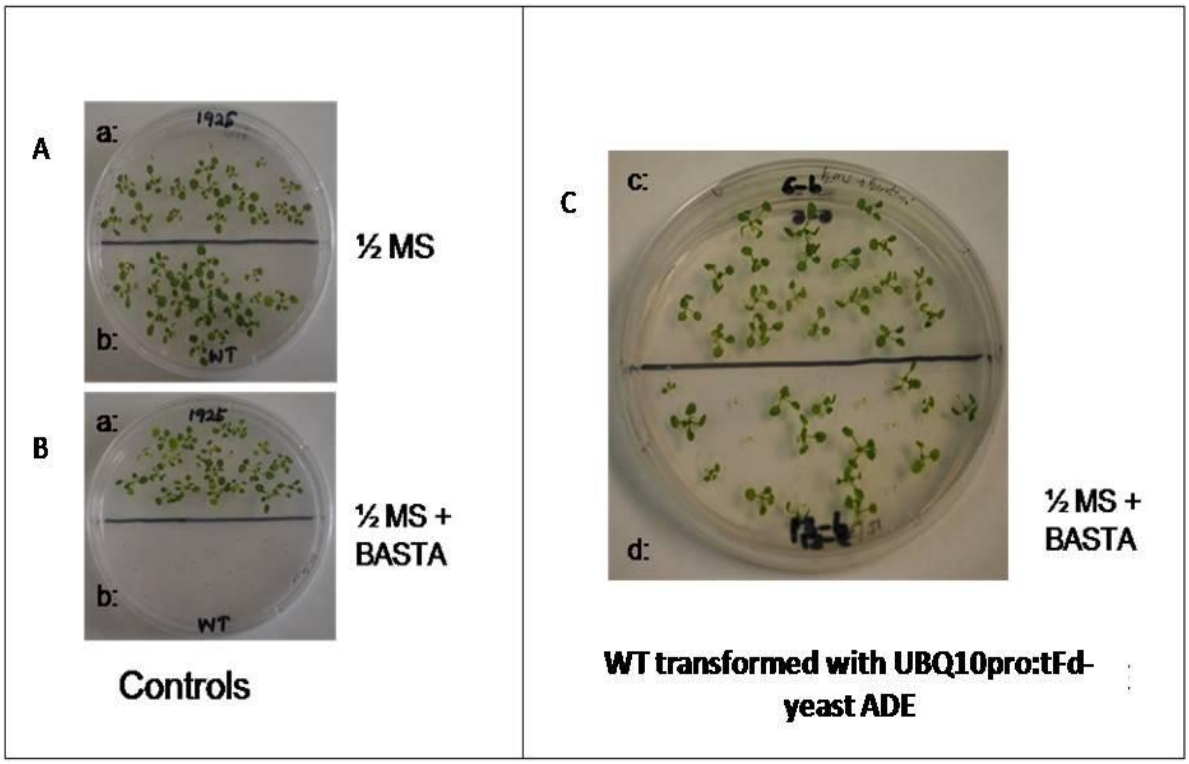

Figure 3-2: Selection of homozygous *UBQ10*$_{pro}$:tFd-yeast ADE transformants

T3 seeds from nine individual T2 plants were germinated on BASTA-supplemented media to identify those that were not segregating for BASTA resistance and thus homozygous for the transgene. A, B control lines, grown in ½ MS medium and ½ MS supplemented with BASTA as indicated. a: BASTA-resistant line; b: WT; C: Two representative T3 lines transformed with *UBQ10*$_{pro}$:tFd-yeast ADE germinated on 1/2 MS medium supplemented with BASTA. c: a non-segregating homozygous T3 line; d: a segregating T3 line.

3.1.2 Detecting the presence of the yeast ADE transgene in *UBQ10$_{pro}$*:tFd-yeast ADE transformants

Having detected what I interpreted to be a specific protein consistent with ADE in the transgenic *UBQ10$_{pro}$*:tFd-yeast ADE lines, I looked for evidence that the transgene was intact and was being transcribed. Plant genomic DNA was extracted from leaves and used as a template for PCR assays designed to detect the full-length coding region of yeast ADE. The yeast ADE full-length CDS (987 bp) was detected in genomic DNA of the *UBQ10$_{pro}$*:tFd-yeast ADE transgenic lines as shown in Figure 3-3; this product was not detected in reactions containing WT DNA as the template.

The presence of the expected transcript was next assayed using cDNA templates from the same transgenic lines. These PCRs produced three distinct products: ˜1000 bp, ˜900 bp, and ˜400 bp. While the signal for the putative full-length CDS fragment (˜1000 bp) was faint, the signal for the shortest band was the strongest. The relative abundance of each fragment was estimated using ImageJ (imagej.nih.gov/ij/) software; the ˜900 bp and ˜400 bp fragments were 1.7 and 34.9 times more abundant than the ˜1000 bp fragment.

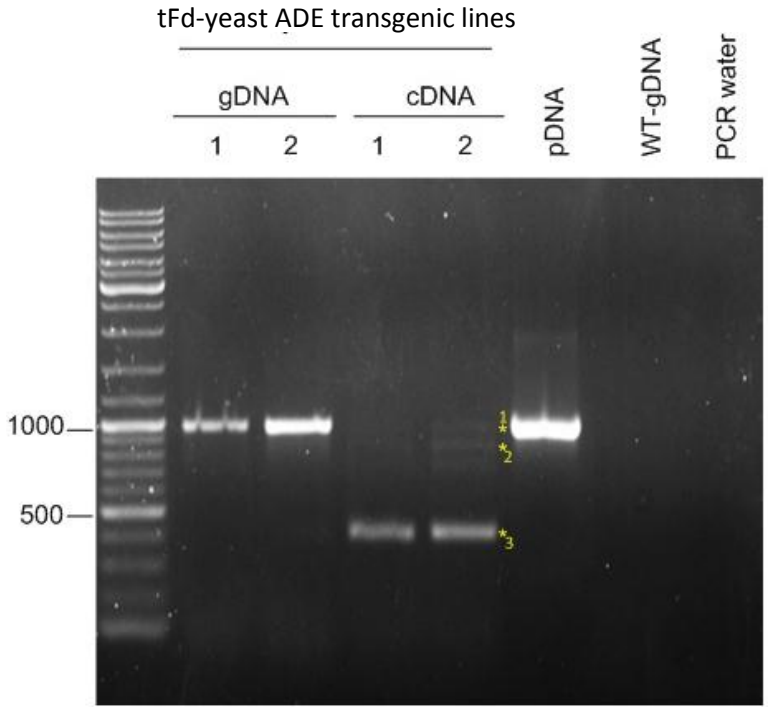

Figure 3-3: Expression of *AHH1* transgene in transgenic plants containing *UBQ10*$_{pro}$:tFd-yeast ADE

Products of PCR reactions using either genomic or cDNA from lines homozygous for *UBQ10*$_{pro}$:tFd-yeast ADE. The fragment corresponding to full-length yeast ADE insert (˜1000 bp) was seen in gDNA of both lines similar to size present in the positive control (pSAT-*UBQ10*$_{pro}$-tFd-yeast ADE plasmid DNA). Three fragments, fragment 1, 2 and 3, presented in cDNA were 1000 bp, ˜900 bp and ˜400 bp in size, respectively.

The sequence of fragment 2 was analyzed by restriction mapping (Figure 3.4), and later by PCRs using both nested primers and flanking primers (Figure 3.5 A). While fragment 2 was amplified with both flanking and nested primers, fragment 3 was amplified only with

flanking primers. The positions of the flanking primers and nested primers on the yeast ADE CDS are shown in Figure 3.5 B.

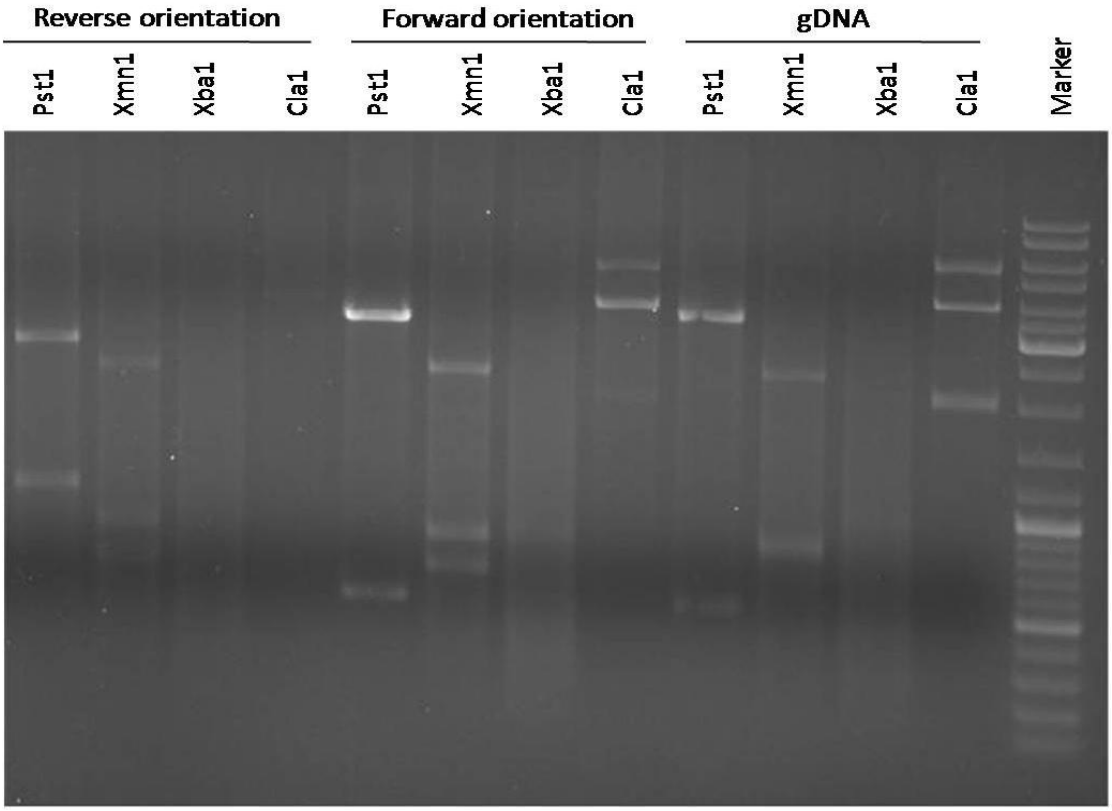

Figure 3-4: Restriction mapping of fragment 2 in pJET1.2, and gDNA

Restriction mapping of fragment 2 cloned in to the vector pJET1.2 in the forward and reverse orientations. Genomic DNA of a transgenic line with *UBQ10*$_{pro}$:tFd-yeast ADE was used the positive control. Restriction digestions were done using PstI, XmnI, XbaI and ClaI. The XbaI digests were not successful.

A

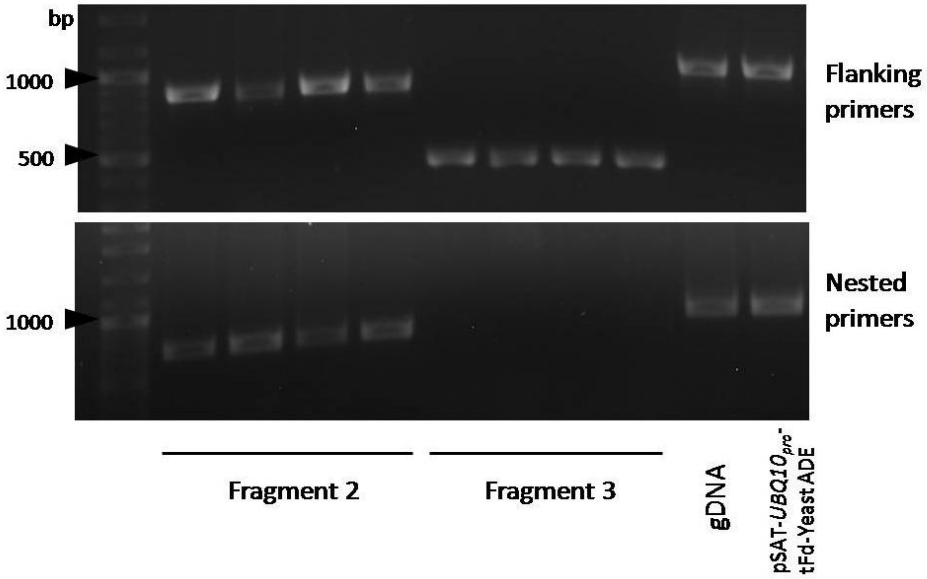

B

1

Atggtttctgtggagtttttacaggagttaccaaaatgtgagcatcacttgcatttggaaggtactctagaacctgacctattgttcccattagcta

3

aaagaaacgatataattctacctgaaggttttcctaaatcggtcgaggaattaaacgaaaagtataagaagtttcgtgatctgcaggatttcttag

attactattatattggtactaatgtcttgattagtgaacaagatttctttgatttggcgtgggcctattttaaaaaagttcacaaacaaggcttggtc

catgctgaagtgttttacgaccctcagtcacatacatctaggggcatctccatagaaacagtcactaaaggtttccaaagagcttgtgacaaagc

cttctctgaatttggtattacatccaagctaattatgtgtctgttaagacacattgaaccagaggaatgtttgaaaactatcgaagaagctacccc

atttattaaagatggtactatctctgccttaggattagattctgctgagaaaccatttcccccacatttatttgttgaatgttacggaaaggccgcct

cattgaataaagatttaaaactaactgcacacgcaggtgaagaaggccccgctcaattcgtctcggatgctttagacttgttgcaagtaacaaga

atcgatcacggtatcaacagtcaatacgacgaggagttattggataggttgtcgcgcgaccagaccatgctaactatttgtcctctctccaacgtg

aagctacaagtagtccaatccgtttcagagttaccactacaaaagtttcttgacagagatgttccattttctttaaattctgatgaccccgcctatttt

ggtggttatatcttagatgtctacactcaagtttcgaaagatttcccacactgggaccatgaaacatgggggtcgtatcgctaagaacgccattaaa

4

ggttcatggtgtgacgataaaagaaagaacggtttgttaagtagagtggacgaagtagtcactaaatattcgcattag

2

Figure 3-5: Amplification of fragment 2 and 3 with flanking and nested primers

A: Gel image of PCR products of yeast ADE CDS amplified with flanking and nested primers. Fragment 2, fragment 3, genomic DNA isolated from two homozygous lines, Lines 1 and 2, as well as pSAT-*UBQ10*$_{pro}$:tFd-yeast ADE (positive control) were resolved by electrophoresis through a 1% (w/v) agarose gel. Two replicates were done for each line. The gel was stained by 0.005% (v/v) Safeview. No amplification of fragment 3 was observed using the nested primers. B: The location of primer binding to the yeast ADE CDS used in the transformation experiments; 1 and 2: the text highlighted in red represent the forward and reverse primers, 3 and 4: the text highlighted in red represent the nested forward and reverse primers.

The three PCR fragments amplified when cDNA recovered from the mRNA isolated by *UBQ10*$_{pro}$:tFd-yeast ADE transformants. According to the sequencing data, fragments 1, 2, and 3 were 987, 867 and 433 bp in length, respectively. As shown in Figure 3.6 A relative to the ADE open reading frame (ORF), fragment 2 arises from a cDNA that is missing bp 460 to 579. Fragment 3 contains the first 20 bp of the ORF and bp 567 to 987. The fact that the second starting points of fragment 2 and 3 are close to each other, i.e. bp 579 and 576, suggested that secondary structure in the mRNA might be a potential reason for the multiple products. Kozak (1989) explains how secondary structure formation inhibits the translation in eukaryotic mRNA.

A

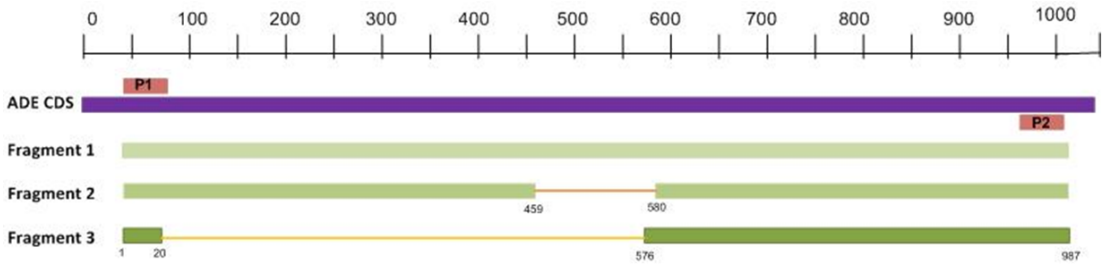
0
100
200
300
400
500
600
700
800
900
1000
P1
ADE CDS
P2
Fragment 1
Fragment 2
459
580
Fragment 3
1
20
576
987

B

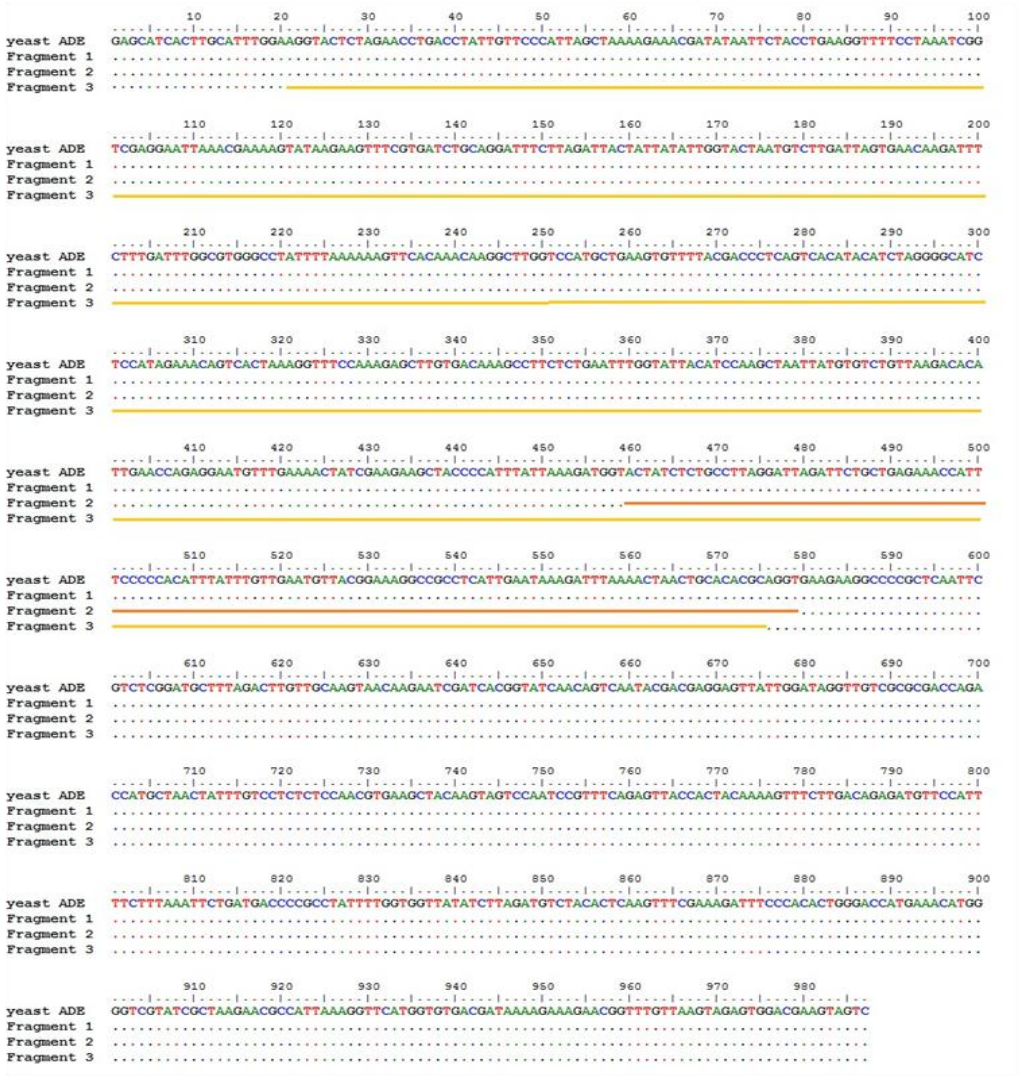
yeast ADE GAGCATCACTTGCATTTGGAAGGTACTCTAGAACCTGACCTATTGTTCCCATTAGCTAAAAGAAACGATATAATTCTACCTGAAGGTTTTCCTAAATCGG
TCGAGGAATTAAACGAAAAGTATAAGAAGTTTCGTGATCTGCAGGATTTCTTAGATTACTATTATATTGGTACTAATGTCTTGATTAGTGAACAAGATTT
CTTTGATTTGGCGTGGGCCTATTTTAAAAAAGTTCACAAACAAGGCTTGGTCCATGCTGAAGTGTTTTACGACCCTCAGTCACATACATCTAGGGGCATC
TCCATAGAAACAGTCACTAAAGGTTTCCAAAGAGCTTGTGACAAAGCCTTCTCTGAATTTGGTATTACATCCAAGCTAATTATGTGTCTGTTAAGACACA
TTGAACCAGAGGAATGTTTGAAAACTATCGAAGAAGCTACCCCATTTATTAAAGATGGTACTATCTCTGCCTTAGGATTAGATTCTGCTGAGAAACCATT
TCCCCCACATTTATTTGTTGAATGTTACGGAAAGGCCGCCTCATTGAATAAAGATTTAAAACTAACTGCACACGCAGGTGAAGAAGGCCCCGCTCAATTC
GTCTCGGATGCTTTAGACTTGTTGCAAGTAACAAGAATCGATCACGGTATCAACAGTCAATACGACGAGGAGTTATTGGATAGGTTGTCGCGCGACCAGA
CCATGCTAACTATTTGTCCTCTCTCCAACGTGAAGCTACAAGTAGTCCAATCCGTTTCAGAGTTACCACTACAAAAGTTTCTTGACAGAGATGTTCCATT
TTCTTTAAATTCTGATGACCCCGCCTATTTTGGTGGTTATATCTTAGATGTCTACACTCAAGTTTCGAAAGATTTCCCACACTGGGACCATGAAACATGG
GGTCGTATCGCTAAGAACGCCATTAAAGGTTCATGGTGTGACGATAAAAGAAAGAACGGTTTGTTAAGTAGAGTGGACGAAGTAGTC

Figure 3-6: Alignment of PCR fragments produced from *UBQ10$_{pro}$*:tFd-yeast ADE cDNA templates

A: Schematic diagram of showing the sizes of fragment 1, 2 and 3 compared to the full-length yeast ADE CDS; AAH1 CDS is 1044 bp in length. The presence of the full-length insert was investigated using flanking primers; the expected size was 987 bp. Fragments 1, 2, 3 were 987, 867 and 433 bp, respectively; B: Alignment of sequenced fragments using ClustalW program in BioEdit software. The missing sequences in fragment 2 and 3 are shown in orange and yellow colored lines, respectively.

3.1.2.1 Prediction of secondary structure in mRNA

The possible hairpin structures in the yeast ADE transcript were analyzed using the program mfold (Zucker, 2003) which was accessed online via Oligocalc (basic.northwestern.edu/biotools/oligocalc.html; Kibbe, 2007). The nineteen potential hairpin formations predicted by the program are shown in Figure 3.7. When the sequence that was absent in fragment 3 was analyzed with mfold, 99 possibilities were predicted (data not shown). Then the possible secondary structure formation in CDS was analyzed using Web server for RNA structure prediction tool (rna.urmc.rochester.edu/RNAstructureWeb/Servers/Predict1/Predict1.html) as shown in Figure 3-8.

Figure 3-7: Hairpin formation possibilities of the sequence missing in the fragment 2 PCR product.

The hairpin formation potential in missing 120 bp sequence (from 460 to 579 bp) of fragment 2. mfold (www.basic.northwestern.edu/biotools/oligocalc.html) showed 19 different predictions. Complementary regions in each sequence are highlighted in red font.

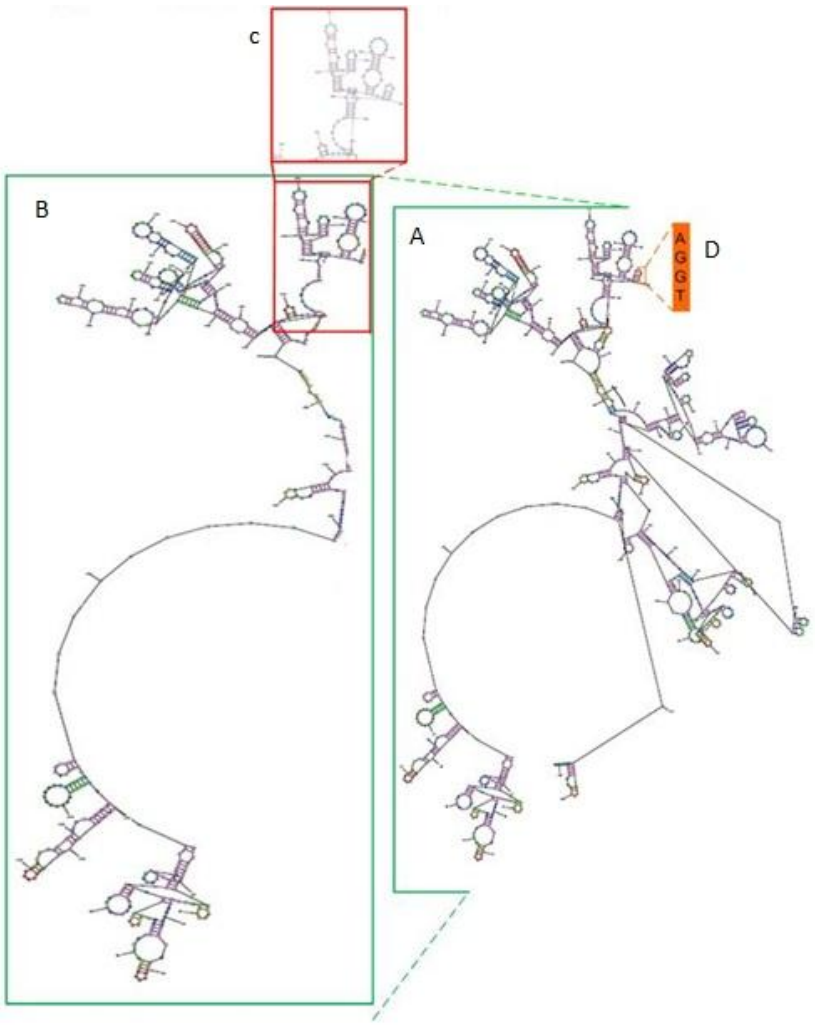

Figure 3-8: The secondary structure formation in yeast ADE mRNA predicted by RNAfold

A: the predicted secondary structure formation along the full length fragment; B: the predicted secondary structure formation in the sequence missing in fragment 3; 3: the predicted secondary structure formation in the sequence missing in fragment 2; D: the additional four bases present in the breaking point of fragment 3 but not in fragment 2 (from 576-579 bp) form a small bulge in the structure.

3.1.3 Detection of expression and plastid localization of the ADE-GFP fusion protein

In this study the transit peptide from the ferredoxin gene of *B. sinuspersici* (tFd) was used to target the yeast ADE into chloroplast in *Arabidopsis*. The localization of the tFd-yeast ADE fusion was evaluated by adding the sequence of GFP to the C-terminus of tFd (*UBQ10*$_{pro:}$tFd-GFP). The localization of the GFP signal in T3 plants transformed with *UBQ10*$_{pro}$:tFd-yeast ADE-GFP was used to indicate the subcellular targeting of ADE. Two homozygous transformant lines containing *UBQ10*$_{pro}$:tFd-GFP and *UBQ10*$_{pro}$:GFP were used as the positive controls for tFd functionality, respectively; WT plants were imaged as the negative control for GFP expression.

Green fluorescence was detected, as expected, in the positive control line and not in the WT plants as shown in (Figure 3-9 A). The GFP signal was observed in the cytosol and nuclei of *UBQ10*$_{pro}$:GFP plants.

Almost all of the GFP detected in the leaves from plants containing *UBQ10*$_{pro:}$tFd-GFP was presented in the chloroplasts as shown in Figure 3-9 A while *UBQ10*$_{pro}$:GFP showed the GFP expression remaining in cytosol (and in nuclei). The plants containing the *UBQ10*$_{pro}$:tFd-yeast ADE-GFP transgene expressed GFP in their chloroplasts in addition to the cytosol and nuclei, when their leaves were viewed with confocal microscopy. The cytosolic GFP expression is more evident in Figure 3-9 B to exist in both mesophyll and epidermal cells.

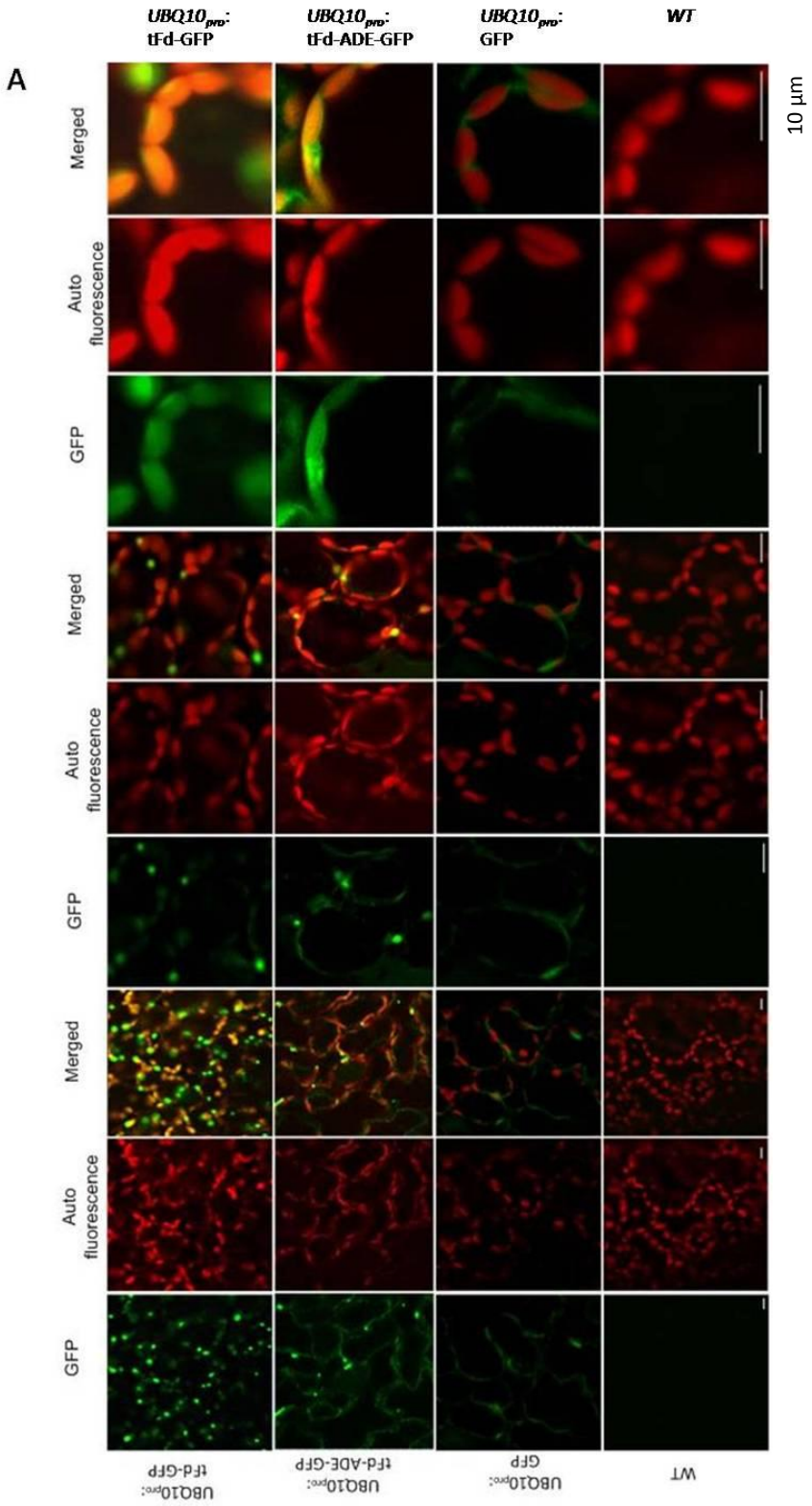
A
UBQ10pro: tFd-GFP
UBQ10pro: tFd-ADE-GFP
UBQ10pro: GFP
WT
Merged
Auto fluorescence
GFP
10 µm

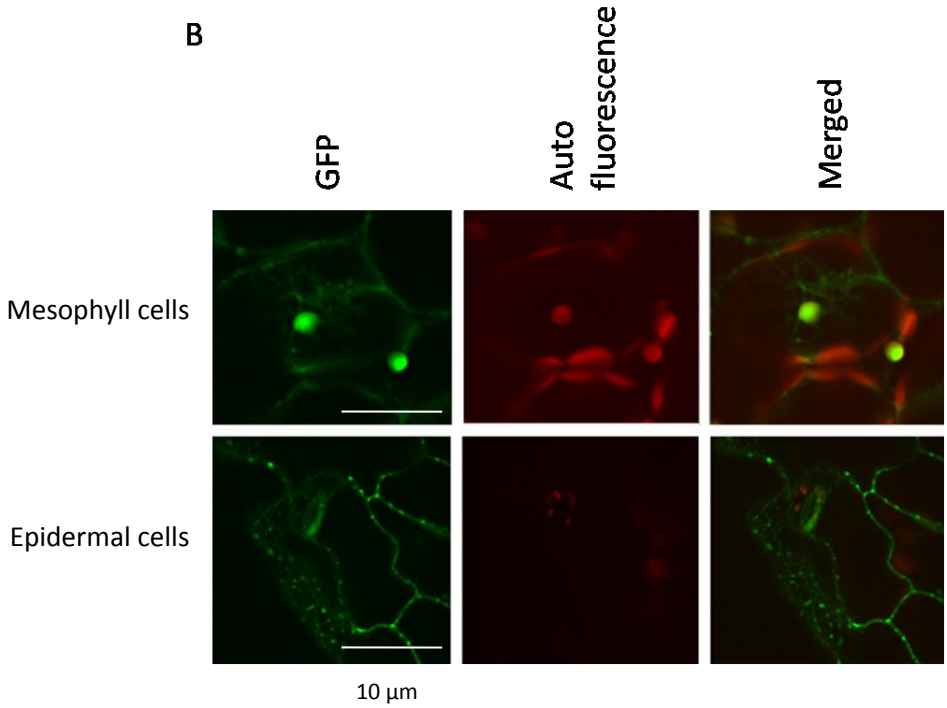

Figure 3-9 Expression of GFP in leaf cells of transgenic lines

A: GFP was expressed in leaf mesophyll cells of lines carrying *UBQ10*$_{pro}$:tFd-yeast ADE-GFP. The figure shows images of the same set of cells in three different magnifications. The fusion of tFd to coding sequence led to the import of the protein into chloroplasts (*UBQ10*$_{pro}$:tFd-GFP and *UBQ10*$_{pro}$:tFd-yeast ADE-GFP). When GFP was expressed from the transgene lacking tFd (i.e. *UBQ10*$_{pro}$:GFP) it was localized in the cytosol. GFP expressed from *UBQ10*$_{pro}$:tFd-yeast ADE-GFP was observed in the cytosol in addition to plastid localization. WT mesophyll cells were imaged as the negative control for these experiments. B: The GFP expression in plastids as well as cytosol in a transgenic line containing *UBQ10*$_{pro}$:tFd-yeast ADE-GFP. Both mesophyll cells and epidermal cells are shown. Scale bars = 10 µm.

3.1.4 Immunoblot analysis of *UBQ10$_{pro}$*:tFd-yeast ADE-GFP transgenic lines

Leaf crude protein extracts prepared from approximately three-week-old-plants grown in agar plates were immunoblotted with anti-αAah1p and anti-GFP and the results are shown in Figure 3-10. Transgenic lines with *UBQ10$_{pro}$*:tFd-yeast ADE-GFP (4+40+26=70 kDa) showed the intact band at 70 kDa as shown in Figure 3-10 A (highlighted with a red star). The positive control, affinity chromatography purified recombinant yeast ADE, showed ADE polypeptide of 40 kDa as shown with a yellow star.

For the immunoblot using anti-GFP antiserum, *35S$_{pro}$:*SAHH-GFP (53+27=80 kDa), *APT1$_{pro}$*:Ex1-GFP (7+27=34 kDa), *UBQ10$_{pro}$*:GFP (27 kDa) were used as positive controls. All the lines showed the GFP alone at 27 kDa; this was not seen in the WT extract. In addition another protein of approximately 70 kDa level was detected in all the extracts including the WT sample. The expected intact polypeptide for the transformants with *UBQ10$_{pro}$*:tFd-yeast ADE-GFP is (40+27=67 kDa) as the tFd sequence get cleaved off when the protein enters into plastids (Lung 2012). However, there was no band at 67 kDa size except the band around 70 kDa. On the other hand the bands at 70 kDa in *UBQ10$_{pro}$*:tFd-yeast ADE-GFP lines were clearly stronger than the rest except *35S$_{pro}$*:SAHH-GFP.

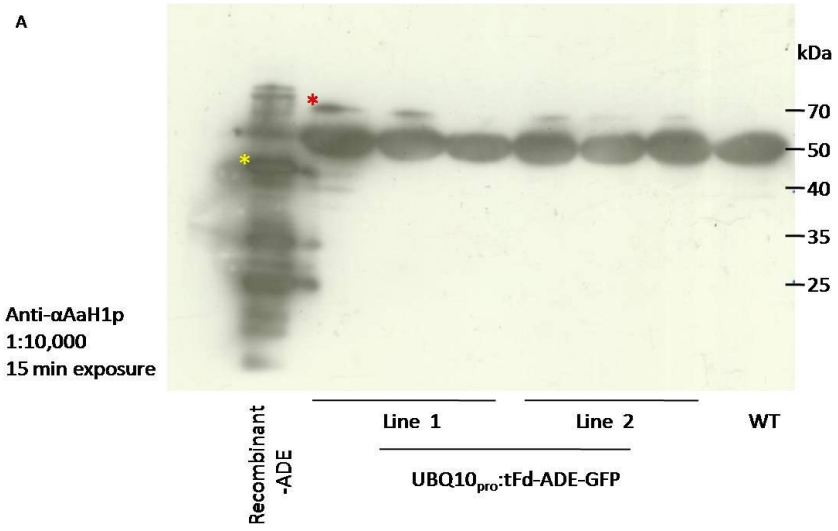
A
kDa
70
50
40
35
25
Anti-αAaH1p
1:10,000
15 min exposure
Recombinant -ADE
Line 1
Line 2
WT
UBQ10pro:tFd-ADE-GFP

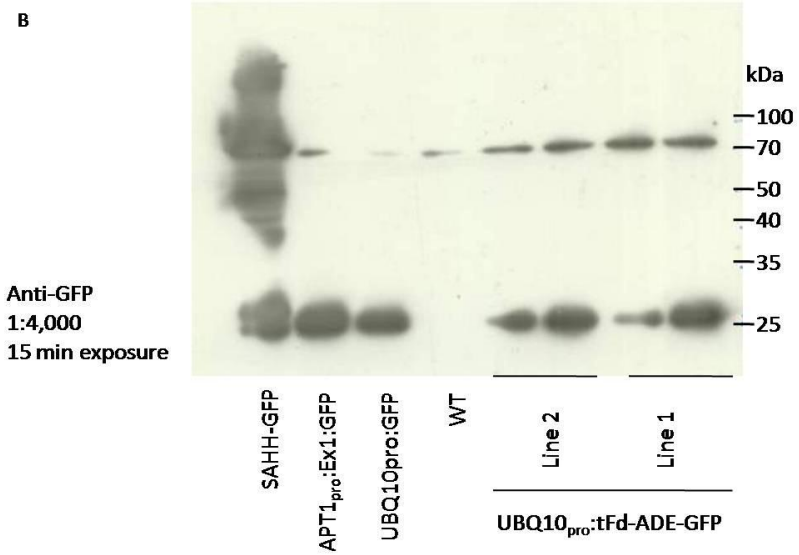
B
kDa
100
70
50
40
35
25
Anti-GFP
1:4,000
15 min exposure
SAHH-GFP
APT1pro:Ex1:GFP
UBQ10pro:GFP
WT
Line 2
Line 1
UBQ10pro:tFd-ADE-GFP

Figure 3-10: Detection of *UBQ10$_{pro}$*:tFd-yeast ADE-GFP by immunoblotting

Western blots to detect expression of the *UBQ10$_{pro}$*:tFd-yeast ADE-GFP in leaf crude protein extracts of two independent BASTA-resistant T3 lines; three independent extracts were prepared for each transgenic line. The quantity of protein that was loaded in each lane was 15 µg. A WT protein crude extract was used as the negative control. Samples were resolved by 12% (w/v) SDS-PAGE and the bound antibody was detected using a rabbit secondary antibody conjugated to HRP. Exposure time was 15 minutes. A: Immunoblot using anti-αAaH1p antibody (1:10,000). A protein of the approximate size of the yeast ADE-GFP fusion protein (40 + 27=67 kDa) is present in five of the six transgenic plant extracts (as shown with a red star); it is not present in the WT extract. In addition, another very strong polypeptide was observed at 50-55 kDa in all the plant extracts, and likely reflects binding to RbcL. Affinity-purified recombinant yeast ADE (the 300 mM imidazole eluate fraction) was used as the positive control for the blot (yellow star).B:Immunoblot analysis of the two extracts of two *UBQ10$_{pro}$*:tFd-yeast ADE-GFP T3 lines using anti-GFP (1:4,000). Three other GFP expression lines were used as positive controls: a fusion to S-adenosylhomocysteine hydrolase (53 kDa); fusion to the first exon of APT1.1 (7 kDa) and GFP alone. All the GF expressing lines had a signal for free GFP at 27 kDa; the WT extract did not. In addition there was another band ˜70 kDa in all the extracts including those prepared from WT plants.

3.1.4.1 Purification of recombinant yeast ADE

As the yeast ADE was expected to be expressed constitutively in the *UBQ10$_{pro}$*:yeast ADE transgenic lines, the next goal was to detect the activity of the enzyme in crude leaf extracts by an *in vitro* enzyme activity assay. Since a positive control was needed for the assay, recombinant yeast ADE was overexpressed using a plasmid that expressed the *S. cerevisiae* ADE from the inducible *lac* promoter. This plasmid was a gift from Dr. Ivo Frébort and the enzyme purification strategy I used was based on the protocol outlined in Pospisilova *et al.* (2008).

Since the lab did not have *E. coli* BL21star™(DE3), the strain recommended for ADE expression, I tried using *E. coli* BL21(DE3) cells and BL21(DE3) pLysS cells. *E. coli* BL21(DE3) cells were more efficient in over expression than *E. coli* BL21(DE3) pLysS cells as shown in Figure 3.11. The protein was strongly induced by the addition of 0.2 mM IPTG followed by overnight incubation at 18^{o}C. However, the solubility of recombinant protein was low and was predominantly present inclusion bodies, as shown in Figure 3.12.

The recombinant protein from soluble fraction was purified by nickel affinity chromatography. The final concentration of purified recombinant yeast ADE enzyme was 2.7 µg/µL. Since the amount of recombinant protein yielded was enough for the enzyme activity assay I did not make any attempt to resolubilize the active enzyme from the inclusion bodies.

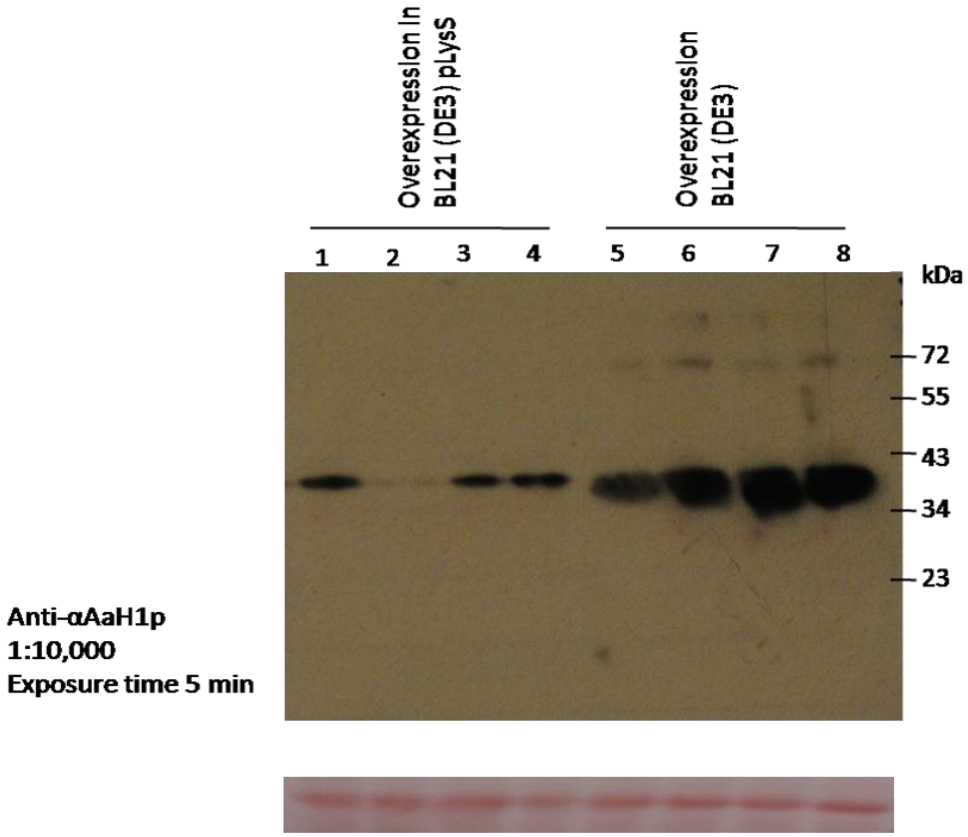

Figure 3-11: Immunoblot of detecting the expression of recombinant yeast ADE using *E. coli* BL21(DE3) pLysS versus BL21(DE3)

AAH1 containing pET 100 plasmids were overexpressed using *E. coli* BL21(DE3) and *E. coli* BL21(DE3) pLysS cells (which contains additional T7 lysozyme gene to suppress the protein expression if it is toxic) (four cultures were prepared from each). After incubation with 0.2 mM IPTG at 18^0C, with shaking at 200 rpm for 16 h, 1 µL from each total culture was analyzed by immunobloting. Lanes 1, 2, 3, and 4 were ran with 1 µL total cultures in which the protein was expressed in BL21(DE3) pLysS cells. Lanes 5, 6, 7, and 8 were ran with 1 µL total culture in which the protein was expressed in BL21(DE3) cells. BL21(DE3) cells were better in overexpression over BL21(DE3) pLysS cells. Ponceau results to evaluate the consistency of the protein loading have also shown.

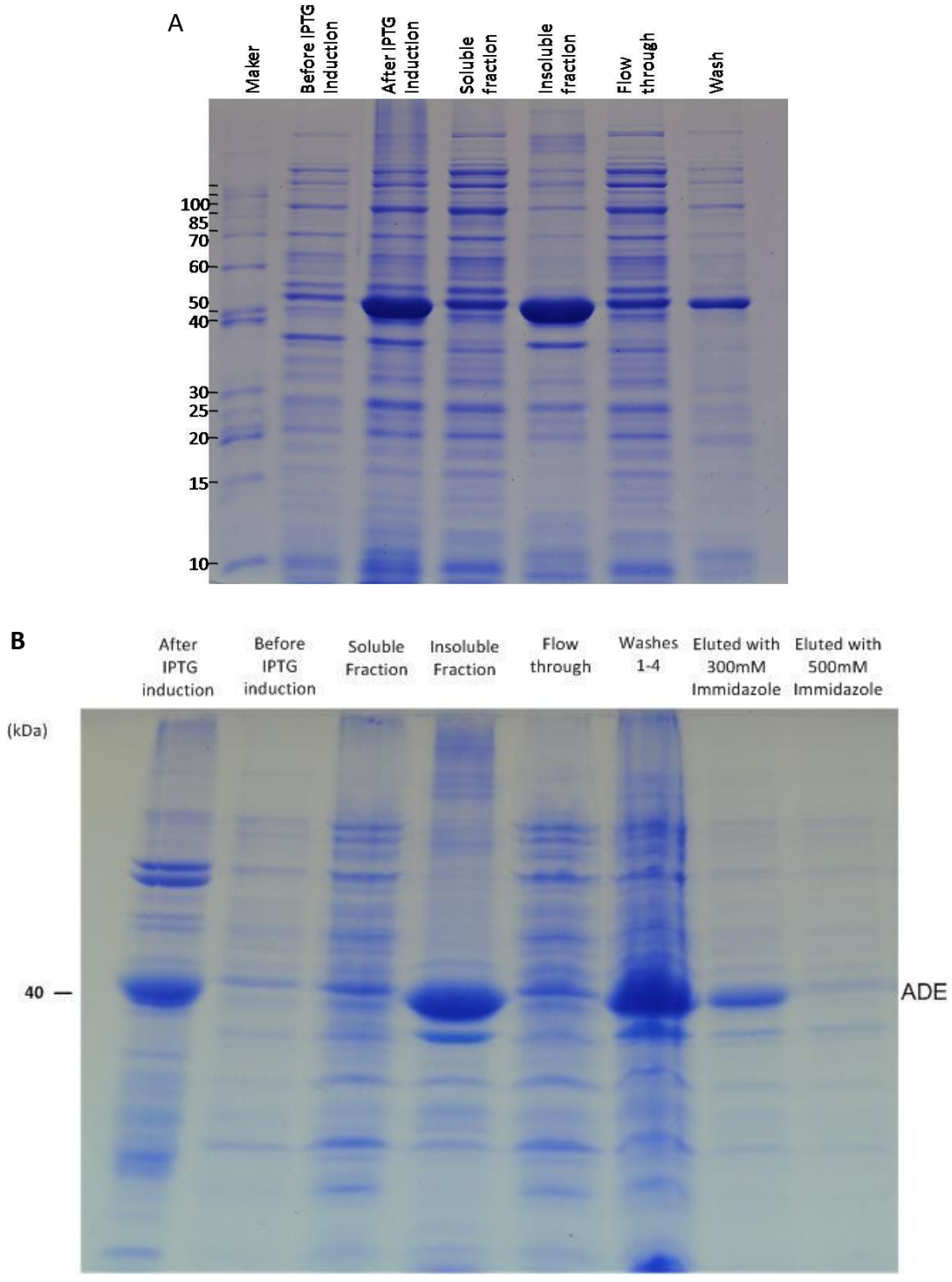
A
Maker
Before IPTG Induction
After IPTG Induction
Soluble fraction
Insoluble fraction
Flow through
Wash
100
85
70
60
50
40
30
25
20
15
10
B
After IPTG induction
Before IPTG induction
Soluble Fraction
Insoluble Fraction
Flow through
Washes 1-4
Eluted with 300mM Immidazole
Eluted with 500mM Immidazole
(kDa)
40
ADE

Figure 3-12: Purification of recombinant yeast ADE from *E. coli* BL21(DE3)

ADE was over expressed *in E. coli* BL21(DE3) cells with pET 100 containing the *AAH1* coding region by induction with 0.2 mM IPTG overnight at 18^{o}C. The gel images stained with Coomassie Brilliant blue shows various stages of the enzyme purification process; before and after IPTG induction, soluble and insoluble fractions, flow through, wash and elution with running buffer containing 300 mM imidazole and 500 mM imidazole. Fermentas PageRuler^{TM} unstained protein ladder was used to estimate the sizes of the polypeptides.

3.1.4.2 Assay of yeast ADE enzyme activity in transgenic lines

The recombinant yeast ADE was used as the positive control to develop the assay of the ADE enzyme activity in the *UBQ10$_{pro}$*:tFd-yeast ADE transgenic plants. I used the assay as explained by Kamat *et al*. 2011. It was a coupled assay in which it produces ammonia in the first reaction and that ammonia leads to the second reaction and oxidizes NADH into NAD^{+}. The activity of the reaction was measured by the oxidation of NADH at 340 nm in the reaction mixture. The assay was optimized before analyzing the crude leaf extracts from the plants with the transgene.

3.1.5 Optimization of the enzyme activity assay

The preparation of stock solutions of GDH, oxo-ketoglutarate, NADH, and adenine using 50 mM HEPES-KOH (pH 7.5) was more effective than using dH_2O as the solvent. In addition, the preparation of GDH, oxo-ketoglutarate, and adenine solutions freshly on each day of assay was always efficient for a better activity. Mixing of GDH by inverting the tube slowly without allowing air incorporation was critical for the success of the assay.

The optimum amount of the GDH coupling enzyme required for the assay was determined to be 0.5 (w/v) by running the assay with NH_4Cl as the substrate in place of adenine as

explain in section 2.6.2. Five µm of recombinant yeast adenine deaminase (with concentration of 2.7 µg/µl) was sufficient to run the assay well. Representative results of the assay after optimization of the reagents are shown in Figure 3-13.

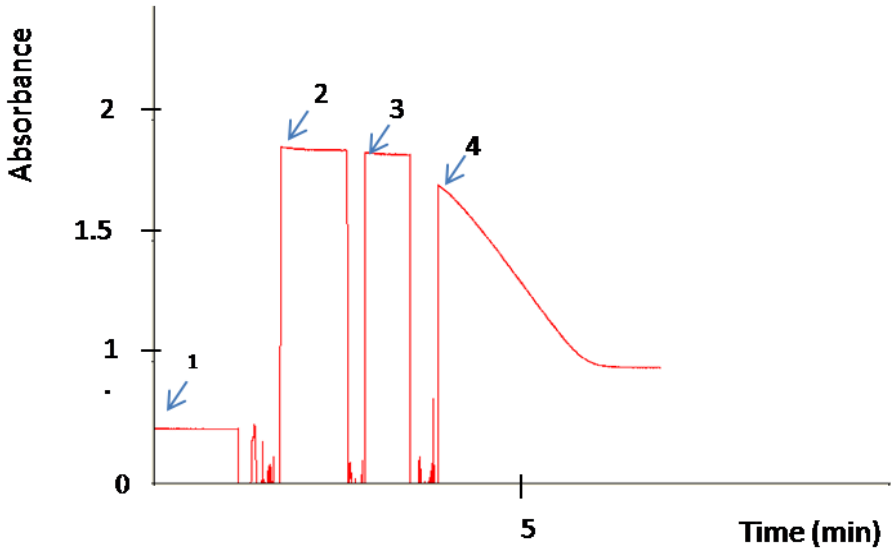

Figure 3-13: Oxidation of NADH happened in the coupled enzyme activity assay after optimization of reagents

The graph shows the absorbance of NADH at 340 nm over the time of the assay. 1: point of mixing HEPES (pH 7.5), NADH, oxo-glutarate and dH_2O, 2: addition of GDH, 3: addition of recombinant yeast ADE, 4: addition of adenine. The reaction was stopped after 6 min (complete NADH oxidation).

3.1.6 Determination of recombinant yeast ADE K_M for adenine

It is important to know an enzyme's K_M for its substrate in order to develop a quantitative assay. K_M value is important to determine the optimum amount of substrate for the reaction to carry on. Pospisilova *et al.* (2008) reported the K_M of yeast ADE for adenine as 55 µM. Thus, I started the K_M estimates using three lower concentrations and five higher concentrations (up to 250 µM) of adenine. Since the range of concentrations with higher values was not enough to reach to a plateau in a Michaelis-Menten plot (data not shown), the adenine concentration was increased up to 700 µM of adenine, as shown in Figure 3-14, the K_M and V_{max} of his-tagged affinity chromatography purified recombinant yeast ADE was determined to be 72.2 µM and 6.6 µmol $min^{-1}mg^{-1}$.

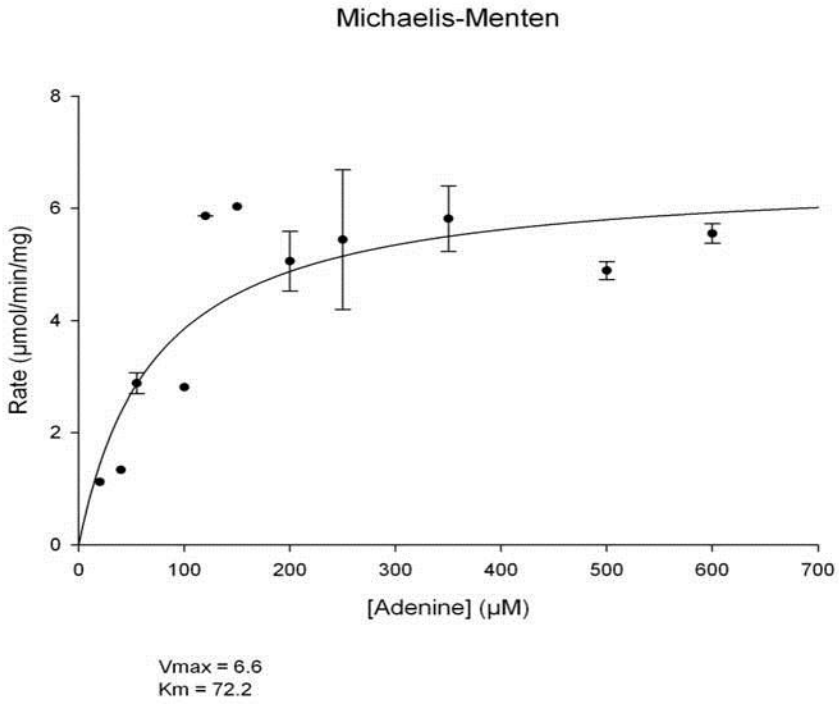

Figure 3-14: Determination of Michaelis-Menten constant (K_M) and V_{max} for recombinant yeast ADE

The ADE activity assay was carried out at a range of concentrations of adenine from 0-700 µM using the optimized conditions. The activity was monitored by measuring the oxidation of NADH at 340 nm. The graph shows the rate of the reaction against different concentrations of adenine. Since the K_M value of yeast ADE was 72 µM, the assay was continued with 800 µM of adenine as the substrate concentration in reaction mixture as it needs to be taken ten times of K_M value. The V_{max} was determined to be 6.6 $\mu molmin^{-1}mg^{-1}$.

3.1.7 Enzyme activity assay with protein crude extracts

After optimizing the assay, I moved into analyzing the leaf crude extracts from the two lines determined to be homozygous for *UBQ10*$_{pro}$:tFd-yeast ADE transgene. The recombinant yeast ADE was used as the positive control. Unexpectedly, a slope for NADH oxidation was observed immediately after adding the crude extract, in the absence of the substrate, adenine. It was proposed that this might be due to impurities in the crude extract, leading me to use desalting to remove all possible small molecules that might be in the extract, including adenine. Unfortunately, desalting of these protein crude extracts using a homemade column of sephadex beads or Nanosep 10 K OMEGA centrifugal devices (VWR, Canada) did not successful in eliminating the non-specific NADH oxidation that occurred before adding adenine. The slope took 120 minutes to come to a plateau. After the slope came to a plateau, the addition of adenine to the reaction mixture did not make any difference due to the complete loss of NADH from the reaction medium. To avoid the loss of NADH due to continuous oxidation, adenine was added when the first slope became a constant and tried to see any difference among two slopes i.e. before and after addition of adenine (Figure 3-15 A). However, no clear difference between two slopes was observed

leading me to conclude that there was no ADE activity in the leaf crude extracts I had prepared.

My subsequent approach to improve the assay involved concentrating the crude extracts by $(NH_4)_2SO_4$ precipitation. Using this technique the protein concentration in the extracts was increased approximately four-fold (e.g. homozygous 1 (lane #4 in figure 3-1) 8.55 mg/mL, homozygous 2 (lane #9 in figure 3-1)-8.18 mg/mL and WT–9.94 mg/mL). Although this step increased the protein concentrations several fold higher, no adenine-dependent NADH oxidation was observed (Figure 3.15 B).

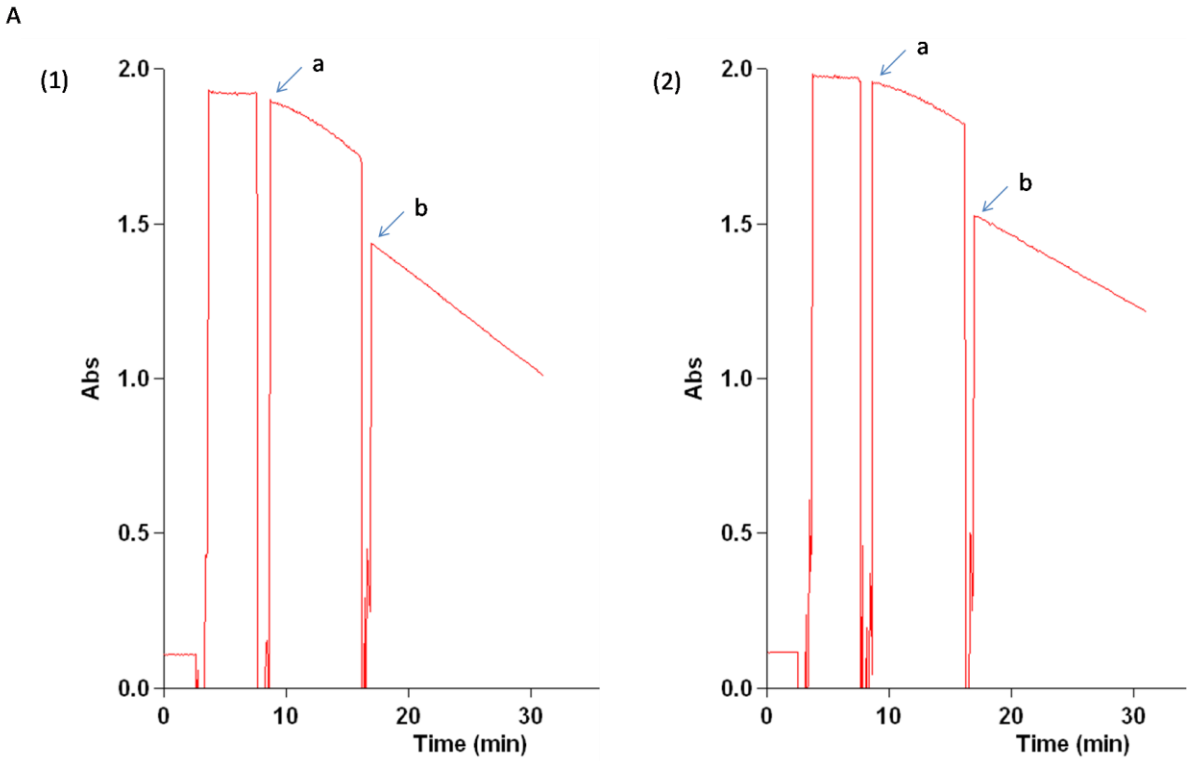

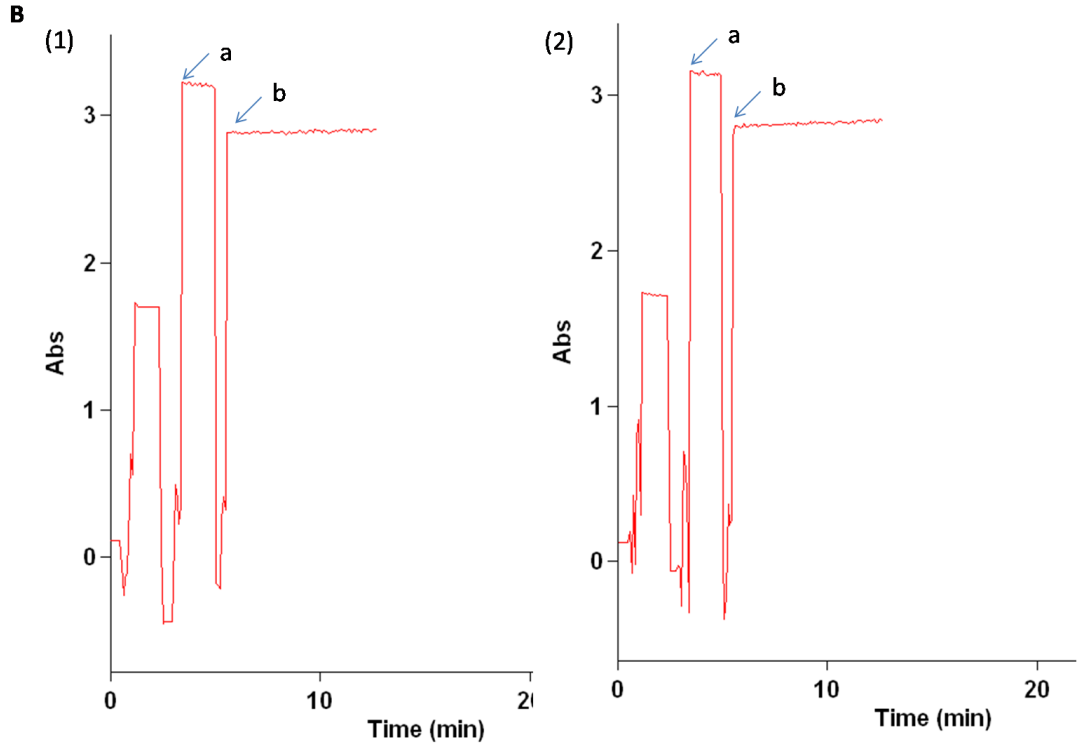

Figure 3-15: Oxidation of NADH with presence of plant protein crude extracts

A: The assay carried out with desalted leaf crude extracts; (1): oxidation of NADH in assay with homolines 1 protein crude extract, a: point of mixing protein crude extract, b: adding of adenine; (2): oxidation of NADH in assay with WT protein crude extract

B: The assay carried out with concentrated and desalted protein crude extract by ammonium sulphate precipitation and centrifugation using 10 K Nanosep centrifugal tubes, respectively. (1): oxidation of NADH in assay with homolines 1 protein crude extract; a: adding of protein crude extract, b: adding of adenine; (2): oxidation of NADH in assay proceeded with WT protein crude extract

Table 4: NADH oxidization of adenine deaminase over expression lines. Values are average ± SD; n = 3 or 4 samples

Enzyme added at Step 3	NADH Oxidization (Slope of the graph)	
	Step 3	**Step 4**
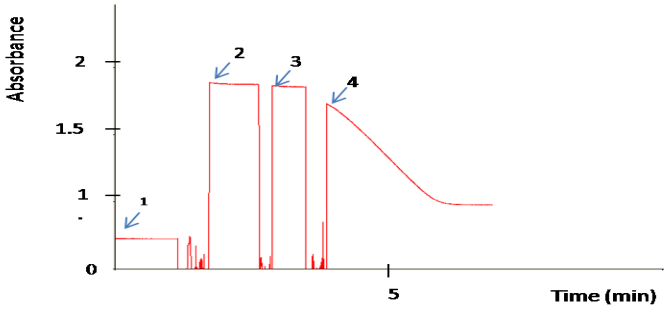		
1. His-tagged purified recombinant Adenine deaminase	0	-0.302
2. Protein crude extract		
a. Yeast ADE over expression line 1	-0.0224	-0.0228
b. Yeast ADE over expression line 2	-0.0241	-0.0252
c. WT protein crude extract (control)	-0.0132	-0.0125
3. Desalted protein crude extract		
a. Yeast ADE over expression line 1	-0.0197	-0.0202
b. Yeast ADE over expression line 2	-0.0194	-0.0226
c. WT protein crude extract (control)	-0.0149	-0.0105
4. Concentrated protein crude extract with $(NH_4)_2SO_4$ precipitation followed by dialysis and use of commercial concentrators.		
a. Yeast ADE over expression line 1	0	0
b. Yeast ADE over expression line 2	0	0
c. WT protein crude extract (control)	0	0

3.1.8 Genetic crossing with APT1-deficient mutants

My plan at the beginning of the research was to detect any involvement of high adenine levels in *apt1* mutants in oxidative stress tolerance, yeast ADE was introduced in *apt1* mutants. After homozygous lines for $UBQ10_{pro}$:tFd-yeast ADE were obtained, they were crossed with *oxt1* and *apt1-3* mutants by using the ADE transgenic line as the maternal parent. F1 seeds were collected and grown on agar media supplemented with BASTA. The recovered seedlings were transplanted into individual pots with soil. The F2 seeds were collected. F2 seeds were grown on BASTA again and recovered plant DNA was tested with primers for *apt1-3* and *oxt1* mutants.

3.2 Chloroplast localization of native APT1.1

APT1 encodes 2 polypeptides: APT1.1 and APT1.2. APT1.1 is expected to be targeted localized in chloroplasts as its first exon contains a plastid targeting sequence. Facciuolo (2009) tried to detect this using GFP fusion protein studies. However he could not distinguish whether it is localized in the chloroplast or on the outer envelope of the chloroplasts. Therefore, in this study I tried to detect the presence of native APT1.1 in chloroplast subfractions by immunobloting with APT1 antibody.

Isolated chloroplasts were fractionated into membrane and stroma fractions and immunoblotted along with intact protoplasts (IP) and intact chloroplasts (IC). IP-oxt1 and affinity chromatography purified his-tagged recombinant APT1 were used as negative and positive controls, respectively in the experiment. The protoplast yield was 1,000,000-1,100,000 protoplasts per milliliter of enzyme buffer.

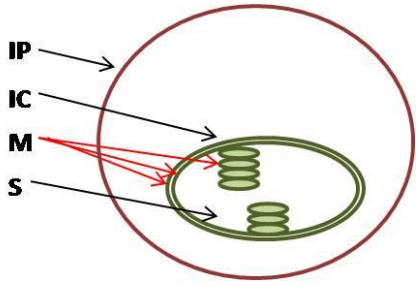

Figure 3-16 Four different chloroplast fractions used to detect the presence of APT1.1

The intact protoplast (IP), intact chloroplast (IC), membrane(M) and stroma (S) fractions are the four fractions used in subfractionation method to detect the localization of APT1.1. Membrane fraction contains outer- and inner- envelope membranes and thylakoid membrane.

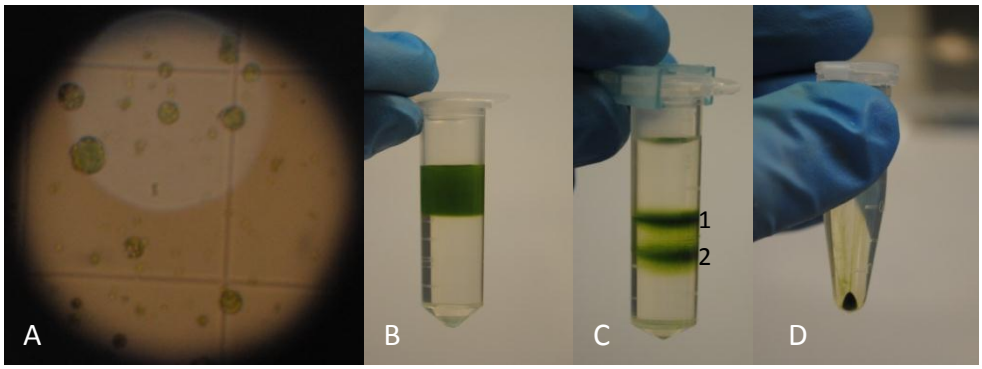

Figure 3-17: Four different stages in the subfractionation procedure: IP, lysed protoplast suspension on the Percoll gradient, Separation of IC at 40%/85% interface of Percoll gradient and the pellet of IC

A: WT-intact protoplasts (IP-WT) after 3 hs of enzyme digestion under compound light microscope (x400); B: Lysed protoplasts (LP) on Percoll gradient (50,000-70,000 LP in one gradient) before centrifugation; C: 1-Broken chloroplasts, 2- IC at 40%/85% interface after centrifugation; D: pellet resulted after centrifugation of intact layer of chloroplasts with 6.5 volumes of HS buffer

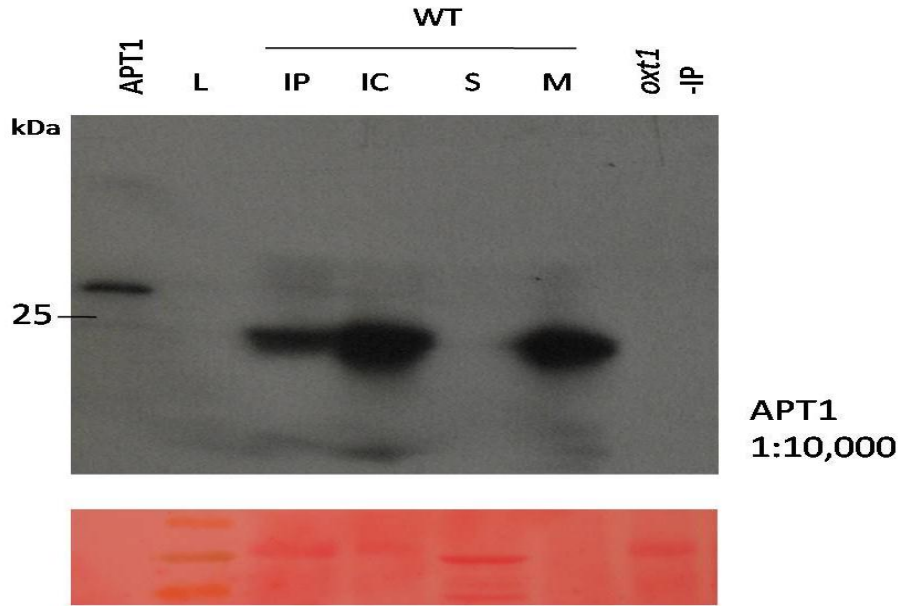

Figure 3-18: Detection of APT1 localization in intact protoplasts, chloroplasts and chloroplast subfractions

Immunoblot for WT-IP, WT-intact chloroplasts (WT-IC), chloroplast membrane fraction of WT (WT-M), chloroplast stroma fraction of WT (WT-S), *oxt1* intact protoplasts (*oxt1*-IP) and affinity purified recombinant APT1 using anti-APT1 in (1:10,000). APT1 polypeptide which is 24 kDa in size was detected in WT-IP, WT-IC and WT-M fractions. WT-S and *oxt1*-IP did not show the band. The APT1 mutant, *oxt1*-IP was used as the negative control for the experiment. The positive control, 18 ng of his-tagged purified recombinant APT1 was seen around ˜26-27 kDa size as it is supposed to be 26 kDa. Protein ladder (L) has run in lane 2. Samples were resolved by 15% (w/v) SDS-PAGE and the bound antibody was detected using a rabbit secondary antibody conjugated to HRP. Exposure time was 15 minutes. Ponceau stained gel has given to show all the fractions worked as expected; RUBISCO was seen in WT-IP, WT-IC, S and *oxt1*-IP fractions and not in his-tagged purified recombinant APT1 and M fractions.

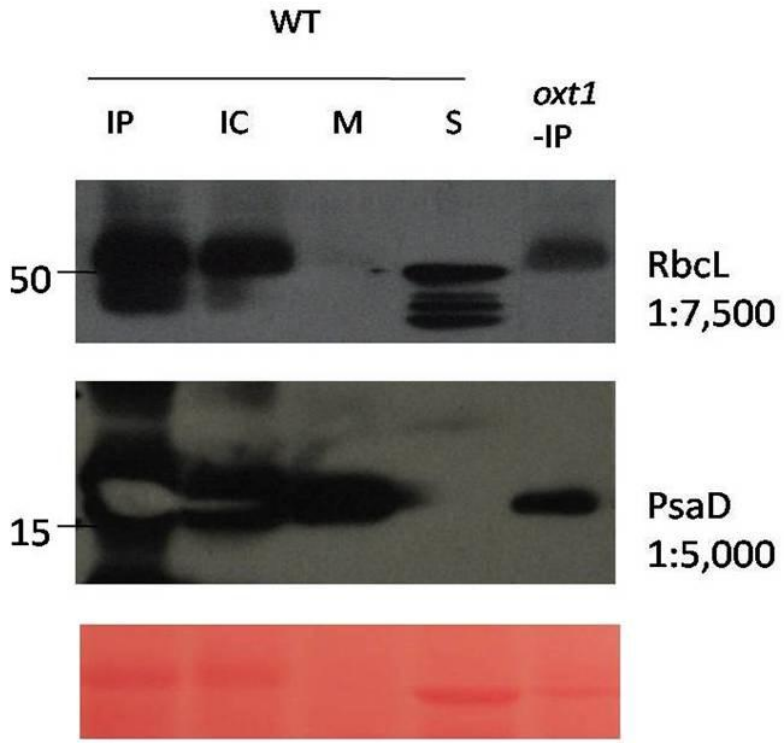

Figure 3-19: Detection of membrane and stroma fractions using anti-RbcL and anti-PsaD

Immunoblot for WT-IP, WT-IC, WT-M, WT-S, and *oxt1*-IP using anti-RbcL in (1:7,500) anti-PsaD (1:5,000). The band for RbcL was detected at 55 kDa in all the fractions except WT- M. The binding of antibody for membrane marker, PsaD, was detected at 17 kDa in all the fractions except WT-S. Samples were resolved by 15% (w/v) SDS-PAGE and the bound antibody was detected using a rabbit secondary antibody conjugated to HRP. Exposure time was 15 minutes. Ponceau stained gel has given to show all the fractions worked as expected; RUBISCO was seen in WT-IP, WT-IC, S and *oxt1*-IP fractions and not in his M fraction.

The APT1 polypeptide was detected in IP-WT, IC-WT, and M-WT fractions at a size of ~24 kDa (Figure 3.17). In addition, the positive control, affinity chromatography purified his-tagged APT1, was detected at a slightly larger molecular weight. The WT stromal fraction

and oxt1 fractions did not have any evidence of APT1. Both positive (his-tagged recombinant APT1) and negative (IP-*oxt1*) controls worked as expected. The Ponceau stained membrane showed RUBISCO in IP-WT, IC-WT, S-WT, and IP-*oxt1* at 55 kDa (Figure 3.17).

IP-WT, IC-WT, S-WT and IP-*oxt1* fractions showed the band for the large subunit of RUBISCO with anti-RbcL at 55 kDa (Figure 3.18). IP-WT, IC-WT, M-WT, and IP-*oxt1* showed the polypeptide of the core subunit of photosystem I in thylakoid membrane against anti-PsaD at 17 kDa. Ponceau stained membrane showing the 55 kDa region in IP-WT, IC-WT, S-WT, and IP-*oxt1* as expected (Figure 3.18).

Chapter 4
Discussion

Oxidative stress arises from ROS is one of the main abiotic stresses that cause huge yield losses in agriculture (Allen 1995; Shkolnik 2009). One part of this study followed up on the observation that the *APT1*-deficient-mutants, *oxt1* and *apt1-3,* have a higher tolerance to chemically induced oxidative stress than WT plants do. The analyses of these mutants by Facciuolo (2009), Shkolnik (2009), and Sukrong *et al.* (2012) led to the hypothesis that the increased plastid content of adenine in these *apt1* mutants is essential for their oxidative stress tolerance.

Part one of the research reported in this thesis involved developing a system to test this hypothesis. The plan was to introduce an enzyme into *oxt1* and *apt1-3* that would reduce their plastid adenine content. The enzyme that was chosen was the yeast ADE that is encoded by the *AAH1* gene. This was directed into the plastids by fusing its coding region with a previously characterized N-terminal transit sequence from the *B. sinuspersici* ferredoxin gene (Lung, 2012). This construct was first introduced into WT *Arabidopsis* plants which were subsequently genetically crossed with the *apt1-3* and *oxt1* mutants. Two additional transgenic lines were used in the study to verify the functionality of the ferredoxin transit sequence.

The second aspect of the research documented in this thesis was focused on defining the plastid localization of APT1.1 in WT *Arabidopsis* plants.

4.1 Yeast ADE was expressed in *Arabidopsis* plants transformed with $UBQ10_{pro}$:tFd-yeast ADE

The yeast *AAH1* gene encoding ADE activity was transformed into WT plants using three constructs as explained in section 2.4.1. The *UBQ10* promoter was used to drive constitutive expression in almost all tissues (such as roots, stems, leaves) of *Arabidopsis* (Grefen *et al*., 2010). Since the ADE gene was from yeast, which does not possess chloroplasts, a chloroplast targeting sequence was added to introduce the enzyme into chloroplasts of plant cells (Lung, 2012). Western blot analysis showed a band at 40 kDa which was suspected to be the *AAH1,* expressed in transgenic plants carrying $UBQ10_{pro}$:tFd-yeast ADE construct (Figure 3.1). This immunoblot was done using α-Aah1p antiserum that was raised in a rabbit against the N-terminal part (amino acids 1–177) of yeast ADE by Escusa *et al*. in 2006. As noted by Pospisilova *et al*. (2008) the exact size of this protein is 39.633 kDa. A signal from the antibody bound to a 40 kDa polypeptide that was suspected to be the yeast ADE was observed on the membrane. Since α-Aah1p is a polyclonal antibody, the epitopes it recognizes may be present in several other polypeptides in the plant extracts in addition to ADE. Thus, the observation of additional bands on the blot is not unexpected. These non-specific bands were observed in all the lines including WT. However, WT did not show the band that I presumed to be yeast ADE (Figure 3.1, compare lanes 1 and 4). When the amino acid sequence of α-Aah1p was Blasted against the predicted *Arabidopsis* protein profile using an NCBI tblastn query (blast.ncbi.nlm.nih.gov/Blast.cgi) two potential proteins, ROOT UVB SENSITIVE 1 (66.39 kDa) and adenosine deaminase like protein (31 kDa), were recovered with 32% and 43% similarities, respectively. These two proteins may be the proteins that potentially led the 77 and 26 kDa levels.

The lack of specificity of the anti-ADE antiserum reduced my confidence in identifying ADE in the plant extracts by immunoblotting. While the binding of this antiserum to a 40 kDa

polypeptide is consistent with ADE expression, it was not conclusive. Immunoblotting of protein crude extracts of transgenic lines with a monoclonal antibody for yeast ADE, if available, would be unequivocal. Alternatively, the 40 kDa protein could be recovered by immunoprecipitation with the available antiserum, the products resolved by SDS-PAGE, and the 40 kDa protein sequenced by mass spectrometry to verify its identity.

4.2 The yeast ADE transgene is transcribed in plants transformed with *UBQ10*$_{pro}$:tFd-yeast ADE

PCR was used to verify the presence of the ADE transgene in the two homozygous transformants. The full-length yeast ADE CDS was detected in genomic DNA as a strong single band identical to the positive control. However, PCRs using cDNA prepared from leaf mRNA of the same transformants as the templates revealed three different DNA products with the fragment corresponding to the full length CDS being the faintest in both samples. The abundance of the shortest fragment of 433 bp was estimated to be approximately 35 times stronger than the full-length fragment based on staining with Safeview. It is not clear whether these products reflect mRNAs that exist in vivo or whether they are the result of artifacts during the cDNA synthesis step of the assay.

Several possible reasons can be suggested for the formation of alternative cDNA product transcripts detected *in vitro*. The end point of two missing regions in fragment 2 and 3 are very close to one another (i.e. at bp 576 and 579). This suggests the possibility of secondary structure formation in the mRNA leading to “a deletion” during the reverse transcription step of the RT-PCR. The possibility of secondary structure formation of the mRNA was predicted using mfold and RNAfold programs. Nineteen different potential hairpin structures were predicted in the missing 120 bp region in fragment 2 while, 99 predictions were given for the missing region of 575 bp in fragment 3 by mfold. Any of those hairpins

can be the reason for missing regions. The ADE CDS was analyzed for possible secondary structure formation using RNA fold; the results are shown in Figure 3.8. The results indicate that there are possible secondary structure formations all along the sequence including in the missing parts. Analysis of mRNA secondary structures using computational tools is only a first step in determining whether it is the reason behind these results. Definite confirmation would require elaborate studies such as making mutations in mRNA strand followed by further cross-linking analyses (Svitkin *et al.* 2001; Williams *et al.*, 2004). The only conclusion that can be made based on these data is there are possibilities of secondary structure formation along the whole strand, with the most stable being in the regions of 21-575 and 460-579 nucleotides.

Alternate splicing is not a possible reason for the PCR evidence of unusual ADE mRNAs in the transformants because alternate splicing takes place in genes with introns (Clancy, 2014). In this study only the CDS of yeast ADE was introduced into the plants. It is questionable whether these secondary structures are happening in vivo in the cells or made during the cDNA formation or during the PCR step.

4.3 The ferredoxin transit sequence targeted ADE-GFP into plastids

In this study it was essential that ADE actually be targeted into chloroplasts. The ferredoxin transit peptide, tFd, was used for this purpose (Lung, 2012). To evaluate the functionality of this import sequence it was fused with GFP. Normally, GFP resides in the cytosol and the nucleus of transgenic cells because it lacks targeting signals and being only 27 kDa it is small enough to diffuse between the two compartments (Ogawa *et al.* 1995). However, by adding the tFd plastid targeting sequence in-frame to GFP the fusion protein was directed for import into plastids as shown in Figure 3.9. $UBQ10_{pro}$:tFd-GFP, the positive control for tFd, showed the localization of GFP in other plastids which do not contain chlorophyll. GFP

expression in non-photosynthetic plastids could be identified by having only the GFP expression but not autofluorescence of chlorophyll. Cells of plants homozygous for the *UBQ10*$_{pro}$: tFd-GFP transgene contained GFP localized in plastids while in cells of plants transformed with the *UBQ10*$_{pro}$:GFP transgene, all the GFP was retained in the cytosol/nucleus. The GFP in cells of plants transformed with the *UBQ10*$_{pro}$:tFd-yeast ADE-GFP transgene was localized in chloroplasts although some fluorescence was also present in the cytosol (Figure 3.9 B). The latter could reflect saturation of the plastid import apparatus due to the overexpression of the transgene from the *UBQ10* promoter. Quattrocchio *et al.* (2013) explained that overexpression of GFP fusion proteins can lead to their mislocation. On the other hand the cytosolic signal in the *UBQ10*$_{pro}$: tFd-yeast ADE-GFP plants may reflect that the GFP is cleaved from a fraction of the fusion proteins in these plants. Quattrocchio *et al.* (2013) reported cleavage of GFP from the fusion protein is very common in transgenic lines.

However, the confocal results proved that the *B. sinuspersici* tFd plastid transit peptide functional normally in *Arabidopsis*. As ADE was sandwiched between the tFd and the GFP sequences the microscopy suggests that the yeast ADE also localizes in chloroplasts of these transgenic lines. Thus, I conclude that ADE expressed from the construct, *UBQ10*$_{pro}$:tFd-yeast ADE is also likely directed into chloroplasts as explained by *Huh et al.* (2003).

Western blot analysis was used to confirm the presence of ADE-GFP in *UBQ10*$_{pro}$:tFd-yeast ADE-GFP transgenic lines. As shown in Figure 3.10 A the results of immunoblot with anti-ADE antiserum were consistent with the expression of some ADE-GFP fusion protein based on the presence of a signal around 70 kDa level. On the other hand, another immunoblot was done with anti-GFP. All the transgenic lines tested including positive controls showed evidence of some free GFP (27 kDa) suggesting GFP was cleaved off the fusion protein in

each case, as Quattrocchio *et al.* (2013) proposed. This is consistent with the presence of GFP in the cytosol in *UBQ10*$_{pro}$:tFd-yeast ADE-GFP lines.

Contrary to expectation the immunoblot of *UBQ10*$_{pro}$:tFd-yeast ADE-GFP lines using anti-GFP antiserum indicated a signal at ˜71-72 kDa in leaf extracts from all the lines including WT. Even so, all the transgenic lines showed the expected fusion protein bands along with GFP alone band at 27 kDa. The expected band for *UBQ10*$_{pro}$:GFP was of 27 kDa as GFP was not a part of a fusion protein. *APT1*$_{pro}$:Ex1-GFP polypeptide was observed at 27 kDa as the plastid peptide, Ex1, gets cleaved off after localization as shown in Facciuolo (2009). Both *UBQ10*$_{pro}$:GFP and *APT1*$_{pro}$:Ex1-GFP showed a band around 70 kDa including in WT, although they would be expected to lack this polypeptide if it truly the ADE-GFP fusion protein. It is possible that the seed lots used for this experiment were contaminated with ADE-GFP expressing seed at the time of collection. These seed lots have to be tested for Basta resistance to confirm this. The expected size for *35S*$_{pro}$:SAHH-GFP is 82 kDa. Since the gel used for this experiment did not resolve polypeptides of 70 to 100 kDa well, it is possible that the strong signal observed slightly above 70 kDa may be the 83 kDa SAHH-GFP polypeptide. The *UBQ10*$_{pro}$:tFd-yeast ADE-GFP lines contained a polypeptide that reacted with the GFP antibody at 70 kDa, the same as the other lines. However, the bands in lines with *UBQ10*$_{pro}$:tFd-yeast ADE-GFP are stronger than in *APT1*$_{pro}$:Ex1-GFP, *UBQ10*$_{pro}$:GFP and WT. Therefore the strong bands might be due to the presence of intact ADE-GFP along with the band for contamination. Observing of the polypeptide of 67 kDa at little above 70 kDa level also possible as immunoblots do not give the bands at the exact place always.

Although transcription of the *UBQ10*$_{pro}$:tFd-yeast ADE transgene was detected and further confirmed by *UBQ10*$_{pro}$:tFd-yeast ADE-GFP analyses, the activity of yeast ADE in transgenic lines was not detected.

4.4 Yeast ADE activity could not be detected in plant crude extracts using an *in vitro* assay

The over expression of yeast ADE was done using both *E. coli* BL21(DE3) cells and BL21(DE3) pLysS cells, though Escusa *et al.* (2006) had used *E. coli* BL21(DE3) Star cells for this purpose. As shown in Figure 3-11**,** BL21(DE3) cells were better over expressers as compared to BL21(DE3) pLysS cells. As Pan and Malcolm (2000) explained BL21(DE3) pLysS cells were more stringent and consistent in expression than BL21(DE3); BL21(DE3) gave higher levels of proteins upon induction. In Figure 3-12 B it is clear that a large amount of ADE is present in the wash fraction which was a cumulative sample from four washes. Taking the sample only from one wash gave a clear banding appearance as in Figure 3-12 A. Incubation of the soluble fraction with the affinity resin for 45 minutes at 4^{o}C prior to running through the column was more effective as it gave more opportunity for the his-tagged protein to bind to the resin.

A coupled *in vitro* assay was used to measure yeast ADE enzyme activity in the plant extracts. In this coupled assay ADE catalyzes the rate-limiting step while GDH is the coupling enzyme. It is a colorimetric assay where the oxidation of NADH is measured at 340 nm (Davitt *et al*. 2005). Since the pH of the reaction medium is critical, use of 50 mM HEPS-KOH (pH 7.5) was more effective in the assay rather than using dH_20 to dissolve adenine, NADH, GDH and oxo-ketogutaric acid.

The K_M value of an enzyme for its substrate is an important characteristic to determine when establishing and enzyme assay. The K_M is defined as the substrate concentration at which the reaction rate is half of its maximum value (for review, see Berg *et al*. 2002). Since the K_M of an enzyme slightly varies depending the strain and conditions they used. Pospisilova *et al.* (2008) reported two K_M values for adenine deaminase from *S. cerevisiae* and *Schizosaccharomyces pombe* as 55 and 32 µM. In this case of my analysis, I determined the K_M value of over expressed yeast ADE for adenine to be 72 µm. This value is within the

range of 55 µm determined by Pospisilova *et al.* (2008). The substrate, adenine, concentration for this assay set at ten times more than the K_M value to avoid any limitations in substrate concentration while conducting the ADE enzyme activity assays. Moreover, the amount of GDH needed in the reaction mixture using ammonium chloride as the substrate as mentioned Figure 2-4 in to avoid any possible limitations in coupling enzyme concentration as well.

After optimization of reagent quantities the order of adding of reagents was changed as HEPES-KOH (pH 7.5), oxo-ketoglutarate, NADH, and dH_2O. Secondly GDH followed by recombinant yeast ADE and finally adenine as shown in Figure 3-13 expecting no slope prior to adding of adenine as the substrate. When the recombinant yeast ADE was replaced by protein crude extract of transgenic line with *UBQ10*$_{pro}$:tFd-yeast ADE, NADH started to oxidize even prior to adding of adenine. This NADH oxidation could be due to several reasons. One is the presence of adenine or adenine-like other substrate for yeast ADE in protein crude extract in the reaction mixture which leads to oxidation of NADH into NAD^+ (Pospisilova *et al*. 2008). Another reason is the presence of some other enzyme and its corresponding substrate to react with and oxidize NADH; phosphoenolpyruvate which reduces into malate while oxidizing NADH into NAD^+ is one example (Smith *et al.* 1989). To overcome these background reactions, the protein crude extract was desalted to remove all the small molecules such as purines, nucleosides, nucleotides and bases. However, desalting itself was not effective and there was no clear difference in the slopes before and after the addition of adenine to the reaction mixture (Figure 3-15 A). As the next attempt I concentrated the leaf crude extract to increase the available ADE concentration proportionally. Although concentrating filters shows the highest concentration efficiency according to Eppler *et al.* (2011), centrifugal tubes could not be used for leaf crude extract since the filters got blocked with debris. On the other hand, ethanol precipitation and speed

vac like methods could not be used as the yeast ADE was required to be active to involve in the subsequent assay. Therefore, ammonium sulphate precipitation was selected as the concentrating method. The precipitation was done for a whole day as mentioned in Methods section 2.6.4. The precipitation was followed by dialysis for a whole day to remove all ammonium ions from the protein solution (Rege and Heng 2010). Since the dialysis made the protein diluted, the protein had to be concentrated again using centrifugation collection devices. After the concentration, the assay was carried on the third day after the initial extraction. However, no NADH oxidation was observed after ammonium sulphate precipitation procedure as shown in Figure 3.15 B.

Several reasons can be proposed for my inability to detect the enzyme activity by this *in vitro* assay. First, it might be due to poor expression of the enzyme in transgenic lines. The enzyme might be expressed at low levels that are insufficient to be detected in the spectrophotometric assay; or the transgene may be expressed but inactive in plant extracts for an unknown reason. A complete lack of expression is ruled out as the explanation as the protein was detected in immunoblot shown in Figure 3-1 and further confirmed by PCR detection of the corresponding transcript and ADE-GFP analyses. Low expression or no active expression is possible due to species incompatibility between yeast and *Arabidopsis*. Since this assay was developed by Kamat *et al*. (2011) on purified recombinant ADE, the assay may not be sensitive enough to detect low ADE levels that exist in leaf protein crude extracts. Despite all the above reasons, yeast ADE is very unstable *in vitro* as documented in Pospisilova *et al.* 2008. Therefore, after 48-72 hs of pre-treatments, yeast ADE may no longer be active. In addition, Pospisilova and Frebort (2007) reported yeast ADE is highly modified post translationally and that can also be a reason to not to show the activity as expected.

However, it is still uncertain whether the actual reason behind not being able to detect the activity by in vitro assay is due to expression problem of enzyme in the transgenic plants or its instability of the enzyme for such *in vitro* assay or the sensitivity of the assay to detect the lower expression of the enzyme. The activity of the ADE could be measured in means of adenine concentrations of leaf crude extracts and chloroplasts by HPLC as done by Shkolnik (2009) if the assay did not work due to instability of ADE as reported by Pospisilova *et al.* 2008. It is also advisable to try with another enzyme assay for ADE which could be more sensitive, such as the assay described by Escusa *et al.* 2006. If above attempts will also fail to detect an activity it is then clear yeast ADE is not active in *Arabidopsis*.

Therefore as a whole I could not prove the system of yeast ADE is a success or a complete failure. As elaborated before the expression of ADE was detected by immunobloting and confirmed further by transcript and GFP analyses. Moreover, GFP fusion expression proved the chloroplast targeting of the construct by tFd. Most importantly, but disappointingly, the enzyme activity could not be detected by the assay. On the other hand taken together these results cannot be considered a complete failure either.

4.5 Native APT1.1 localizes in chloroplasts

APT1.1 is predicted to be localized in chloroplasts as the gene contains an Exon1 with transit peptide at its N-terminal. Facciuolo (2009) tried to detect this by GFP fusion proteins but he could not distinguish whether the APT1.1 is in the chloroplast or not. Therefore, in this study I fractionated chloroplasts and detected the presence of APT1.1 by immunoblotting. First the intact protoplasts (IP) were isolated from leaves, lysed and extracted intact chloroplasts (IC). Then the chloroplasts were fractionated into stroma (S) and membrane (M) fractions. APT1.1 was detected in each fraction by immunoblotting all the fractions with anti-APT1.

The dilution of protoplasts into 80,000-100,000 protoplasts per milliliter was effective in later steps of the fractionation procedure. Breaking only 30,000-50,000 protoplasts through the 10 µm mesh to avoid crushing of chloroplasts by blocked pores was also critical to obtain a good IC yield. In addition, layering about 50,000-70,000 broken protoplasts on each Percoll gradient of 500 µl in each phase, also was important for a good IC yield. Furthermore, making the percoll gradient slowly with small drops using the 200µl pipetman instead of the 1000µl without mixing up between the two layers and have clear interface was also important to have good yield of IC.

According to chloroplast subfractionation results, APT1 could be seen in IP, IC and M fractions of WT plants in addition to the positive control, affinity chromatography purified recombinant APT1. As shown in figure 3-17, APT1 band was observed at 24 kDa in IP, IC and M while the band was at 26 kDa in the positive control. The reason was 6xhis-tagged recombinant APT1 was ran as the positive control and as Sauerand Stolz (1994) reported 6xhis tag at the C-terminal adds 2 kDa to the recombinant protein. Immunoblots with RbcL and PsaD evidenced all the fractions worked well. RbcL and PsaD are control antibodies for stroma and membrane fractions, respectively.

The observation of the APT1 polypeptide in the M fraction helps to narrow down its localization to the membrane part of the chloroplasts. However, in a chloroplast there are three membranes as outer envelope membrane, inner envelope membrane and thylakoid membrane. It is still not clear in which membrane APT1 is localized. Therefore, this chloroplast subfractionation followed by immunoblotting did not conclusively prove if APT1.1 localizes in chloroplasts. Because, the polypeptide might be bound to the outer envelope instead of localizing in the chloroplasts. To confirm the localization more precisely further analysis such as immunogold localization should be used. Immunogold localization uses electron microscopy to detect the binding of the antiserum (Kaur et al. 2002). The

primary antibodies designed to bind a specific protein are reacted with secondary antibodies attached with colloidal gold particles. Gold is used for its high electron density which increases electron scatter to give high contrast dark spots (Kaur *et al.* 2002). I initiated this analysis at the end of my studies by fixing and embedding WT and *oxt1* leaf tissues in LR White. These were sent to the lab of a collaborator, Dr. Klaus von Schwartzenberg (University of Hamburg) which has expertise in this method. The preliminary results shown in Figure 4-1, are consistent with APT1 residing in the thylakoid membrane.

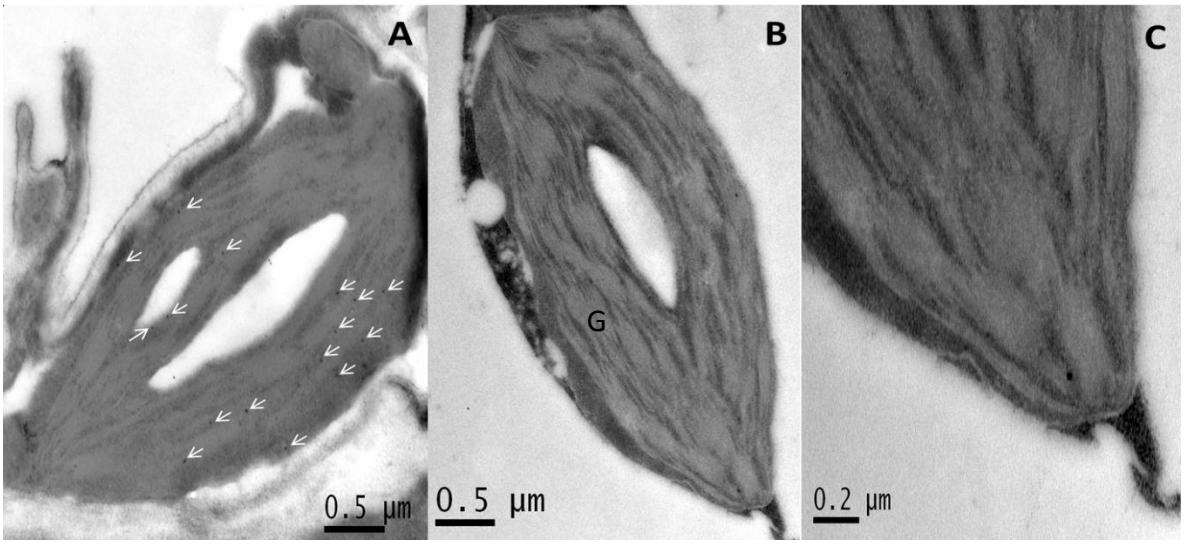

Figure 4-1: Fig. 2. Subcellular localization of APT1.1 in chloroplasts, using immunogold electron microscopy

Labeling is carried out using a polyclonal antibody to APT1 and then followed by secondary antibody bound to 20 nm gold particles. Labeling is seen in WT chloroplasts (A) with no labeling present in *oxt1* chloroplasts (B and C). *oxt1* used as the negative control. The white arrows show gold particles. G: grana (stack of thylakoids).

Chapter 5

Suggestions for future work

Based on the evidence presented in this thesis it is clear that further experiments are needed to confirm the success of this test system. Some of these include:

1. The suspected band of polypeptide to be yeast ADE has to be sequenced for confirmation.
2. The adenine levels in chloroplasts and leaf crude extracts have to be analyzed by HPLC as explained in Shkolnik (2009).
3. The activity of yeast ADE in crude extracts has to be confirmed using an alternate assay such as Escusa *et al.* (2006).
4. WT plants transformed with yeast ADE were crossed with *oxt1* and *apt1-3*. Now the seeds are at F2 stage. Next, homozygous seeds from each line (i.e. *oxt1* and *apt1-3* transformed with yeast ADE) have to be selected and grown stress inducing medium. Figure 5-1 shows a model with expected outcome.

This thesis presents attempts to develop a system to determine involvement of adenine in oxidative stress tolerance in plants. In this system yeast ADE that uses adenine as the major substrate was expressed in chloroplasts of model plant *A. thaliana*.

The foundation to develop this system was based on two major findings. First, according to Sukrong *et al. (*2012), WT plants with normal APT activity (100%) and normal adenine levels (1 $nmolg^{-1}FW$) are susceptible to chemically induced (AT and BSO) oxidative stress (Figure 5.1 A) while *apt* mutants with 1-6% APT activity and 1.5-6 times higher adenine content than WT are resistant to this oxidative stress (Figure 5.1 B). Interestingly, when

these susceptible WT plants can be recovered by supplementing with exogenous adenine up to 150 µM. On the other hand, *apt* mutants lose their tolerance above 50 µM of exogenous adenine perhaps because some unknown threshold is exceeded. Secondly, Shkolnik (2012) separated chloroplasts by sucrose gradient, measured adenine contents in chloroplasts using HPLC and found 12-fold higher adenine content of *apt* mutant chloroplasts. Based on these evidences, we designed and developed a system that could utilize the increased adenine in chloroplasts of *apt* mutants. For this, yeast ADE expression was targeted to chloroplasts along with transit peptide for ferredoxin (tFd; Figure 5.1 C, D) using the $UBQ10_{pro}$: tFd: yeast ADE construct.

The transgenic plants having $UBQ10_{pro}$: tFd: yeast ADE in WT background is susceptible to chemically induced oxidative stress as a result of both APT and yeast ADE utilizing the adenine in its chloroplasts (Figure 5.1 C). Similarly, this construct in *apt* background is also susceptible to oxidative stress as the higher adenine content was utilized by the Yeast ADE (Figure 5.1 D). Together these two systems can provide evidence that the stress tolerant ability of these plants is due to increased adenine contents. To further confirm that adenine is the key factor involved in chemically induced oxidative stress in these systems, the susceptible plants can be exposed to a continuous supply of exogenous adenine (Figure 5.1 C, D). Although, the continuous supply of adenine to the susceptible WT plants with the $UBQ10_{pro}$: tFd: yeast ADE construct might not recover its growth due to utilization of adenine by both APT and yeast ADE. However, the continuous supply of adenine to the susceptible *apt* plants with the $UBQ10_{pro}$: tFd: yeast ADE could be recovered its tolerance as a result of accumulating adenine after saturating the yeast ADE within the system.

This model was developed with the assumption that adenine metabolism occurs only in chloroplasts by chloroplast localized APT1.1. However, in reality this may not be true as the

other APT isoforms that are localized in the cytosol may also contributing to the whole plant responses.

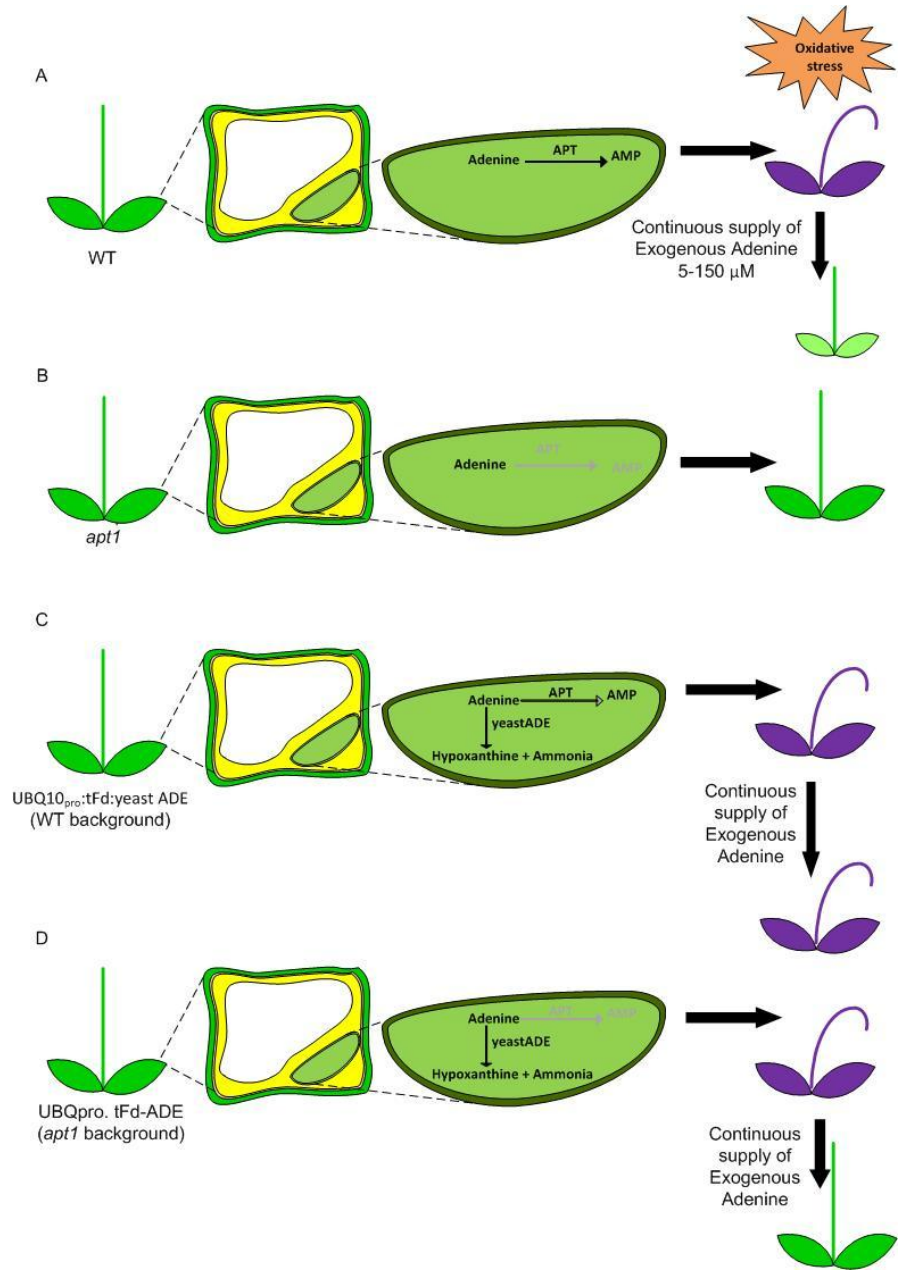

Figure 5.1: Model that explains the involvement of chloroplast adenine in developing tolerance to chemically induced oxidative stress

In WT, the adenine content is regulated by APT. WT plants do not survive under oxidative stress. Exogenous supply of adenine up to 150 µm improves the growth under oxidative stress medium. The *apt1* mutants have several folds increased levels of adenine and the plants are oxidative stress tolerant. The yeast ADE transformed WT plants are supposed to be not recovered by exogenous supply of adenine as the adenine content is continuously metabolizes by APT and yeast ADE. However, *apt1* mutants transformed with yeast ADE are supposed to be susceptible to stress as yeast ADE can lower the increased level of adenine and recovered back by exogenous supply of adenine.

References

Allen, R.D., (1995). Dissection of Oxidative Stress Tolerance Using Transgenic Plants. Plant Physiology 107:1049-1054

Allen, M., Qin, W.S., Moreau, F. and Moffatt, B.A. (2002). Adenine phosphoribosyltransferase isoforms of *Arabidopsis* and their potential contribution to adenine and cytokinin metabolism. Physiologia Plantarum115:56–68

Ashihara, H. and Ukaji, T. (1985). Presence of adenine phosphoribosyltransferase and adenosine kinase in chloroplasts of spinach leaves. International Journal of Biochemistry 17:1275-1277

Arabidopsis Genome Initiative (2000). Analysis of the genome sequence of the flowering plant *Arabidopsis thaliana*. Nature. 408:796-815

Bashor, C., Denu, J.M., Brennan, R.G. and Ullman, B. (2002). Kinetic mechanism of adenine phosphoribosyltransferase from *Leishmania donovani*. Biochemistry. 41:4020-31

Berg, J.M., Tymoczko, J.L. and Stryer, L. (2002). Biochemistry. 5th edition. New York: W H Freeman. Section 20.1, The Calvin Cycle Synthesizes Hexoses from Carbon Dioxide and Water

Berget, S. M., Moore, C., and Sharp, P. A. (1977). Spliced segments at the 5' terminus of adenovirus 2 late mRNA. Proceedings of the National Academy of Sciences 74:3171–3175

Biswal, B. Mohapatra, P.K., Biswal, U.C. and Raval, M.K. (2012). Leaf Senescence and Transformation of Chloroplasts to Gerontoplasts. Advances in Photosynthesis and Respiration 34: 217-230

BRENDA in 2013: integrated reactions, kinetic data, enzyme function data, improved disease classification: new options and contents in BRENDA. Schomburg, I., Chang, A., Placzek, S., Söhngen, C., Rother, M., Lang, M., Munaretto, C., Ulas, S., Stelzer, M., Grote, A., Scheer, M., Schomburg, D. Nucleic Acids Research 41:764-772

Broderick, T. P., Schaff, D. A., Bertino, A. M., Dush, M. K., Tischfield, J. A. and Stambrook, P. J. (1987). Comparative anatomy of the human APRT gene and enzyme: nucleotide sequence divergence and conservation of a nonrandom CpG dinucleotide arrangement. Proceedings of the National Academy of Sciences 84:3349-3353

Bruce, B.D. (2000). Chloroplast transit peptides: structure, function and evolution. Trends in cell biology 10:440-447

Bruce, B.D. (2001). The paradox of plastid transit peptides: conservation of function despite divergence in primary structure. Biochimica et Biophysica Acta 1541:2-21

Cadenas, E. and Packer, L. (2013). Methods in Enzymology: Hydrogen peroxide and cell signaling, part B. 527:284

Chan, C. X. and Bhattacharya, D. (2010). The Origin of Plastids. Nature Education 3(9):84

Chen, K.Y. and Li, H.M. (2007). Precursor binding to an 880-kDa Toc complex as an early step during active import of protein into chloroplasts. Plant Journal 49:149–158

Cho, U. and Seo, N. (2005). Oxidative stress in *Arabidopsis thaliana* exposed to cadmium is due to hydrogen peroxide accumulation. Plant Science 168:113–120

Clancy, S. (2014) Chemical structure of RNA. Nature Education 7:60

Daum, B., Nicastro ,D., Austin, J. 2nd, McIntosh, J.R. and Kuhlbrandta, W. (2010). Arrangement of Photosystem II and ATP Synthase in Chloroplast Membranes of Spinach and Pea. The Plant Cell 22:1299-1312

Davitt, K., Song, Y., Patterson, W., Nurmikko, A.V., Gherasimova, M., Han, J., Pan, Y. and Chang, R.K. (2005). 290 and 340 nm UV LED arrays for fluorescence detection from single airborne particles. Optics Express 13:9548-9555

Emanuelsson, O., Nielsen, H., Brunak, S. and von Heijne, G. (2000). Predicting subcellular localization of proteins based on their N-terminal amino acid sequence. Journal of Molecular Biology 300:1005-1016

Emanuelsson, O., Nielsen, H. and von Heijne, G. (1999). ChloroP a neural network-based method for predicting chloroplast transit peptides and their cleavage sites. Protein Science 8: 978-984

Epplera, A., Weigandta, M., Schulzea, S., Hanefelda, A., Bunjes, H. (2011). Comparison of different protein concentration techniques within preformulation developmentInternational Journal of Pharmaceutics 421:120-129

Escusa, S., Camblong, J., Galan, J. M., Pinson, B. and Daignan-Fornier, B. (2006). Proteasome- and SCF-dependent degradation of yeast adenine deaminase upon transition from proliferation to quiescence requires a new F-box protein named Saf1p. Molecular Microbiology 60:1014-1025

Facciuolo, A. (2009). The functional significance of the alternative first exons of the *Arabidopsis thaliana APT1* gene. M.Sc. Thesis. University of Waterloo. Waterloo. ON

Fujibe, T., Saji, H., Arakawa, K., Yabe, N., Takeuchi, Y., and Yamamoto, K.T. (2004). A Methyl Viologen-Resistant Mutant of Arabidopsis, Which Is Allelic to Ozone-Sensitive *rcd1*, Is Tolerant to Supplemental Ultraviolet-B Irradiation. Plant Physiology 134:275-285

Groth, D.P. and Young, L.G. (1971). On the formation of an intermediate in the adenine phosphoribosyltransferase reaction. Biochemical and Biophysical Research Communications 43: 82–87

Gupta, A.S., Heinen, J., Holaday, A.S., Burke, J.J.J. and Allen, R.D. (1993). Increased resistance to oxidative stress in transgenic plants that over-express chloroplastic Cu/Zn superoxide dismutase. Proceedings of the National Academy of Sciences USA 90:1629-1633

Hayashi, H., Alia I, Mustardy, L., Deshnium, P., Ida, M. and Murata, N. (1997). Transformation of *Arabidopsis thaliana* with the codA gene for choline oxidase; accumulation of glycinebetaine and enhanced tolerance to salt and cold stress. The Plant Journal 12:133-142

Heazlewood, J.L., Verboom, R.E., Tonti-Filippini, J., Small, I. and Millar, A.H. (2007). SUBA: the *Arabidopsis* Subcellular Database. Nucleic Acids Research 35: (Database issue) D213-D2188

Heiber, T. Steinkamp, T., Hinnah, S., Schwarz, M., Flugge, U.I., Weber, A. and Wagner, R. (1995). Ion channels in the chloroplast envelope membrane. Biochemistry 34: 15906-15917

Hochstadt-Ozer, J. and Stadtman, E.R. (1971).The Regulation of Purine Utilization in Bacterial Adenine phosphoribosyltransferase in isolated membrane preparations and its role in transport of adenine across the membrane. The Journal of Biological Chemistry 246: 5304-5311

Huh, W., Falvo, J.V., Gerke, L.C., Carroll, A.S. Howson, R.W., Weissman, J.S. and O'Shea, E.K. (2003). Global analysis of protein localization in budding yeast. Nature Publishing Group 425: 686-691

Inoue, H., Li, M. and Schnell, D.J. (2013). An essential role for chloroplast heat shock protein 90 (Hsp90C) in protein import into chloroplasts. Proceedings of the National Academy of Sciences of the United States of America 110:3173-3178

Itali, R., Suzuki, K., Yamaguchi, H., Nakanishi,H., Nishizawa, N., Yoshimura, E. and Mori,S. (2000). Induced activity of adenine phosphoribosyltransferase (APRT) in iron-deficient barley roots: a possible role for phytosiderophore production. Journal of Experimental Botany 51: 1179-1188

Jarvis, P. (2008). Targeting of nucleus-encoded proteins to chloroplasts in plants. New Phytologist 179: 257-285

Jarvis, P. and Soll, J. (2001). Erratum to: ''Toc, Tic, and chloroplast protein import''. Biochimica et Biophysica Acta 1541:64–79

Kamat, S.S., Bagaria, A., Kumaran, D., Hampton, D.P.H., Fan, H., Sali, A., Sauder, J.M., Burley, S.K., Lindahl P.A., Swaminathan, S. and Raushel, F.M. (2011). Catalytic mechanism and three-dimensional structure of adenine deaminase. Biochemistry 50:1917–1927

Kasuga, M., Liu, Q., Miura, S., Yamaguchi-Shinozaki, K. and Shinozaki, K. (1999). Improving plant drought, salt, and freezing tolerance by gene transfer of a single stress-inducible transcription factor. Nature Biotechnology 17: 287-291

Kazantsev, A.V. and Pace, N.R. (2006). Bacterial RNase P: A new view of an ancient enzyme. Nature Reviews Microbiology 4: 730

Kaur, R., Dikshit, K.L. and Raje, M. (2002). Optimization of immunogold labeling TEM: An ELISA-based method for evaluation of blocking agents for quantitative detection of antigen. The Journal of Histochemistry & Cytochemistry 50: 863–873

Keeling, P.J. (2004). Diversity and evolutionary history of plastids and their hosts. American Journal of Botany 91: 1481–1493

Kessler, F. and Blobel, G. (1996). Interaction of the protein import and folding machineries of the chloroplast. Proceedings of the National Academy of Sciences of the United States of America 93: 7684-7689

Kikuchi, S., Hirohashi, T. and Nakai, M.(2006). Characterization of the preprotein translocon at the outer envelope membrane of chloroplasts by blue native PAGE. Plant Cell Physiology 47:363-371

Koshiishia, C., Katoa, A., Yamab,S., Crozierc, A. and Ashihara, H. (2001). A new ca¡eine biosynthetic pathway in tea leaves: utilisation of adenosine released from the S-adenosyl-L-methionine cycle. FEBS Letters 499: 50-54

Kozak, M. (1989). Circumstances and mechanisms of inhibition of translation by secondary structure in eucaryotic mRNAs. Molecular and Cellular Biology 9: 5134-5142

Kruzniak, E. (2002). Transgenic plants: An insight into oxidative stress tolerance mechanisms. Acta Physiologiae Plantarum 24: 97-113AC

Lee, D. and Moffatt, B. A. (1994). Adenine salvage activity during callus induction and plant growth. Physiologia Plantarum 90:739-747

Ma, J.K., Drake, P.M.W., Chargelegue, D., Obregon, P. and Prada, A.(2005). Antibody processing and engineering in plants, and new strategies for vaccine production. Vaccine 23:1814-1818

Meyer, S., Temme, C. and Wahle, E. (2004). Messenger RNA Turnover in Eukaryotes: Pathways and Enzymes. Critical Reviews in Biochemistry and Molecular Biology 39:197-216

Miras, S., Salvi, D., Ferro, M., Grunwald, D., Garin, J., Joyard, J. and Rolland, N. (2002). Noncanonical transit peptide for import into the chloroplast. Journal of Biological Chemistry 277: 47770-47778

Mittler, R. (2002). Oxidative stress, antioxidants and stress tolerance. Trends in Plant Science 7:405-410

Miyagawa, Y., Tamoi, M. and Shigeoka, S. (2000). Evaluation of defense system in chloroplasts to photo oxidative stress caused by paraquat using transgenic tobacco plants expressing catalase from *Escherichia coli.* Plant and Cell Physiology 41:311-320

Moffatt, B.A. and Ashihara, H. (2002). Purine and Pyrimidine Nucleotide Synthesis and Metabolism. Arabidopsis Book 1:e0018

Moffatt, B.A. and Somerville, C. (1988). Positive selection for male-sterile mutants of Arabidopsis lacking adenine phosphoribosyltransferase activity. Plant Physiology 86: 1150–1154

Moffatt, B.A., McWhinnie, E.A., Agarwal, S.K. and Schaff, D.A. (1994). The adenine phosphoribosyltransferase-encoding gene of *Arabidopsis thaliana*. Gene 143: 211-216

Nurmohamed, S. and Vincent, H.A. (2011). RNA Turnover: The missing link polynucleotide phosphorylase activity may be modulated by metabolites in *Escherichia coli.* Journal of Biological Chemistry 286**:** 14315–14323

Nygaard, P., Duckert, P., and Saxild, H.H. (1996). Role of the adenine deaminase in purine salvage and nitrogen metabolism and characterization of ade gene in *Bacillus subtilis*. Journal of Bacteriology 178:846

Ogawa, H., Inouyett, S., TsujIt, F.I, Yasuda, K. and Umesono, K. (1995). Localization, trafficking, and temperature-dependence of the Aequorea green fluorescent protein in cultured vertebrate cells. Cell Biology 92:11899-11903

Page, M.G.P. and Burton, K. (1978). The Location of Purine Phosphoribosyltransferase Activities in *Escherichia coli* Biochemical Journal 174: 717-725

Pan, S.H. and Malcolm, B.A. (2000). Reduced background expression and improved plasmid stability with pET vectors in BL21 (DE3). Bio Techniques 29:1234-1238

Pilon-Smith, E.A.H., Zhu, Y.L., Sears, T. and Terry, N. (2000). Overexpression of glutathione reductase in *Brassica juncea:* effects on cadmium accumulation and tolerance. Physiologia Plantarum 110: 455-460

Pospisilova, H., Sebela, M., Novak, O. and Frebort, I. (2008). Hydrolytic cleavage of N6-substituted adenine derivatives by eukaryotic adenine and adenosine deaminases. Bioscience Reports 28:335-347

Pyke, K.A. (1994). Arabidopsis-Its Use in the Genetic and Molecular Analysis of Plant Morphogenesis. New Phytologist 128:19-37

Pyke, K.A. (1999). Plastid Division and Development. The Plant Cell 11:549–556

Quattrocchio, F.M., Spelt, C. and Koes, R. (2013). Transgenes and protein localization: myths and legends. Trends in Plant Science 18: 1360-1385

Raghow, R. (1987). Regulation of messenger RNA turnover in eukaryotes. Trends in Biochemical Sciences 12:358-360

Rege K. and Heng, M. (2010). Miniaturized parallel screens to identify chromatographic steps required for recombinant protein purification. Nature Protocols 5:408-417

Reinbothe, S., Rossig, C., Gray, J. and Reinbothe, C. (2014).Plastid Import of a Transit Sequence-Less Precursor Protein in *Arabidopsis thaliana.* Cellular and Molecular Biology 60:1-10

Reinbothe, .S, Runge, S., Reinbothe, C., van Cleve, B. and Apel, K. (1995). Substrate-dependent transport of the NADPH:protochlorophyllide oxidoreductase into isolated plastids. Plant Cell 7: 161-172

Ribard, C., Rochet, M., Labedan, B., Daignan-Fornier, B., Alzari, P., Scazzocchio, C., and Oestreicher N. (2003).Sub-families of a/b Barrel Enzymes: A New Adenine Deaminase Family. Journal of Molecular Biology 334: 1117–1131

Richardson, L.G.N., Paila, Y.D., Siman, S.R., Chen, Y., Smith, M.D. and Schnell, D.J (2014). Targeting and assembly of components of the TOC protein import complex at the chloroplast outer envelope membrane. Frontiers in Plant Science 5:1-14

Robb, F.T., Park, B,J, and Adams, M.W.W (1992). Characterization of an extremely thermostable glutamate dehydrogenase: a key enzyme in the primary metabolism of the hyperthermophilic archaebacterium, *Pyrococcus furious.* Biochimica et Biophysica Acta. 11211:267-272

Sarver, A.E. and Wang, C.C. (2002). The Adenine Phosphoribosyltransferase from *Giardia lamblia* has a unique reaction mechanism and unusual substrate binding properties. Journal of Biological Chemistry 277:39973-39980

Sauer, N. and Stolz, J. (1994). SUC1 and SUC2: two sucrose transporters from Arabidopsis thaliana; expression and characterization in baker's yeast and identification of the histidine-tagged protein. The Plant Journal 6:67-77

Schleiff, E., Soll, J., Kuchler, M., Kuhlbrandt, W. and Harrer, R. (2003). Characterization of the translocon of the outer envelope of chloroplasts. Journal of Cell. Biology 160:541–551

Schmid, M., Davison, T.S., Henz, S.R., Pape, U.J., Demar, M., Vingron, M., Schölkopf, B., Weigel, D., and Lohmann, J.U. (2005). A gene expression map of *Arabidopsis thaliana* development. Nature Genetics 37:501 - 506

Schnorr, K. M., Gaillard, C., Biget, E., Nygaard, P., and Laloue, M. (1996). A second form of adenine phosphoribosyltransferase in *Arabidopsis thaliana* with relative specificity towards cytokinins. The Plant Journal 9:891-898

Schoor, S. (2007). Determining the subcellular localization of adenosine kinase and SAH hydrolase and their roles in adenosine metabolism. M.Sc. Thesis. University of Waterloo, Waterloo, ON

Schwartzenberg, K.V., Núñez, M.F., Blaschke, H., Novak P.I.O., Motyka, V. and Strnad, M. (2007). Cytokinins in the Bryophyte *Physcomitrella patens*: Analyses of activity, distribution, and cytokinin

oxidase/dehydrogenase over expression reveal the role of extracellular cytokinins. Plant Physiology 145:786–800

Senecoff, J. F., McKinney, E. C., and Meagher, R. B. (1996). *De novo* purine synthesis in *Arabidopsis thaliana* (II. the PUR7 gene encoding 5 [prime]-phosphoribosyl-4-(Nsuccinocarboxamide)-5-aminoimidazole synthetase is expressed in rapidly dividing tissues). Plant Physiology 112:905-917

Shi, W., Tanaka, K.S., Crother, T.R., Taylor, M.W., Almo, S.C., Schramm, V.L. (2001). Structural analysis of adenine phosphoribosyltransferase from *Saccharomyces cerevisiae*. Biochemistry 40:10800-10809.

Shikanai, T., Takeda, T., Yamauchi, H., Sano, S., Tomizawa, K.I., Yokota, A. and Shigeoka, S. (1998). Inhibition of ascorbate peroxidase under oxidative stress in tobacco having bacterial catalase in chloroplasts. FEBS Letters 428:47-51

Shkolnik, V. (2009). Purine metabolite effects on growth and oxidative signaling plants. M.Sc. thesis. University of Massachusetts Lowell, Massachusetts, The United States

Smith, A.M., Hylton, C.M. and Rawsthorne S. (1989). Interference by phosphatases in the spectrophotometric assay for phosphoenolpyruvate carboxylase. Plant Physiology 89:982-985

Sukrong, S, Yun, K, Stadler, P, Kumar, C, Facciuolo, T., Moffatt, B.A. and Falcone, D.L. (2012). Improved growth and stress tolerance in the *Arabidopsis oxt1* mutant triggered by altered adenine metabolism. Molecular plant 5:1310-1332.

Sunker, R., Bartels, D. and Kirch, H. (2003). Overexpression of a stress-inducible aldehyde dehydrogenase gene from *Arabidopsis thaliana* in transgenic plants improves stress tolerance. The plant journal 35:452-464.

Svitkin, Y.V., Pause, A., Haghighat, A., Pyronnet, S., Witherell, G., Belsham, G.B. and Sonenberg, N. (2001). The requirement for eukaryotic initiation factor 4A (elF4A) in translation is in direct proportion to the degree of mRNA 5' secondary structure. RNA 7:382-394

The Arabidopsis Information Resource (TAIR), www.arabidopsis.org/about arabidopsis.html on Mar 2, 2014

Tischfield, J.A. and Ruddle, F.H. (1974). Assignment of the gene for adenine phosphoribosyltransferase to human chromosome 16 by mouse-human somatic cell hybridization. Proceedings of the National Academy of Sciences 71:45-49

Tzfira, T., Tian, G.W., Lacroix, B., Vyas, S., Li, J., Leitner-Dagan, Y., Krichevsky, A., Taylor, T., Vainstein, A. and Citovsky, V. (2005). pSAT vectors: a modular series of plasmids for autofluorescent protein tagging and expression of multiple genes in plants. Plant molecular biology 57:503-516

Ventura, S. and Villaverde, A., (2006). Protein quality in bacterial inclusion bodies. Trends in biotechnology 24:179-185

Villarejo, A., Buren, S., Larsson, S., Dejardin A, Monne, M., Rudhe, C., Karlsson, J., Jansson, S., Lerouge, P., Rolland, N., von Heijne, G., Grebe, M., Bako, L. and Samuelsson, G. (2005). Evidence for a protein transported through the secretory pathway en route to the higher plant chloroplast. Nature Cell Biology 7:1124-1131

Wang, W., Vinocur, B. and Altman, A. (2003). Plant responses to drought, salinity and extreme temperatures: towards genetic engineering for stress tolerance. Planta 218:1-14

Wang, W.X., Vinocur, B., Shoseyov, O. and Altman, A. (2001a). Biotechnology of plant osmotic stress tolerance: physiological and molecular considerations. Acta Horticulture 560:285-292

Williams, A.D., Portelius, E., Kheterpal, I., Guo, J., Cook, K.D., Xu, Y., and Wetzel, R. (2004). Mapping Ab amyloid fibril secondary structure using scanning proline mutagenesis. Journal of Molecular Biology 335:833–842.

Wilson, G.M., Sutphen, K., Chuang, K. and Brewer, G. (2001). Folding of A1U-rich RNA Elements Modulates AUF1 Binding: Potential roles in regulation of mRNA turnover. Journal of Biochemistry 276: 8695–8704

Wilson, J. M., O'Toole, T. E., Argos, P., Shewach, D. S., Daddona, P. E. and Kelley, W. N. (1986). Human adenine phosphoribosyltransferase: complete amino acid sequence of the erythrocyte enzyme. Journal of Biochemistry 261: 13677-13683

Wu, S., Yu, Z., Wang, F., Li, W., Yang, Q., Ye, C., Sun, Y., Jin, D., Zhao, J. and Wang, B. (2008). Identification and characterization of a novel adenine phosphoribosyltransferase gene (ZmAPT2) from maize (*Zea mays* L.). DNA Sequence 19:357-65

Zhang, X., Chen, Y., Lin, X., Hong, X., Zhu, Y., Li, W., He, W., An, F. and Guo, H. (2013). Adenine Phosphoribosyl Transferase 1 is a key Enzyme catalyzing cytokinin conversion from nucleobases to nucleotides in *Arabidopsis.* Molecular Plant 5:1661-72

Yoo, S.D., Cho, Y.H., Sheen, J. (2007) *Arabidopsis* mesophyll protoplasts: a versatile cell system for transient gene expression analysis. Nature Protocols 2:1565-1572

Zarella-Boitz, J.M., Rager, N., Jardim, A. and Ullman, B. (2004).Subcellular localization of adenine and xanthine phosphoribosyltransferases in *Leishmania donovani.* Molecular and Biochemical Parasitology 134: 43-51

Zhang, C. (2000). The involvement of adenine phosphoribosyltransferase in microsporogenesis of *Arabidopsis thaliana*. M.Sc. Thesis. University of Waterloo, Waterloo, ON

Zhang, X., Henriques, R., Lin, S., Niu, Q., and Chua, N. (2006). *Agrobacterium*-mediated transformation of *Arabidopsis thaliana* using the floral dip method. *Nature Protocols* 1:641-646

Zhang, C., Guinel, F.C. and Moffatt, B.A. (2001). A comparative ultra-structural study of pollen development in *Arabidopsis thaliana* ecotype Columbia and male-sterile mutant *apt1-3.* Protoplasma 219:59-71

Zhou, C., Li, J., Zou, J., Liang, F., Ye, C., Jin, D., Weng, M. and Wang, B. (2006). Cloning and characterization of a second form of the rice adenine phosphoribosyltransferase gene (OsAPT2) and its association with TGMS. Plant Molecular Biology 60:365-376

Zrenner, R., Stitt, M., Sonnewald, U. and Boldt, R. (2006). Pyrimidine and purine biosynthesis and degradation in plants. Annual review of Plant Biology 57:805-836

Zybailov, B., Rutschow, H., Friso, G., Rudella, A., Emanuelsson, O., Sun, Q. and van Wijk, K.J. (2008) Sorting Signals, N-Terminal Modifications and Abundance of the Chloroplast Proteome. PLoS ONE 3: e1994.